CHARACTERIZATION OF THE MOLECULAR MECHANISMS INVOLVED IN ETHIONAMIDE ACTIVATION IN MYCOBACTERIA

ANG LAY TENG MICHELLE

(B.Sc (*Life Sciences, Hons.*), NUS)

A THESIS SUBMITTED

FOR THE DEGREE OF
DOCTOR OF PHILOSOPHY
DEPARTMENT OF MICROBIOLOGY
YONG LOO LIN SCHOOL OF MEDICINE
NATIONAL UNIVERSITY OF SINGAPORE

2014

Declaration

I hereby declare that this thesis is my original work and it has been written by me in its entirety. I have duly acknowledged all the sources of information which have been used in the thesis.

This thesis has also not been submitted for any degree in any university previously.

Ang Lay Teng Michelle

29 October 2014

Acknowledgements

My deepest gratitude goes to my supervisor, A/P Sylvie Alonso for all the unwavering support she has provided me throughout this journey. Her constant encouragement, inspiring guidance and intellectual opinions were critical driving forces in helping me to achieve my research goals. Much of this project was also completed with the invaluable assistance from past and present SA Lab BSL3 team members thanks to the exemplary teamwork: Ms. Lin Wenwei, Ms. Vanessa Koh, Ms. JuliaMaria Martinez Gomez and in particular, Ms. Zarina Zainal Rahim Siti, for her dedicated mentorship during my initiation at SA lab and her technical support in this project. I would also like to thank all other past and present members of SA lab for their support, suggestions and assistance, in particular, Grace, Jowin, Weixin, Jian Hang, Regina, Yok Hian, Eshele, Annabelle, Liching and Emily.

Special thanks also goes to all our project collaborators and advisors involved in this project who have provided valuable technical assistance, constructive suggestions and helpful critiques – Dr Alain Baulard, Dr Nicholas West, Dr Katarína Mikušová, Dr Jana Korduláková, Petronela Dianišková, Jan Madacki, Dr Pablo Bifani, Dr. Shui Guanghou, Dr Anne Bendt, Dr Sukumar Sudarkodi, A/P Marcus Wenk, A/P Kevin Pethe, Dr Paola De Sessions and Dr Martin Hibberd. I would also like to thank my thesis advisory committee (TAC) – A/P Thomas Dick, Dr Manjunatha Ujjini, and my own supervisor again, for all their invaluable suggestions and comments throughout the course of my project.

Last but not least, I would not have come this far without the constant support and love from my family. To my mum and dad, thank you for giving me the freedom to pursue my dreams and always encouraging me to reach for the stars. To my younger sisters, Eunice and Celeste, thank you for all the crazy and fun sister bonding times that helped maintain my sanity through the stressful periods. I would also like to express my great appreciation and gratitude for my husband, Jega, for continuously motivating me with various forms of positive encouragement throughout the ups and downs of my research. Finally, I thank my dog Yoshi, for unknowingly being my de-stressing companion through the most challenging of times.

Table of Contents

Summary

Approximately one-third of the world population is presently infected with the highly infectious *Mycobacterium tuberculosis* (Mtb), and this worldwide endemic appears to be deteriorating. Underlying this endemic is the emerging epidemic of multi-drug resistant (MDR-TB) and extreme-drug resistant TB strains (XDR-TB) that have severely undermined control efforts. With dwindling treatment options for MDR and XDR-TB that are decades old, it has become imperative to either identify novel anti-TB drugs or develop shorter, more efficient anti-TB therapies with existing drugs. While improving the efficacy of existing drugs may require a shorter timeframe than the former strategy, this approach however necessitates further understanding in the mechanism of action of mycobacterial drugs and their bio-activation, especially drugs which have been suggested to have multiple targets and pathways, such as isoniazid (INH) and ethionamide (ETH), thus increasing the exploitation potential for drug improvements.

One of the most efficient second-line drugs to date for the treatment of MDR-TB is ETH; however its associated hepatotoxicity and gastric intolerability have restricted its use as an alternative treatment reserved for MDR-TB cases only. As a pro-drug that requires activation within the mycobacterial cell in order to exert its bactericidal effects, the current model for ETH bio-activation involves a Bayer-Villiger monooxygenase EthA and a repressor, EthR, which binds to the promoter region of *ethA*. However, the molecular mechanisms of ETH activation by EthA have not been completely deciphered yet. To add on, while most studies to date have focused on dissecting the role of EthA in ETH activation, few attempts have been made to understand its physiological role in Mtb. This thesis aims to further characterize the role of the EthA/R system in both the physiology and virulence of mycobacteria, and in ETH bio-activation.

To address the first aim, *ethA/R* knockout mutants and complemented strains were constructed in both *M. bovis* BCG (BCG) and Mtb backgrounds. Our results indicate that absence of the *ethA/R* locus led to greater persistence of BCG in the mouse model of mycobacterial infection, which correlated with greater adherence to mammalian cells. Furthermore, analysis of cell wall lipid composition by thin-layer chromatography and mass spectrometry revealed differences between the BCG *ethA/R* KO mutant and the parental strain in the

relative amounts of alpha and keto-mycolates. The work presented in this section suggests that the *ethA/R* locus is involved in the composition of cell wall mycolates in mycobacteria, specifically the relative amounts of alpha and keto-mycolic acids, which impacts the adherence properties of mycobacteria to mammalian cells *ex vivo* and their ability to colonize their host.

The second part of this thesis further investigates the bio-activation of ETH by the EthA/R system. Interestingly, we discovered that ETH killing efficacy against Mtb was greater in macrophages than during *in vitro* growth. We demonstrated that this effect was neither accountable by changes in *ethA* or *ethR* gene expression during macrophage infection nor mediated by spontaneous activation of ETH by macrophages alone. We concluded that the apparent greater killing efficacy of ETH in macrophage may be due to accumulation of the drug within the phagosomal compartment where mycobacteria reside, thereby leading to higher drug concentration compared to the actual concentration in the culture medium.

In the second sets of experiments, we demonstrated for the first time that the deletion of the entire *ethA/R* locus in BCG and three different Mtb backgrounds (namely Erdman, H37Rv and CDC1551) leads to different levels of resistance to ETH. While *ethA/R* deletion in BCG led to high levels of ETH resistance, *ethA/R* KO mutants in Mtb backgrounds displayed retained drug susceptibility and dose-dependent killing in response to ETH, suggesting the existence of an alternative EthA/R-independent pathway of ETH bio-activation in Mtb. Expression of *ethR* in *ethA/R* KO strains did not increase ETH resistance therefore supporting that the alternative pathway of ETH bio-activation is not modulated by EthR. Full-genome sequencing of spontaneous ETH-resistant mutants isolated from Erdman *ethA/R* KO Mtb identified several candidates, including *mshA,* which is involved in mycothiol biosynthesis. These gene candidates may have potential roles in ETH drug resistance that may specifically be involved in ETH bio-activation. Validation of the role of *mshA* in ETH drug resistance showed that deletion of the *mshA* locus in all Mtb *ethA/R* KO strains conferred even higher levels of resistance to ETH compared to their *ethA/R* single KO counterpart. These observations therefore suggest that *mshA* is not involved in ETH bio-activation and is more likely to be involved in the downstream steps after ETH catalysis. Most importantly, this is the first report to demonstrate that the simultaneous removal of both *ethA/R*and *mshA* loci is able to completely abrogate ETH susceptibility in all Mtb strains.

List of Tables

List of Figures

List of Acronyms & Abbreviations

Bacteria Strains and Mutants

BCG – *Mycobacterium bovis* bacillus Calmette-Guérin

CDC1551 – *Mycobacterium tuberculosis* CDC1551

E. coli – Escherichia coli

Erdman – *Mycobacterium tuberculosis* Erdman

WT – wild type/parental strain

*ethA/R*KO – *ethA/R* Knockout Mutant

H37Rv – *Mycobacterium tuberculosis* H37Rv

*m/e*KO – *mshA/ethA/R*Knockout Mutant

Mtb – *Mycobacterium tuberculosis*

MTBC – *Mycobacterium tuberculosis* Complex (MTBC)

Drugs

CCD – cytochalasin D

EMB – Ethambutol

ETH – Ethionamide

INH – Isoniazid

ISO – Isoxyl

PZA – Pyrazinamide

PAS – Para-amino Salicylic Acid (PAS)

PZA – Pyrazinamide

RIF – Rifampicin

TAC- Thiacetazone

TMC-207 – Bedaquiline

Chemicals

ADS – Albumin Dextrose Saline

AG – Silver

CSPD - Disodium 3-(4-methoxyspiro {1,2-dioxetane-3,2'-(5'-chloro)tricyclo [3.3.1.1^{3,7}]decan}-4-yl)phenyl phosphate

DMEM – Dulbecco modified Eagle medium

EDTA – Ethylenediaminetetraacetic acid

FBS – Fetal Bovine Serum

HCl – Hydrochloric Acid
HEPES – 4-(2-hydroxyethyl)-1-piperazineethanesulfonic Acid
KOH – Potassium Hydroxide
M-CSF – Recombinant Macrophage Colony-stimulating Factor
OADC – Oleic Albumin Dextrose Catalase
PMA – Phorbol 12-myristate 13-acetate
PBS – Phosphate Buffered Saline
PBST – Phosphate Buffered Saline Tween

Cell Lines

A549 – Human Pulmonary Epithelial Cells
BMMO – Murine Bone Marrow-derived Macrophages
Huh7 – Human Hepatocytes
THP1 – Human Macrophages

Molecules, Proteins and Enzymes

Ac2PIM2 – Diacylated Phosphatidylinositol Di-mannoside
Ac1PIM1 – Mono-acylated Phosphatidylinositol Di-mannoside
ACP – Acyl Carrier Protein
BVMO – Bayer-Villiger Monooxygenase
CL – Cardiolipin
CmrA – Corynebacterineae Mycolate Reductase A
DIMs – Phthiocerol Dimycoserosates
ETH-SO – S-oxide derivative of Ethionamide
ETH-OH – 2-ethyl-4-hydroxymethylpyridine
FAD – Flavine Adenine Dinucleotide
FAME – Fatty Acid Methyl Ester
FAS-I – Fatty acid synthase-I
FAS-II – Fatty acid synthase-II
FGS – Full Genome Sequencing
GSH – Glutathione
GAG – Glycosaminoglycans
HRP – Horseradish Peroxidase
hsp60 – Heatshock Protein 60
MAME – Mycolic Acid Methyl Ester

MSH – Mycothiol

NAD/NADH – Nicotinamide Adenine Dinucleotide

NADP/NADPH – Nicotinamide Adenine Dinucleotide Phosphate

PEE – Phosphatidylethanolamine

PI –Phosphatidylinositol

PIMs – Higher Phosphatidylinositol Mannosides

STPK – Mycobacterial Serine/Threonine Protein Kinase (STPK)

TDM – Trehalose-6,6'-dimycolate

TMM – Trehalose Monomycolate

Others

CFU – Colony Forming Unit

CMI – Cell-mediated Immunity

DTH – Delayed-type Hypersensitivity

ECL – Chemiluminescence

ETH^{Rlow} – Low Ethionamide-resistance

ETH^{Rhi} – High Ethionamide-resistance

ETH^{R} – Ethionamide-resistant

ESI-MRM – Electrospray Ionization-based Multiple Reaction Monitoring

FDA – US Food and Drug Administration

gDNA – genomic DNA

HR-NMR – High Resolution Magic Angle Spinning-Nuclear Magnetic Resonance

INDELs – Insertion/deletions

INH^{R} – Isoniazid-resistant

LED-FM – Light-emitting Diode Fluorescence Microscopy

MAs - Mycolic Acids

MBC – Minimum Bactericidal Concentration

MDR-TB – Multi-Drug Resistant Tuberculosis

MIC – Minimum Inhibitory Concentration

MOI – Multiplicity of Infection

NR – Non-replicating

NRT – No Reverse Transcriptase Controls

NS-SNPs – Non-Synonymous Single Nucleotide Polymorphisms

NTC – No Template Controls

OD – Optical Density

PE - Proteins that contain highly conserved Proline-Glutamate residues in N-terminal domains

PCR – Polymerase Chain Reaction

PGRS - Polymorphic CG-repetitive Sequences

PVDF – Polyvinylidene Difluoride

RD – Regions of Differences

ROS – Reactive Oxygen Species

RNIs – Reactive Nitrogen Intermediates

SD – Standard Deviation

SDS-PAGE – Sodium Dodecyl Sulfate Polyacrylamide Gel Electrophoresis

SNPs – Single Nucleotide Polymorphisms

TB – Tuberculosis

TDR-TB – Totally-Drug Resistant Tuberculosis

TLC – Thin Layer Chromatography

WHO – World Health Organization

XDR-TB – Extensively-Drug Resistant Tuberculosis

ZN – Ziehl-Neelsen

Chapter 1: Literature Review

1.1 Tuberculosis: A Persistent Adversary through the ages since Europe's Great White Plague to Today's Global Hallmark of Drug Resistance

Tuberculosis is a chronic granulomatous disease that has persisted throughout history since the inception of early civilization to present, accumulating monikers such as Consumption, Phthisis, Scrofula, Pott's disease, and the Great White Plague. As one of the most eminent epidemics of the past, the Great White Plague was used to describe the tuberculosis epidemic in Europe which started in the early 17th century and lasted up to two hundred years, during which up to 25% of deaths in Europe were attributed to this complex and debilitating disease (1, 2). The death toll from tuberculosis began to fall in Europe towards the beginning of the 20th century with the general improvement of living standards and the advent of antituberculosis drugs and BCG vaccination in the early 1960s (2). However, due to globalization, the current HIV/AIDS epidemics, complicated and lengthy drug regimens causing poor drug compliance, and the development of multi/extensively/totally-drug resistant *M. tuberculosis* strains (largely fuelled by the above three factors), the disease has presently resurged with a vengeance in staggering proportions globally and is ratified as one of the leading causes of morbidity and mortality, causing 1-7 million tuberculosis-related deaths worldwide annually (3, 4).

Upon the declaration of tuberculosis as a global public health emergency by the World Health Organization (WHO) in 1993, response from the international community was criticized as 'sluggish and inadequate' (2), and the incidence of tuberculosis cases continued to increase at an alarming rate.

Since then, the disease has eventually been recognized by these global organizations as a formidable threat that could have serious repercussions in terms of social and financial development internationally. The Stop TB strategy was initiated by WHO in 2006 with the ultimate goal of reversing the spread of tuberculosis by 2015 (5).

Unfortunately, regardless of continuous efforts by public health officials worldwide to curb the spread of *Mycobacterium tuberculosis* (Mtb)infections, pulmonary tuberculosis (TB) remains endemic worldwide. With approximately one-third of the world population presently infected with this highly infectious pathogen (6), the situation appears to be deteriorating, with WHO reporting 8.6 million incident cases of tuberculosis, 1 million deaths from HIV-negative tuberculosis-infected individuals and an additional 0.3 million deaths from HIV-associated tuberculosis in 2012(7).

Underlying these statistics is an emerging epidemic of multi-drug resistant (MDR-TB) and extensively-drug resistant TB strains (XDR-TB) that have severely undermined control efforts (8, 9), resulting in concerned appeals by the WHO for urgent action by TB control programmes worldwide as the multiplication of these strains spin out of control. Even more alarmingly, a handful of totally-drug resistant TB strains have surfaced in Iran and India in recent years. While the number of diagnosed MDR-TB cases nearly doubled between 2011 and 2012, leading to 94,000 confirmed MDR-TB cases; in reality, WHO estimates that there were 450,000 new MDR-TB cases in 2012 alone (7). These statistics are even more alarming with the knowledge that on average, an estimated 9.6% of MDR-TB cases develop into XDR-TB (7). By

the end of 2012, 92 countries reported at least one case of XDR-TB. This implies that globally, less than one in four MDR-TB patients have been detected, necessitating the need for wider and better TB detection and diagnostics. A large-scale and orchestrated effort largely led by the WHO Global TB Program together with WHO regional and country offices has been implemented worldwide to tackle this multi-factorial perseverant disease.

1.2 Tuberculosis pathophysiology: Active versus Latent TB

In an infected individual, tuberculosis generally develops as a consequence of one of the following three processes: progression of primary infection (primary active TB), exogenous reinfection (re-infection with a new strain of Mtb in a previously infected individual), or endogenous reactivation (reactivation of dormant TB in a previously infected individual) (3, 10, 11). The disease typically manifests in the lungs with ~80% of the diagnosed cases being classified as pulmonary TB (12), but can also affect extrapulmonary organs and tissues including the pleura, brain, testicles, spleen and liver, particularly in immunosuppressed persons and young children. Miliary tuberculosis, an extremely serious form of the disease leading to the widespread dissemination of TB into the human body coupled with tiny (1-5mm) lesions comprises 10-20% of extrapulmonary TB cases (13, 14).

The primary phase of TB infection commences with the inhalation of mycobacteria through the respiratory tract, which forms the major portal of entry for this pathogen (15). Alveolar macrophage in the lung peripheries then phagocytose these mycobacteria through interaction with several cell surface receptors, including complement receptor, mannose receptor, surfactant protein A, scavenger receptor and Fc receptor (16). More unconventionally, several lines of evidence also suggest the interaction of mycobacteria with epithelial cells in the respiratory tract including type II pneumocytes by attaching with glycosaminoglycans (GAG) (17-20).Mtb-infected macrophages subsequently reach the lung parenchyma, leading to the recruitment of other cells including the epithelioid and foamy macrophages, multinucleated giant

cells which are surrounded by a peripheral rim of B and T cell lymphocytes followed by a fibrous capsule, delineating the battlefield between Mtb and the host's immune system through the formation of the classic TB granuloma (21-24) (Fig. 1). The initiation of tuberculosis requires the establishment of only a single primary pulmonary tubercle comprising of bacilli surrounded by a wall of immune cells in the lung.During TB infection, individual lesions in the same host may progress at discordant rates, leading to varying maturation stages and subsequently, to different granuloma types which can be categorized as caseous, cellular and fibrotic (22, 24) (Fig. 1).

Disease progression varies widely depending on the complex interplay of both host and pathogen factors, and can be further characterized into 5 non-distinct stages that usually overlap, which are elaborated in detail in Fig. 2: 1) Ingestion with possible destruction of bacilli by pulmonary alveolar macrophages; 2) Exponential growth of bacilli within nonactivated macrophages that entered the developing tubercle from the bloodstream as monocytes; 3) Development of a solid caseous centre in the tubercle upon delayed-type hypersensitivity (DTH) response (due to the accumulation of high concentrations of tuberculin-like product) leading to arrested bacillary growth and subsequent killing of bacilli-laden macrophages; 4) Either tubercle and its caseous centre enlarging with hematogenous bacilli dissemination in immunocompromised hosts due to weak cell-mediated immunity (CMI); or tubercule stabilization orregression in immunocompetent hosts; and lastly, 5) Liquefaction of the caseous centre, extracellular bacillary growth, cavity formation, and bronchial dissemination of the bacilli (25).

In most healthy individuals, initial infection involving minute amounts of Mtb (1-5 bacilli) is asymptomatic, with primary lesions spontaneously resolving on their own. However, 5-10% of primarily infected individuals go on to develop local or systemic TB within the next 1-2 years (23, 26). During active disease, it is thought that mycobacteria may exist as subpopulations in different metabolic states in order to survive the vastly differing microenvironments within a single granuloma (27). In contrast, about 2 billion people comprising one third of the world are estimated to harbour latent TB (22). During latent disease, Mtb is thought to enter a dormant state in which the replication rate is substantially slower than that during active growth (28). 90-95% of primary TB cases asymptomatically develop into latent TB cases which can only be detected via the tuberculin skin test 3-8 weeks later, a diagnostic TB test that can identify the presence of both actively replicating and dormant non-replicating (NR) Mtb (12, 23, 29). NR Mtb can persist in the tissues throughout a latently-infected TB individual's lifetime, during which Mtb may migrate from primary lesions usually formed at the base of the lungs via lymphatics and the bloodstream to secondary sites located at the apical zones of the lungs, leading to the formation of secondary granulomas (12).

About 1 in 10 latent TB cases may reactivate into active TB under circumstances of weakened or compromised immunity, multiplying to high densities within the granulomas. Massive numbers of Mtb antigens appear to trigger the immune response that lead to the occurrence of caseous necrosis, liquefaction, cavity formation and the eventual release of the tubercle bacilli into the airways of highly contagious pulmonary TB patients (23, 26). This

infection-disease-infection cycle mediated by the reactivation of latent TB is believed to be one of the many mechanisms by which Mtb perpetuates its survival (12), leading to its persistence through history.

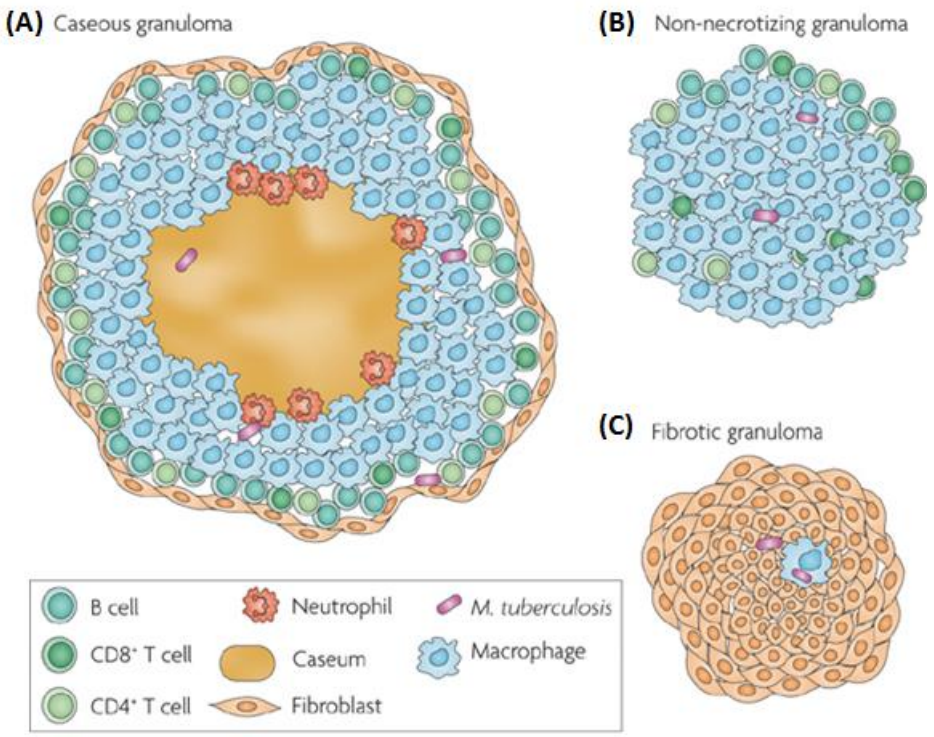

Figure 1: Types of Granulomas that can be found in an Mtb-infected host.

During TB infection, individual lesions in the same host may progress at discordant rates, leading to varying maturation stages and subsequently, different granuloma types which can be categorized as **(A)** Caseous granuloma, also known as the classic TB granuloma, which is composed of epithelial macrophages, neutrophils, a cuff of lymphocytes (CD4+ and CD8+ T cells and B cells) and occasionally surrounded by peripheral fibrosis. Found in both active and latent infections, this granuloma has a caseous centre in a necrotic stage that consists of dead macrophages and other cells. Mycobacteria exist in different microenvironments here, either in macrophages, the hypoxic centre or the fibrotic rim. **(B)** Non-necrotizing granuloma, also known as the cellular granuloma, are primarily found during active TB and largely consists of macrophages and lymphocytes with mycobacteria residing within macrophages. **(C)** Fibrotic lesions are more often found in latent TB and comprise mostly of fibroblasts with a minimal number of macrophages; however it is not clear where the bacilli reside (possibly in macrophages or in the fibrotic area) or what the microenvironment is like. Figure reproduced with permission from Barry *et al.* 2001(30).

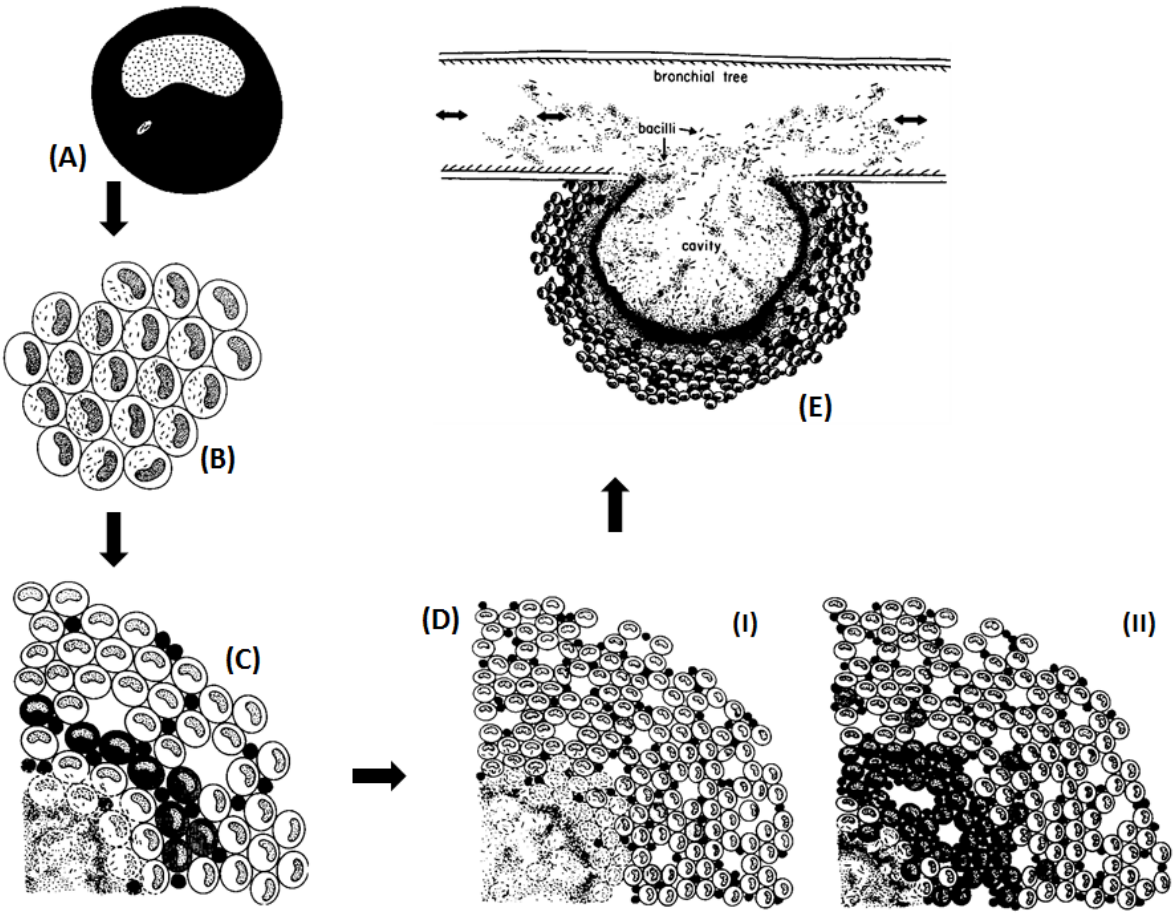

Figure 2: Tubercule development during tuberculosis disease progression

(A) Stage 1: An alveolar macrophage that has ingested and killed two bacilli in a phagocytic vacuole. The darkly shaded cytoplasm in this macrophage depicts a high degree of activation, ie. high levels of lysosomal and oxidative enzymes. Most alveolar macrophages are nonspecifically activated by the variety of inhaled particles that they ingest. An alveolar macrophage is usually able to kill an inhaled bacillus, except when the bacillus is unusually virulent or the macrophage is poorly activated. **(B**) Stage 2: An early primary pulmonary tubercle, in which bacilli have multiplied exponentially within newly arrived macrophages that have immigrated into the lesion from the bloodstream. Being nonactivated and incompetent, their cytoplasm is unshaded to depict the lack of activation. In fact, the phagocytic vacuoles in the cytoplasm of these nonactivated macrophages provide an ideal environment for mycobacterial multiplication, allowing macrophages and bacilli to exist in symbiosis. The bacilli multiply while the macrophages accumulate without harming neither host nor parasite. **(C)** Stage 3: A 3-week old tubercle comprised of a caseous necrotic center and a peripheral accumulation of partly activated macrophages (lightly shaded) and lymphocytes (small dark cells). Initial caseation occurs when the tissue-damaging DTH response to a high concentration of tuberculin-like products kills the nonactivated macrophages that have allowed the bacilli to multiply logarithmically within them. Dead and dying macrophages are depicted by fragmented cell membranes. Intact and fragmented bacilli are present, both within macrophages and within the caseum. Tubercle bacilli do not multiply in solid caseum. **(D)** Stage 4: **(I)** A 4-5 week old tubercle and its caseous center enlarging with hematogenous bacilli dissemination in immunocompromised hosts. Several partly activated macrophages are lightly shaded to indicate that these immunosuppressed hosts develop only relatively weak cell-mediated immunity (CMI). Escaping bacilli from the edge of this centre are ingested by poorly activated incompetent macrophages with intracellular environments that favour their multiplication. High concentrations of tuberculin-like products induce tissue-damaging DTH which kills these new bacilli-laden macrophages, enlarging the caseous necrotic center. This cycle may repeat multiple times, resulting in the development of metastatic lesions due to lung tissue destruction and bacilli spreading via the lymphatic and hematogenous routes to other sites. **(II)** A 4-5 week old established tubercule in healthy immunocompetent humans who show positive tuberculin reactions and yet no clinical and often no X-ray evidence of the disease. Bacilli escaping from the caseous centre are ingested by highly activated macrophages (darkly shaded) surrounding the caseum which inhibit bacilli multiplication and eventually destroy them, hence retaining a small caseous centre. Such effective macrophages were activated by T cells and their cytokines. If the caseous centre remains solid and does not liquefy, the disease will be arrested by this CMI response, leading to stabilization or regression in immunocompetent hosts. **(E)** Stage 5: Bacilli may multiply extracellularly to large numbers in liquefied caseum, which get discharged from cavities into a bronchus, thereby moving to the airways and allow the bacilli to disseminate to other parts of the lung and to the external environment. High concentrations of tuberculin-like products are produced and local tissues are destroyed, including the walls of adjacent bronchi. The large quantities of bacilli and their antigens in liquefied caseum may overwhelm a formerly effective CMI, causing progression of the disease in immunocompetent humans. Also, among such large numbers of bacilli, mutations causing antimicrobial resistance may occur. Figures reproduced with permission from reference (31) and (25).

1.3 The Mycobacterium tuberculosis complex (MTBC)

Being predominantly environmental organisms found in the soil, mycobacteria have since evolved through several transitions from the environment to pathogenicity. Several organisms, including various strains of *M. tuberculosis*, the human pathogen *M. africanum* and a clade of animal-infecting mycobacteria including *M. bovis*, have been classified as a closely related group of variants of a single species known as the *M. tuberculosis* complex (28). These are the etiological agents for both human and animal tuberculosis with pathogenicity differences amongst the various Mycobacterium species (32). The animal-adapted *M. bovis* ecotypes branch from a presumed human-adapted lineage of *M. africanum* that is currently restricted to West Africa (28). On the other hand, human-adapted Mtb strains can be grouped into several main lineages, each of which is primarily associated with distinct geographical distribution (28) (Fig.3).

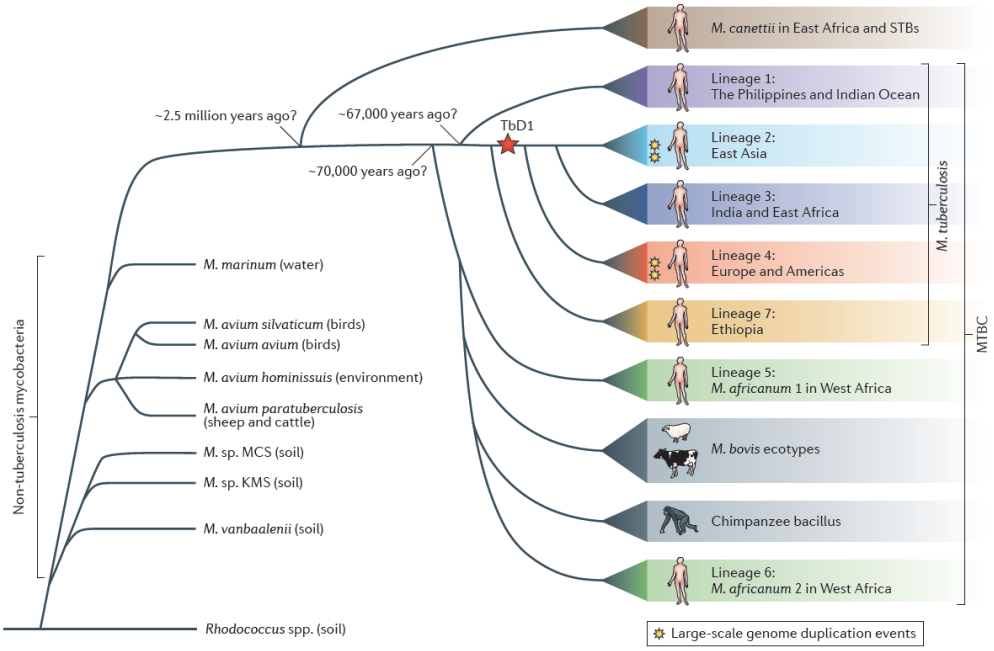

Figure 3: Evolutionary Relationship between selected mycobacteria and members of the MTBC.

The MTBC was thought to arise as a clonal expansion from a smooth tubercle bacillus (STB) progenitor population that originated from soil bacteria. Human-adapted *M. tuberculosis* strains are grouped into seven main lineages, each of which is primarily associated with distinct geographical distribution. TbD1 indicates the deletion event specific for *M. tuberculosis* lineages 2, 3 and 4. Evolutionary distances are not to scale. All species shown are from the genus *Mycobacterium.* Figure reproduced with permission from Galagan2014. (28)

1.3.1 *Mycobacterium* Microbiology

The etiological agent of tuberculosis is *M. tuberculosis,* which belongs to the *Mycobacterium* genus under the *Actinobacteria* class. Mycobacteria are best characterized by their Gram-positive thick, complex, lipid-rich, waxy cell wall which contributes to their acid-fastness. They are generally divided into two major groups, the fast growing mycobacteria eg. *M. smegmatis,* and the slow growing mycobacteria eg. *M. tuberculosis* and *M. bovis.* Members of the MTBC are non-motile, non-sporing, straight or slightly curved rods about 3 x 03µm in size. They usually appear as single or small clumps in sputum and other clinical specimens, and as twisted rope-like colonies termed *serpentine cords* (Fig. 4B) in liquid. Colonies on solid media are typically of an off-white (buff) colour with a dry breadcrumb-like appearance (Fig. 4A). The Ziehl-Neelsen (ZN) staining technique, which is a type of acid-fast stain, is the classic method used for mycobacteria visualization (Fig. 4C). However, light-emitting diode fluorescence microscopy (LED-FM), which involves fluorochrome-labelled auramine O (which has an affinity for the mycolic acid contained in the cell wall of mycobacteria) (33) has increasingly been employed due to its ease of utilization, higher sensitivity (~8-10%) and similar specificity as compared to the Ziehl-Neelsen staining for the detection of sputum smear positive TB cases (34-36) (Fig. 4D).

Although mycobacteria have been shown to be able to survive and persist in a non-replicating state under anaerobic conditions (37), they are obligate aerobes (although *M. bovis* grows better in conditions of reduced oxygen tension) that grow best at the optimal temperature of 35-37°C. These tubercle

bacilli can survive very well and for extremely long periods in either external or internal environments so long as they are not exposed to ultraviolet light due to their heat sensitivity (32).

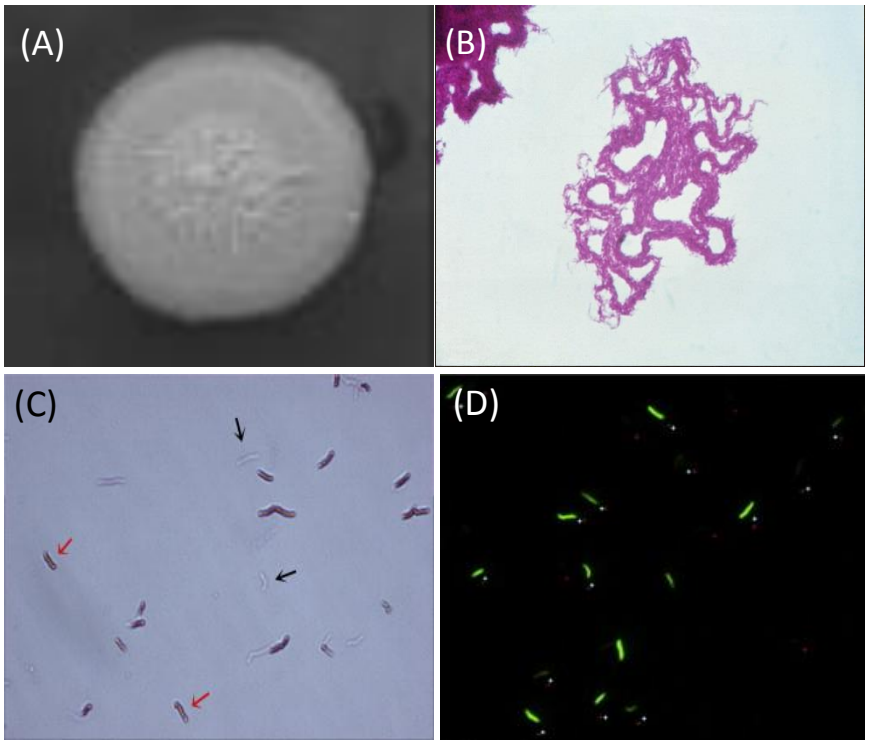

Figure 4: Visualizing *Mycobacterium tuberculosis*

(A) Mtb colony on solid media with a dry breadcrumb-like appearance.
(B) Ziehl-Neelsen stained microcolonies of Mtb showing 'serpentine cord' formation.
(C) Ziehl-Neelsen stained Mtb bacilli appear as purple rods (red arrows) viewed under phase contrast and bright field light.
(D) Auramine-Rhodamine fluorochrome stain showing Mtb bacilli rods (blue dot) viewed under fluorescent light.
Pictures reproduced with permission from (A), Vilceheze *et al.*2008 (38), (B), Wellcome Images (32), (C)&(D) Ryan *et al.* (39)

1.3.2 Avirulent *M. bovis* BCG versus *M. tuberculosis*

As one of the most widely used vaccines in the world for over 50 years, the live attenuated vaccine strain bacillus Calmette-Guérin (BCG) is an attenuated derivative of *M. bovis*, the virulent bacillus that is closely related to *M. tuberculosis* as discussed above (40). For over 50 years, BCG has been used to immunize over 3 billion people in immunization programs against tuberculosis. Although its protective efficacy against TB has been highly variable, the introduction of the BCG vaccine has been shown to reduce the overall risks of tuberculosis (41). The original BCG Pasteur Strain was developed from *M. bovis* by 230 serial passages in liquid culture with stable deletions and/or multiple mutations that eventually gave rise to an avirulent phenotype in both humans and animals, neither causing progressive disease nor pathogenic symptoms characteristic of tuberculosis (42).

Fourteen regions of differences (RD) present in the reference laboratory strain *M. tuberculosis* H37Rv have been identified to be absent from avirulent BCG, which could shed clues on chromosomal genes related to pathogenicity (43). In particular, the genetic differences between avirulent BCG and virulent *M. tuberculosis* strains could be further narrowed down to three distinct genomic regions of difference; designated RD1 to RD3. RD3 is a 9.3kb genomic segment whose role for virulence was deemed doubtful due to its absence in most clinical isolates; RD2, a 10.7kb DNA segment which was found to have been deleted after the original derivation of BCG, and most importantly, RD1. Through the re-introduction of RD1 into BCG and proteomic studies, this 9.5-kb DNA segment was shown to play a role in the

regulation of multiple genetic loci, thus attributing the loss of virulence by BCG to the deletion of this regulatory region (44). Proteome comparison between *M. tuberculosis* and BCG revealed the expression of at least 10 additional proteins and higher levels of many other unidentified proteins (44), which was accounted for by the loss of the RD1 region. These identified genetic differences could also account for the multiple physiological differences that also exist between BCG and *M. tuberculosis* (45, 46).

In light of these crucial findings, although BCG is considered to be closely related to *M. tuberculosis* and hence is commonly used in place of *M. tuberculosis* for research due to its higher safety profile, these important physiological and genetic differences should be taken into consideration when using BCG as a surrogate organism for the study of *M. tuberculosis* virulence and drug resistance.

1.3.3 Strain variants of *M. tuberculosis*: Erdman, H37Rv and CDC1551

Although all three strains belong to the same Lineage 4 (Euro-American), H37Rv and Erdman are very common laboratory strains whilst CDC1551 has been referred to as a "clinical" strain (47, 48). Several studies have shown that the laboratory-derived strains H37Rv and Erdman display distinct phenotypes both *in vitro* and *in vivo* when compared to CDC1551 (47, 48). It is indeed well known that repeated *in vitro* passages of strains may lead to genetic changes acquired during growth in culture such as the loss of PDIM, an important cell wall component associated with mycobacterial virulence, which is often documented in laboratory-derived strains (49). However, since its isolation from a clinical case, CDC1551 has also been passaged a substantial number of times *in vitro* and should be regarded nowadays more like a lab-adapted strain than a clinical isolate. Regardless, the numerous handling and *in vitro* passages of these individual strains in various labs could translate into the acquirement of stable mutations in these strains specific to each lab; and this should be noted during the comparison of whole genomes of various Mtb strains.

1.4 Mtb Virulence: Challenging the Classic Paradigm of Mtb Virulence

Over four decades of experimental work support the classical notion that the *in vivo* niche of *M. tuberculosis* is primarily the membrane-bound phagosome of macrophages, though conceding that growth in other cell types and even extracellular spaces are also important (50). Live *M. tuberculosis* was first demonstrated to exist inside phagosomes that failed to fuse with lysosomes even after 1-4 days of infection through classical electron microscopy (EM) studies (51, 52). These important findings strongly suggest that *M. tuberculosis* was able to avoid the lysosome in order to survive and replicate. Subsequent immuno-EM studies supported this discovery by revealing Mtb-containing vacuoles with uniformly surrounded membranes that contained endosome markers (51-55). Further studies have extensively investigated the mechanism of phagosome maturation arrest which was found to involve bacterial manipulation of several host molecules such as sphingosine kinase (56) and Coronin-1 (57).

However, while the conventional thought on *M. tuberculosis* virulence has generally been agreed to mainly revolve around the rather unusual ability of the bacteria to survive and replicate within the macrophage while concurrently evading the host immune system in comparison to other bacteria, there appears to be accumulating evidence to suggest that phagosome escape into the cytosol can occur during *M. tuberculosis* infection, challenging this classical paradigm. A number of EM studies have reported unusual observations of *M. tuberculosis* bacilli without visible host membranes typically after several

days of infections (58-62), and further investigations have found that the RD1-encoded ESX-1 specialized secretion system is critical for phagosome escape (58, 62). Additional studies also corroborate the notion that *M. tuberculosis* utilizes the ESX-1 pathway to gain access to the cytosol through membrane permeabilization during the early stages of infection (63-68).

Although the mechanism of virulence for *M. tuberculosis* remains poorly understood, it is almost certainly multifactorial; and in light of these unconventional findings, the role of a number of critical factors in mycobacteria virulence should certainly be revisited. These factors should include other aspects of Mtb-host interactions that have been previously reviewed such as defence against host-induced stress (69) and other mycobacterial virulence compounds or genes such as proteases (70), lipids (30, 71, 72), regulators (73), sigma factors (74), secretion systems (75, 76), etc. These virulence determinants can be widely categorized based on their function, molecular features or cellular localization into: 1, Lipid and fatty acid metabolism; 2, cell envelope proteins which include cell wall proteins, lipoproteins and secretion systems; 3, macrophage-interacting proteins; 4, protein kinases; 5, proteases; 6, metal-transporter proteins; 7, gene expression regulators including two component systems, sigma factors and other transcriptional regulators and lastly 8, other virulence proteins of unknown function, including PE and PE_PGRS families.

1.4.1 Mycobacteria Cell Wall and Structure in relation to virulence

The convoluted and distinct cell wall of *M. tuberculosis* comprises of numerous complex lipids that play dual roles as both critical structural components and virulence factors that mediate host cell interactions (77, 78). Its cell wall comprises of a standard inner membrane made up of a peptidoglycan-arabinogalactan polymer that is linked to an outer membrane-like structure termed the mycomembrane (79) (Fig. 5). Unique to mycobacteria and related actinobacteria, mycolic acids consisting of β-hydroxyl fatty acids with long α-alkyl side chains line the inner layer of the mycomembrane, covalently linked to arabinogalactan in the standard inner membrane. Besides forming structural components for the mycobacterium cell wall, mycolic acids can also be esterified to glycerol and trehalose. A large variety of non-covalently attached lipids and glycolipids including additional mycolic acids in the form of the glycolipid trehalose-6,6'-dimycolate (TDM) and a family of structurally related phthiocerol dimycoserosates (DIMs) make up the outer mycomembrane, which is eventually coated with a capsular layer of extractable glycans, lipids, and proteins (80) that form the surface of *M. tuberculosis*. The extremely hydrophobic outer surface forms a reservoir for a myriad of bacterial products that can play a role in host cell interactions. These lipids have been proposed as key mediators of the host-pathogen interaction during Mtb infection (78), affecting host cells and tissues not just through surface mediation but also subsequent immunity. Clearly, the complex and unique mycobacterial cell wall plays a critical role in Mtb virulence that necessitates further exploration.

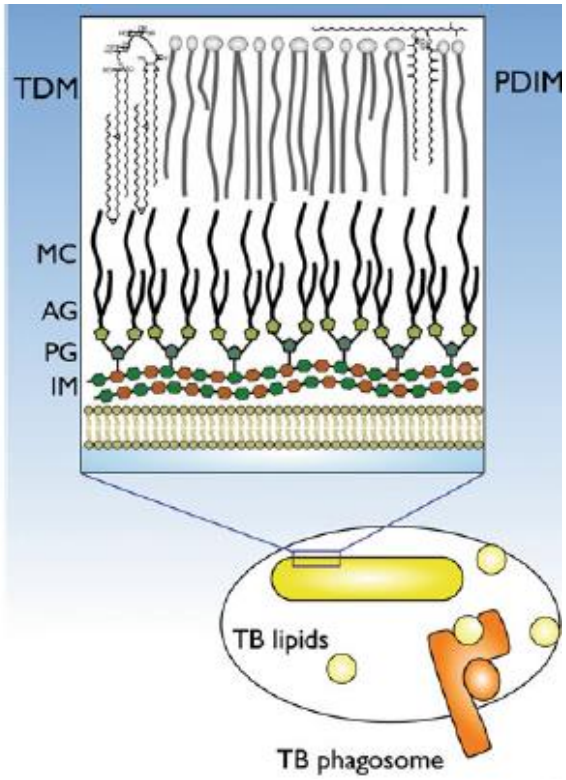

Figure 5: The *M. tuberculosis* cell wall is complex and distinct from other bacteria species.

The *M. tuberculosis* cell wall comprises of a standard inner membrane of peptidoglycan-arabinogalactan polymer that is linked to the outer mycomembrane. The outer mycomembrane is lined with an inner layer of mycolic acids and an outer layer of several lipids and glycolipids, including additional mycolic acids such as TDM and DIMs. Finally, the surface of the mycobacterium is encased with a capsular layer of glycans, lipids and proteins.
Figure adapted with permission from Stanley *et al.* 2013 (78).

1.4.2 Mycolic Acid Synthesis as a Lipid Virulence Factor in Mycobacteria

Characterized by very hydrophobic C_{54} to C_{63} fatty acids with C_{22} to C_{24}α side chains, mycolic acids are generally similar in length but are divided into three distinct structural classes based on their structure variations, having either cyclopropanation (*cis* or *trans*) or keto or methoxy groups (77, 81). α-mycolic acids remain the most abundant form (>70%), with methoxy- and keto-mycolic acids forming minor components (10-15%) (82). α-mycolic acids are *cis, cis*-dicyclopropyl fatty acids that can vary structurally in the length of the terminal alkyl group and the number of methylene groups between the cyclopropane rings and the carboxyl group. Methoxy- and keto-mycolic acids can also vary structurally with either *cis*- or *trans*-cyclopropane rings (77) to give rise to individual subspecies.

Mycobacteria utilize the two component fatty acid synthetase (FASI-FASII) system that is homologous to eukaryotic systems (83) to produce long chains of fatty acids of up to 86-95 carbon atoms in length from a hypothetical medium length fatty acid as its precursor (30) (Fig. 2). The biosynthesis of mycolic acids can be summarized into 5 distinct stages (77): 1, Fatty acid synthase-I (FAS-I) produces a C_{26} saturated straight chain fatty acid forming the α-alkyl branch of mycolic acids; 2, Fatty acid synthase-II (FAS-II) produces the C_{56} fatty acids for the formation of the meromycolate backbone; 3, Various cyclopropane synthases introduce functional groups to the meromycolate chain; 4, Generation of the mycolic acid upon the condensation reaction between the α-branch and the meromycolate chain catalysed by the polyketide synthase Pks13 and a subsequent reduction reaction by

corynebacterineae mycolate reductase A (CmrA); 5, Transfer of mycolic acids to arabinogalactan and other acceptors eg. trehalose via the antigen 85 complex.

However, despite the accumulation of knowledge in mycolic acid biosynthesis in the last 30 years, synthesis of the individual mycolic acids species remains vague and poorly understood. What is clear though, is an established link between mycolic acid metabolism and virulence; as key enzymes involved in the FASI-FASII system and subsequent mycolic acid modifications such as β-keto acyl synthetase KasB (84) and methoxy mycolic acid synthase 4 MmaA4 (85), have been identified as key players in mycobacteria virulence (Fig. 6).

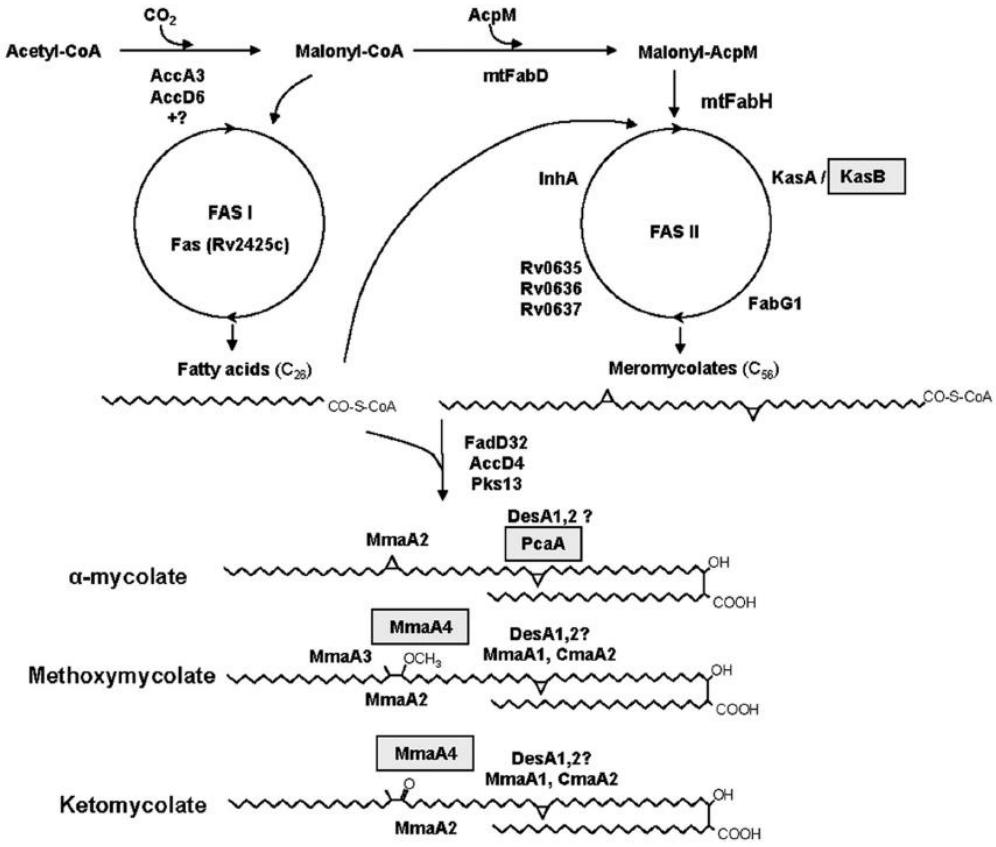

Figure 6: Biosynthesis of Mycolic Acids in Mycobacteria

A-mycolates, methoxymycolates and ketomycolates are synthesized from end products of the FAS I and FAS II pathway through a series of modifications via key enzymes. The genes highlighted in grey have been proposed as virulence factors for *M. tuberculosis*.
Figure reproduced with permission from Forrellad et al. 2013 (43)

1.5 Current and Future Anti-TB Drug Therapies

The conventional drug therapy for active TB consists of a cocktail of first-line drugs including intensive phase treatment of 2 months of isoniazid (INH), rifampicin (RIF), pyrazinamide (PZA), ethambutol (EMB) and a subsequent continuation phase treatment of 4 months of INH and RIF (21, 22), a lengthy drug regime that lasts 6-9 months. MDR-TB, on the other hand, requires an even more complicated and lengthy drug regime, including a combination of eight to ten drugs with therapies lasting up to 18-24 months; only of which four of these drugs were actually developed solely for TB treatment (86). These include the second-line drugs such as cycloserine, ethionamide (ETH), para-amino salicylic acid (PAS) and streptomycin (87-89). Over the years, numerous biochemical, genetic, crystallography studies have been conducted to identify the molecular targets and analyse the mode of actions of these drugs (90) (Table 1). Besides these, for various reasons such as ease of use, toxicity, unclear efficacy and unsuitable drug combinations, other less commonly used drugs such as isoxyl (ISO), thiacetazone (TAC), kanamycin and clofazimine also exist for the treatment of MDR and XDR-TB (87, 90). The clinical efficacies of these drugs against Mtb are further summarized in Table 2 (87).

Unique amongst other general antibiotics, several of the anti-TB drugs in use today including INH, ETH, and pyrazinamide (PZA) are pro-drugs that require activation *in situ* to an activated form for its bactericidal activity against *M. tuberculosis* (91). Of this work's interest are the classic antitubercular pro-drugs that have proven activity on the essential pathway of

mycolic acid synthesis in Mtb, namely, INH, ETH, ISO and TAC. Their respective chemical structures are depicted in Figure 7. INH is a powerful efficacious first-line drug regarded as a highly valuable weapon for the treatment of TB (92); whilst ETH remains as one of the most effective second-line drugs currently still in use for MDR-TB treatment today. Both TAC and ISO are prodrugs used in the 1970s and 1980s especially in Africa and Latin America due to their low cost. However, due to numerous life-threatening side effects such as hepatotoxicity and an unexpectedly high frequency of mutant strains arising during treatment, these drugs are commonly discontinued in the midst of treatment (93-95).

Additionally, novel anti-TB drug candidates are continually being developed amongst research and pharmaceutical communities, including several promising TB drugs that are currently under review in clinical trials (Fig.8). As of 2013, WHO reports a total of 10 new or repurposed anti-TB drugs that are currently in Phase II or Phase III clinical trials, the highest-profile drug being bedaquiline (TMC-207) (7). Although in Phase II clinical trials back then, bedaquiline underwent accelerated approval for use in the treatment of MDR-TB patients by the US Food and Drug Administration (FDA) in 2012 due to its novel mechanism of action and the potential of this drug to treat MDR-TB. Despite the constant search for novel drug candidates over the decades, bedaquiline became the first new TB drug to be approved for use in 40 years, underscoring the challenging and arduous development of the TB drug discovery pipeline. Other promising drugs under research and development for TB treatment include PA-284 (96), a novel nitroimidazole

compound and moxifloxacin (97), a wide-spectrum fluoroquinolone antibiotic, both of which are being tested as part of several potential combination regimens (98).

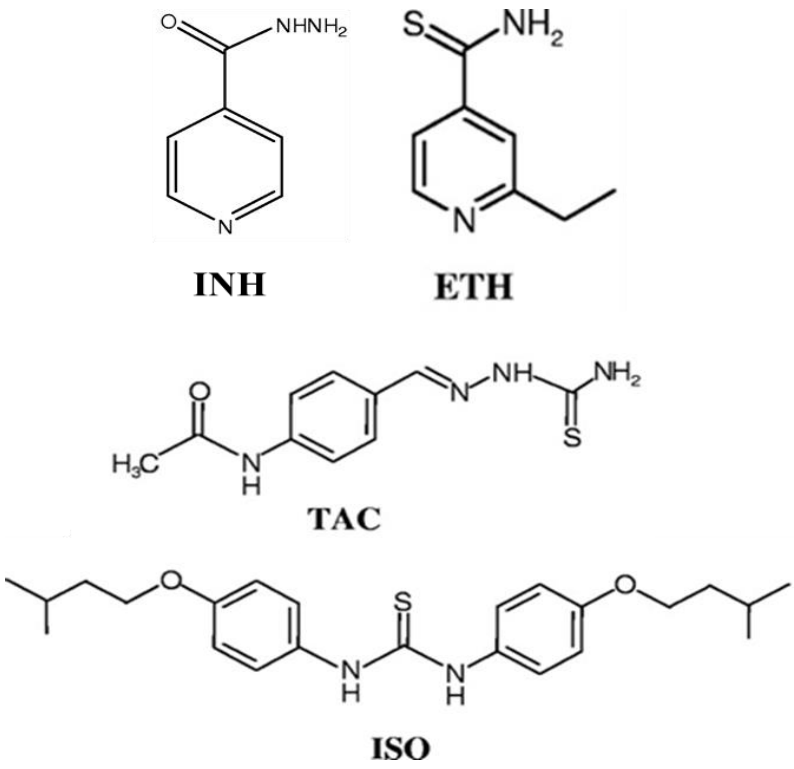

Figure 7: Structures of Drugs that inhibit Mycolic Acid Synthesis

Isoniazid (INH) is a hydrazide, while ethionamide (ETH), thiacetazone (TAC) and isoxyl (ISO) are thiocarbamide-containing drugs that inhibit mycolic acid synthesis in mycobacteria; however their individual mode of actions on mycolic acid synthesis differs.

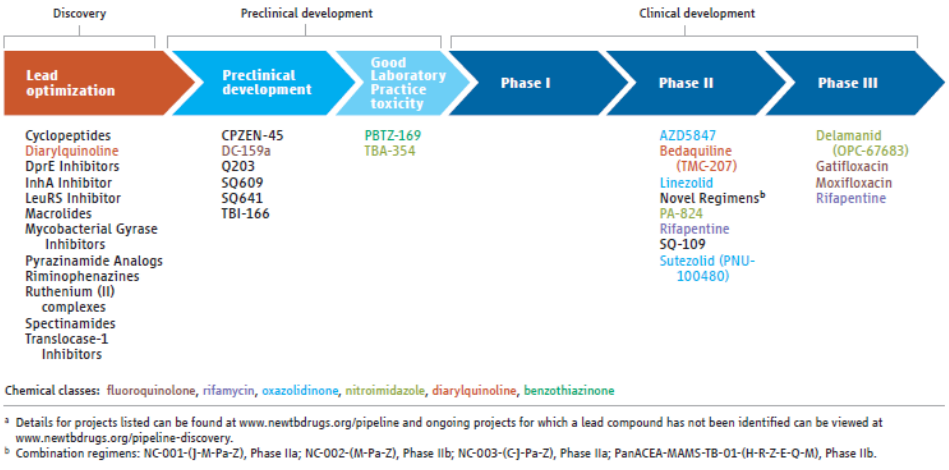

Figure 8: Developmental Pipeline for novel TB drugs as of July 2013

Figure adapted from WHO Global TB Report 2013 (7).

Drug (year of discovery)	Target	Effect
First-line drugs		
Isoniazid (1952)	Enoyl-[acyl-carrier-protein] reductase	Inhibits mycolic acid synthesis
Rifampicin (1963)	RNA polymerase, beta subunit	Inhibits transcription
Pyrazinamide (1954)	S1 component of 30S ribosomal subunit	Inhibits translation and *trans*-translation, acidifies cytoplasm
Ethambutol (1961)	Arabinosyl transferases	Inhibits arabinogalactan biosynthesis
Second-line drugs		
Para-amino salicylic acid (1948)	Dihydropteroate synthase	Inhibits folate biosynthesis
Streptomycin (1944)	S12 and 16S rRNA components of 30S ribosomal subunit	Inhibits protein synthesis
Ethionamide (1961)	Enoyl-[acyl-carrier-protein] reductase	Inhibits mycolic acid biosynthesis
Ofloxacin (1980)	DNA gyrase and DNA topoisomerase	Inhibits DNA supercoiling
Capreomycin (1963)	Interbridge B2a between 30S and 50S ribosomal subunits	Inhibits protein synthesis
Kanamycin (1957)	30S ribosomal subunit	Inhibits protein synthesis
Amikacin (1972)	30S ribosomal subunit	Inhibits protein synthesis
Cycloserine (1955)	D-alanine racemase and ligase	Inhibits peptidoglycan synthesis

Table 1: Main Tuberculosis Drugs in Clinical Use Today and the their respective mechanism of drug action and targets

Table reproduced with permission from Zumla *et al.* 2013 (90)

	Efficacy against *M tuberculosis*
Group 1: Oral first-line agents	
Isoniazid, rifampicin, pyrazinamide, ethambutol	In-vitro and in-vivo clinical data support use. Historical and clinical evidence suggests that these agents are most potent oral antituberculosis medications. Ethambutol is generally bacteriostatic, but at high doses (25 mg/kg) can be bactericidal.[24] In-vitro and in-vivo clinical data support use
Group 2: Injectables	
Streptomycin, kanamycin, amikacin, capreomycin	Bactericidal. In-vitro and in-vivo clinical data support use[25-28,29]
Group 3: Fluoroquinolones	
Ciprofloxacin, ofloxacin, levofloxacin, moxifloxacin, gatifloxacin, sparfloxacin	Bactericidal. In-vitro and in-vivo clinical data support use.[30-32] Newer agents (moxifloxacin, gatifloxacin, sparfloxacin) have lower minimum inhibitory concentrations,[33,34] but clinical importance of this feature unknown
Group 4: Bacteriostatic second-line drugs	
Ethionamide, cycloserine, P-aminosalicylic acid	Bacteriostatic. In-vitro and in-vivo clinical data support use[26-29,35-39]
Group 5: Other drugs (potentially useful agents with conflicting animal or clinical evidence or agents with unclear efficacy because of possible cross-resistance)	
Clofazimine	Bacteriostatic in vitro.[40] Conflicting animal model data. MIC90 <1·0 mg in vitro. Concentrations attainable in vivo, particularly in macrophages.[41,42] Activity in murine and guinea pig models, but no activity in rhesus monkey model[43] (between-species differences may be explained by peak serum differences)[44]
Amoxicillin/clavulanic acid	β lactams in combination with b lactamase inhibitors bactericidal in vitro.[45] Conflicting clinical data of early bactericidal activity. One report showed significant decrease in colony-forming units when used alone for 7 days[46] and suggests possible role,[47] whereas another showed no effect[48]
Clarithromycin	Although in-vitro antimycobacterial properties reported,[49,50] including increase in ability when used in combination with standard antituberculosis drugs against multidrug-resistant strains, data from animal and in vivo studies conflicting.[28,51-53] Clinical usefulness remains to be determined
Rifabutin	May be useful against some isolates of MDR-TB (resistant to rifampicin in vitro but sensitive to rifabutin). Clinical experience suggests no role in routine use in treatment of MDR-TB because of cross-resistance with rifampicin[32,54-56]
Thiacetazone	In-vivo and in-vitro evidence of bacteriostatic activity. Cross-resistance frequently seen between thiacetazone and both isoniazid and ethionamide. High rate of side-effects in HIV-1 patients; use not recommended in patients with suspected HIV-1 infection[57-59]
High-dose isoniazid	Animal model supports use. Conflicting clinical data. Cessation of INH generally recommended in confirmed MDR-TB, however high doses (16–20 mg/kg twice weekly) might have a role.[60,61] In one study, regular doses of no benefit.[61] Supporting data in a mouse model[62]

Potency of drugs decreases from top to bottom of table.

Table 2: Categorized Anti-TB drugs and their Clinical Efficacies against *M. tuberculosis*

Table reproduced with permission from Mukherjee et al. 2004 (87)

1.5.1 The Emergence of Multi-Drug Resistant, Extensively-Drug Resistant and Totally Drug-resistant TB Strains

While first-line drugs such as INH and RIF have historically been successful in the treatment of TB infections (99); today, poor compliance with prolonged regimens, in conjunction with the growing acquired immunodeficiency disease pandemic, have compounded the problem and fuelled the emergence of MDR-TB and XDR-TB (100, 101).

MDR-TB strains are defined as resistant against at least the two first-line anti-TB drugs INH and RIF (102); XDR-TB as *M. tuberculosis* strains resistant to fluoroquinolone and to any of the three injectable drugs (capreomycin, kanamycin and amikacin) in addition to INH and RIF (103); and totally-drug resistant TB (TDR-TB) as strains that are resistant to all first and second-line drug classes (ie. aminoglycosides, cyclic polypeptides, fluoroquinolones, thioamides, serine analogues, and salicylic acid derivatives) (104). Increase in drug resistance in Mtb clinical isolates has impeded the full success of tuberculosis control. An estimated 4.3% of newly and previously treated TB cases are MDR-TB, whilst XDR-TB has been associated with the rapid death of HIV-infected individuals (105, 106).

MDR-TB cases currently represent nearly 5% of the world's annual TB burden (107), and treatment inevitably necessitates the usage of second-line drugs which are less effective and often poorly tolerated with increased toxicity (108). An alarmingly increasing number of XDR-TB cases have been reported worldwide in recent years as well (109), for which neither first nor

second-line anti-TB drugs are efficient. Koul *et al.* raises the terrifying possibility of a return to a situation akin to the pre-antibiotic TB era (110).

1.5.2 Isoniazid; A Highly Efficacious First-Line Anti-TB Drug

As one of the most commonly prescribed first-line drugs for TB treatment, INH, a derivative of the vitamin nicotinamide, is a highly effective hydrazide that is inexpensive, generally well tolerated and available worldwide. By passive diffusion through the mycobacterial cell wall, INH only shows bactericidal activity on dividing bacteria, but is non-functional against mycobacteria in stationary phase or hypoxic mycobacteria (111, 112). INH bactericidal activity has been limited exclusively against mycobacteria, especially slow growing mycobacteria (113). Due to its specific and exceptional potency against Mtb, the molecular mechanism of action of INH has been the subject of intense research by scientists since its discovery in 1952 (114).

The most consensual mechanism described to date proposes the catalysis of the pro-drug INH into an active metabolite via the mycobacterial catalase peroxidase KatG to form a INH-NAD adduct (114). The formation of this adduct inhibits InhA, the NADH-dependent enoyl ACP reductase of the FASII system, resulting in the inhibition of mycolic acid synthesis, accumulation of long-chain fatty acids and finally, cell lysis (114-117) (Fig. 9). Understandably, *katG* and *inhA* mutations have been implicated in INH resistance; however several other genes including *ndh*, *msh* and *nat* have also been proposed to contribute to INH resistance. Notably, only mutations in *inhA* display dominant INH-resistance phenotypes, ie. conferring INH resistance when non-

functional mutant alleles of *inhA* replace or complement the wild type gene, whilst all other mechanisms of resistance (eg. *katG, ndh, msh* and *nat*) are recessive, whereby INH susceptibility is restored in these mutants upon introduction *in trans* of the corresponding wild type gene (114, 116). Furthermore, between 40 up to 95% of INH-resistant (INH^R) Mtb clinical isolates are associated with *katG* mutations, forming the majority of INH^R clinical Mtb isolates (118, 119). Another 8-20% INH^R clinical Mtb isolates have mutations either in the promoter of *inhA* or its open reading frame. Mutations in at least 16 other genes including *ndh, kasA, aphC*, have been implicated in INH^R clinical Mtb isolates as well, although their roles in INH resistance remains unascertained in a large proportion of these genes (119). Approximately 10-25% of INH^R strains do not contain mutations in any of the known gene targets for INH resistance, suggesting the need for further research in the mechanisms of INH resistance (119).

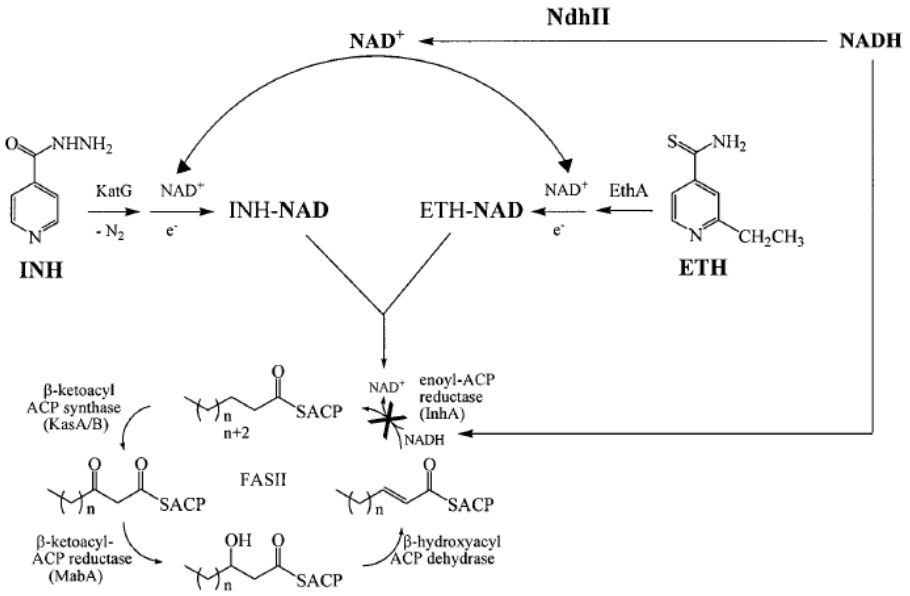

Genes with alleles that transfer resistance or susceptibility to INH or ETH upon transformation

	INH resistance	ETH resistance
katG	+	-
ethA	-	+
inhA	+	+
ndh	+	+

Figure 9: Proposed mechanism of action of INH and ETH on the FASII pathway by Vilcheze *et al.* 2005.

INH is activated by the catalase-peroxidase KatG, while ETH is activated by the monooxygenase EthA into their respective activated forms. The formations of an INH-NAD or ETH-NAD adduct with the activated forms of either drug and NAD+ inhibit the common target InhA, the NADH-dependent enoyl-ACP reductase of the FASII system. InhA inhibition results in mycolic acid biosynthesis inhibition and subsequent cell lysis. Resistance to INH or ETH is associated with gene mutations in the activators of the drugs, katG and ethA respectively. Since activated INH and ETH share a common downstream pathway, hence, co-resistance to INH and ETH is associated not just with inhA mutations, but also ndh mutations, which increase the NADH intracellular concentration and cause resistance by competitively binding InhA to inhibit drug-NAD adduct.
Figure reproduced with permission from Vilcheze *et al.* 2005 (116)

1.5.3 Ethionamide; A Highly Efficacious Second-Line Anti-TB Drug

Ethionamide (ETH) is one of the most efficient second-line drugs to date for the treatment of MDR-TB. Despite its clinical use in humans for over 40 years since its first synthesis in 1956, ETH prescription has been largely limited to patients relapsing with MDR-TB strains due to the high dosage required to achieve clinical efficacy which leads to serious hepatotoxicity, gastro-intestinal disturbances and other adverse toxicity issues (120).

As a structural analog of INH, ETH is a thioamide pro-drug that like INH, inhibits a common molecular target InhA, a NADH specific enoyl-acyl carrier protein reductase, to eventually inhibit mycolic acid synthesis (121, 122) (Fig. 9). However, while both INH and ETH exert inhibitory actions on InhA, the pathways for pro-drug activation and mode of action toward the enzyme are different (118, 123-125). This was apparent during studies conducted to investigate the resistance patterns of ETH and INH. ETH-resistant strains were still sensitive to INH, whilst INH-resistant strains showed a slight increase in sensitivity to ETH (126). Since the discovery of EthA as the mycobacterial enzyme responsible for ETH activation (124), in the past decade or so, much of the research on ETH has mainly focused on further elucidating its poorly understood mechanism of action with the penultimate aim of improving its killing efficacy. To date, whilst significant progress have been made, the full molecular mechanisms involved in ETH activation have yet to be fully characterized. Here, the 5 key major findings contributing to the understanding of ETH metabolism in *M. tuberculosis* up till today are highlighted and summarized.

1.5.3.1 The pro-drug ETH requires activation by EthA.

In 2000, through a series of genetic and transfection experiments, both DeBarber *et al*. and Baulard *et al*. teams independently reported the identification of a gene, Rv3854c, in the *M. tuberculosis* genome encoding for a protein, EthA that was found to be responsible for the activation of ETH (124, 127). Hence, it was deduced that INH and ETH are activated by two different mycobacterial enzymes, namely KatG and EthA respectively (118, 124, 127). The rarity of cross-resistance to both drugs was thus realized to be due to a higher frequency in *katG* mutations than in *inhA,* suggesting the use of ETH to be ideal for the treatment of INH-resistant TB (128). To further support these findings, resistance to ETH has been associated with mutations in *ethA* and *inhA* but not *katG* (126, 129), suggesting that ETH activation is solely dependent on EthA. Additionally, the overexpression of *ethA* in *M. smegmatis* has been shown to dramatically decrease the minimum inhibitory concentration (MIC) of ETH, suggesting that the bactericidal activity of ETH is directly correlated with its activation process by EthA (124).

In vitro and *in vivo* studies have shown that ETH activation results in the production of various intermediates and derivative metabolites (Fig. 10 & 11), among which the active major compound, ETH* has yet to be structurally identified (127, 130, 131). Hanoulle *et al*. have proposed a model for the intracellular metabolization of ETH to depend on EthA, which is a membrane associated protein, through a molecular sorting mechanism of the ETH metabolites (Fig. 11) (128). Using high resolution magic angle spinning-NMR (HR-NMR), ETH activation was studied to observe the distribution of ETH-

derived metabolites inside and outside the bacteria, while monitoring the kinetics of the drug transformation. ETH was found to be metabolized by EthA into ETH-SO and ETH*, and subsequently into ETH-OH. Only one of these three molecules, ETH*, was observed to accumulate exclusively within the bacterial cells whilst the remaining two were exclusively found in the extracellular milieu, suggesting ETH* to be the prime active compound candidate for antibiotic action. However, due to difficulties in purifying an intracellular compound, its molecular definition remains undeciphered. Vanelli *et al*. and Fraaije *et al*. have also shown that EthA is membrane associated when produced in *E. coli* and recombinant EthA is able to convert ETH to ETH-SO *in vitro*(130, 132). This suggests that EthA is a membrane-associated protein responsible for the activation of ETH into the three metabolites and subsequently, their sorting. In the absence of EthA, ETH is either quickly expelled or unable to penetrate the mycobacterial cell (128, 131).

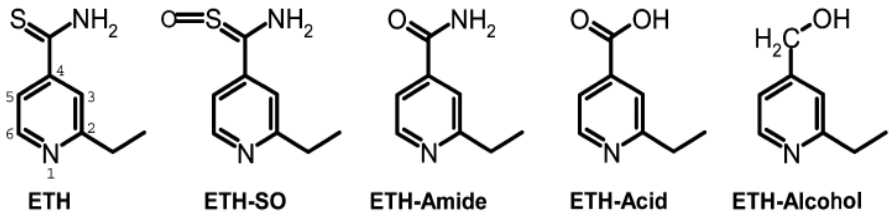

Figure 10: ETH and other proposed metabolites

From Left to Right: Ethionamide (ETH), ETH S-oxide (ETH-SO), 2-ethyl-4-amidopyridine (ETH-amide), 2-ethyl-4-carboxypyridine (ETH-acid) and2-ethyl-4-hydroxymethylpyridine (ETH-alcohol; ETH-OH)
Figure reproduced with permission from Hanoulle *et al.*(128)

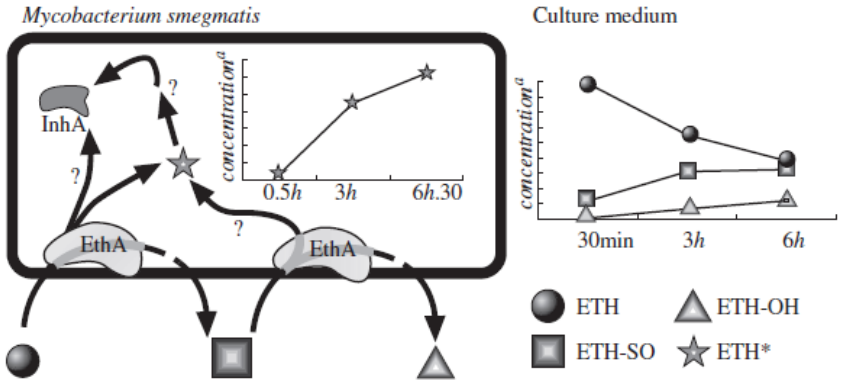

Figure 11: Model of the compartmentalized activation of ethionamide.

Ethionamide is metabolized by EthA into ETH-SO, which is subsequently transformed into ETH-OH. Both metabolites are exclusively present outside of the bacterial cell and accumulate over time (see culture medium graph). In parallel, ethionamide is metabolized into ETH*, which accumulates exclusively in the cytoplasmic compartment (see intracellular graph).
Figure reproduced with permission from Hanoulle *et al*. (128)

1.5.3.2 EthA is a Bayer-Villiger monooxygenase.

EthA belongs to the flavine adenine dinucleotide (FAD)-containing monooxygenase family and has been classified as a Bayer-Villiger monooxygenase (BVMO) (130). The single FAD group catalyses NADPH- and O_2-dependent monooxygenation of ETH to its corresponding S-oxide, ETH-SO, and is also capable of further oxidizing ETH-SO to its final cytotoxic species for the antibiotic action of ETH (130). However, while EthA has been shown to accept various ketones as substrates, the nature of its physiological substrate remains unknown. While Fraaije *et al*. have proposed a detoxifying function for EthA and other mycobacterial BVMOs (132), the physiological role of EthA in the mycobacterial cell has not been determined either. Transcriptome analysis has revealed that *ethA* expression is down regulated upon starvation (133) and upregulated under low-iron conditions (134), suggesting a role for EthA in the pathogen's virulence.

Interestingly, the analysis of ETH-resistant *M. tuberculosis* clinical isolates have revealed cross resistance to TAC and ISO, two other thiocarbamide-containing anti-TB drugs as well (127). Like ETH, TAC and ISO have been shown to target the mycolic acid biosynthesis, albeit through a different mode of action (Fig. 12). The mechanism of action of TAC remains poorly understood, while ISO as well as its derivatives are able to inhibit the synthesis of both fatty acids and mycolic acid subtypes (135). Biochemical analysis of [^{14}C] acetate-labeled cultures suggests that these three drugs inhibit mycolic acid biosynthesis via different mechanisms through binding to specific targets (91). Most importantly, Dover *et al*. have demonstrated that

EthA is a common activator of thiocarbamide-containing drugs, suggesting broad substrate specificity for this enzyme (91).

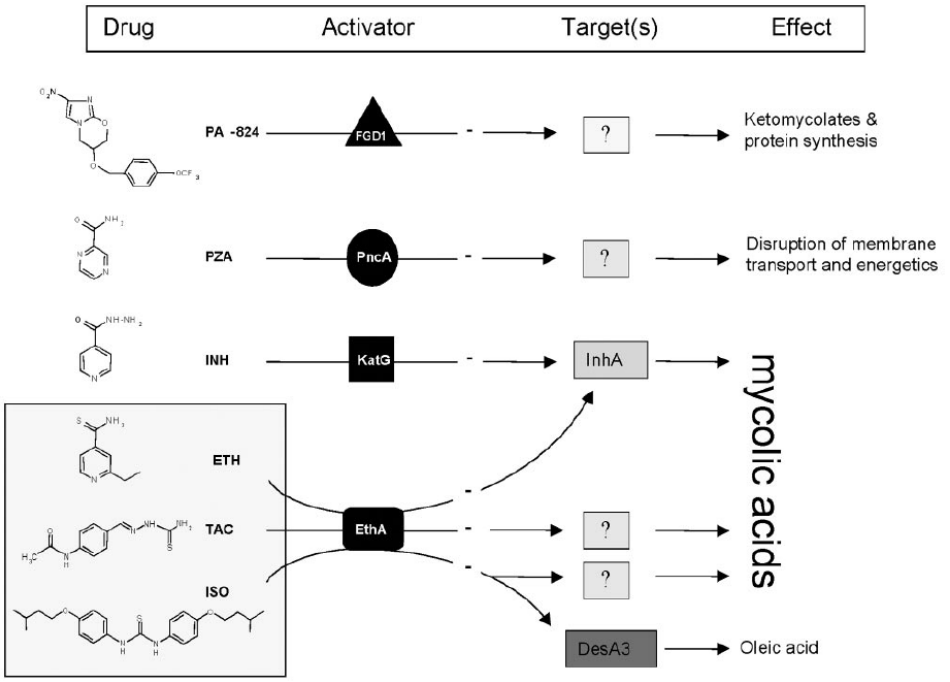

Figure 12: Summary of the activation mechanisms of isoniazid (INH), ethionamide (ETH), thiacetazone (TAC) and isoxyl (ISO) antitubercular drugs.

INH is activated by the catalase-peroxidase KatG, whilst EthA acts as a common activator for ETH, TAC and ISO to generate a range of radicals to attack multiple targets and specific targets in the cell. Once activated, ETH inhibits mycolic acid biosynthesis by targeting InhA, which is also the primary target of activated INH. In contrast, activated TAC or ISO inhibits mycolic acid biosynthesis through InhA-independent mechanisms, which remain to be determined.
Figure reproduced with permission from Dover et al.(91)

1.5.3.3 ethA expression is regulated by EthR.

Previous genetic studies have suggested that EthA production is negatively regulated by the product of the neighbouring gene *ethR* (124, 127, 136). EthR is a repressor that belongs to the TetR/CamR family of transcriptional regulators. Overexpression of *ethR* resulted in ETH resistance; yet chromosomal inactivation of *ethR* led to ETH hypersensitivity, suggesting that EthR represses *ethA* expression in *M. tuberculosis* (136). Engohang-Ndong *et al*. have established that EthR acts as a repressor of *ethA* expression through direct binding to the *ethA* upstream promoter region (136) (Fig. 13). *ethA* and *ethR* genes are divergently transcribed with their +1 transcription start separated by a putative 76-bp divergent promoter. Electrophoretic mobility shift assays indicated a direct and specific physical interaction between recombinant EthR and the *ethA-R* intergenic region (136). Surface plasmon resonance analyses suggest that EthR binds cooperatively as a homo-octamer to its operator, thus preventing RNA polymerase from interacting with both *ethA* and *ethR* promoters, effectively repressing both *ethA* and *ethR*(136). Consequently, the repression of the entire *ethA/R* locus by EthR may be responsible for the poor activation of ETH by EthA, contributing to the innate resistance of mycobacteria to this antibiotic (137). This could also be a plausible reason for the necessary high clinical dosage of ETH to achieve satisfactory killing efficacy which leads however to the adverse and intolerable side effects experienced by patients on ETH medication.

1.5.3.4 The repressor activity of EthR is negatively regulated by Serine/Threonine phosphorylation, and can be modulated by a small inhibitor molecule.

As a repressor that belongs to the TetR/CamR family of transcriptional regulators, characteristically, the regulation of its target gene(s) should be controlled by a small molecule effector able to induce a conformational change in its repressor which would result in a loss in its capacity to bind its DNA operator (138). Earlier, the X-ray crystal structure of EthR in a ligand-bound conformation (EthRHexOc) was reported and described as a homodimer with a ligand bound to each EthR monomer, the ligand subsequently being identified as hexadecyl octonoate (HexOc) (139). In the presence of HexOc, EthRHexOc is unable to bind to its target DNA and thus to repress *ethA* transcription (137). This finding strongly suggests that *ethA* gene expression is tightly regulated and involves more than one modulator.

The transcriptional repressor EthR was later identified as a specific substrate of the mycobacterial serine/threonine protein kinase (STPK) PknF. Phosphorylation of EthR by PknF negatively affected the DNA-binding activity of EthR, suggesting that EthR is negatively regulated by serine/threonine phosphorylation (140), which further affirms the role of STPK-dependent regulatory mechanisms in the bio-activation process of ETH.

Additionally, Willand *et al*. have identified synthetic inhibitors of EthR, demonstrating that one of the compounds (BDM14801) was able to actively repress EthR thereby leading to a ten-fold improvement of ETH potency against *M. tuberculosis* (141). The discovery of these EthR inhibitors with the ability to boost the antimycobacterial efficacy of ETH demonstrates the

importance for further understanding of the bio-activation mechanism of ETH which could potentially lead to improvements in the therapeutic index of ETH.

1.5.3.5 The mycothiol synthesis pathway is implicated in ETH resistance

The mycothiol synthesis pathway involves 5 enzymes, namely glycosyltransferase MshA, phosphatase MshA2, deacetylase MshB, ligase MshC and acetyltransferase MshD (142) (Fig.14). Recently, biochemical studies identified glycosyltransferase MshA and its downstream product, mycothiol, the mycobacterial analogue for glutathione to be involved in ETH bio-activation in *M. tuberculosis*. Although the mechanisms have yet to be fully deciphered, the authors observed a mycothiol-dependent increase in the rate of NADPH conversion during the activation of ETH by recombinant EthA; and noted an absence in the formation of the ETH-NAD adduct in the presence of NAD+, NADPH, recombinant EthA and mycothiol. These findings imply that mycothiol is not involved in the formation of the ETH-NAD adduct, but rather in the activation steps of ETH, hypothetically through the stabilization of ETH intermediates or its active form (142). Further studies by the same group have also illustrated that mutations in *mshA* and *mshC* genes appear to contribute to low-level resistance to INH, but were highly resistant to ETH, leading the authors to conclude that mutations in the mycothiol biosynthesis genes may contribute to INH or ETH resistance across mycobacterial species (143).

Additionally, a separate research group studied the effect on INH and ETH susceptibility upon the disruption of *mshA, mshB* and *mshC* in *M. smegmatis.*

It was observed that while the disruption of *mshA* led to both ETH and INH resistance, *mshB* disruption led to ETH resistance but retained INH sensitivity in *M. smegmatis*. Interestingly, the same authors also found that *mshC*-disrupted *M. smegmatis* mutants remained sensitive to ETH but were INH resistant. These observations led them to suggest the involvement of either mycothiol or its early intermediates in ETH bio-activation, possibly through an indirect effect of the regulation or activation of enzymes that participate in ETH bio-activation (144) .

Regardless of the slightly different drug susceptibility profiles obtained from both groups which could be highly attributed to the use of different Mycobacteria species, it is apparent that the mycothiol synthesis pathway plays a role in ETH resistance, and further studies are required to understand how this pathway can contribute to ETH bio-activation.

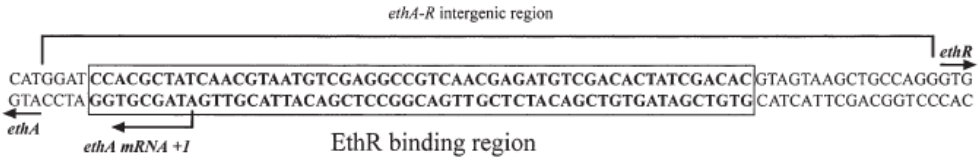

Figure 13: The *ethA/R* intergenic region forms the promoter for the *ethA/R* operon.

ethA and *ethR* are divergently transcribed in opposite directions with the *ethA/R* intergenic region acting as the common promoter for both proteins. The transcriptional regulator EthR can bind to the *ethA/R* intergenic region at the indicated EthR binding region to repress the expression of both genes.
Figure reproduced with permission from Engohang-Ndong *et al,* 2004 (136).

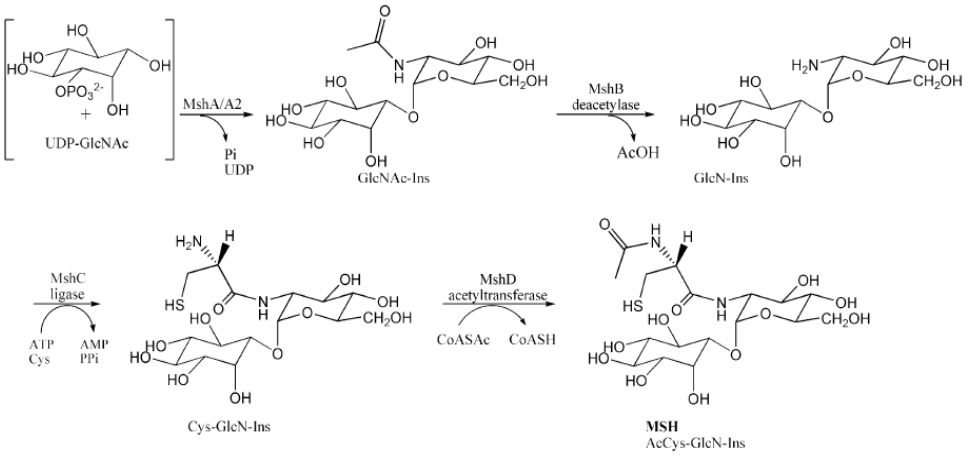

Figure 14: Mycothiol biosynthesis pathway

Mycothiol biosynthesis is first initiated by the glycosyltransferase MshA and the phosphatase MshA2 to an intermediate product, which is then deacetylated by the deacetylase MshB, followed by the addition of a cysteine group by the ligase MshC. The final product is completed by the acetylation of the cysteine amino group by the acetyltransferase MshD.
Figure adapted from Vilcheze *et al.* 2008 (38)

1.6 The role of the ethA-ethR locus in ETH bio-activation and Mycobacterium tuberculosis necessitates further exploration

The major discoveries with regards to ETH bio-activation reported in the above sections have prompted novel therapeutic perspectives for improving ETH efficacy, particularly against MDR-TB. Based on the literature reviewed in this section, a summary model for the modulation of *ethA-ethR* expression as it is understood today is depicted in Figure 15. A full understanding and deciphering of the molecular mechanisms involved in ETH activation is a pre-requisite for scientists and clinicians to be able to propose novel strategies to improve ETH potential such that the high dosage of ETH can be reduced, thereby minimizing its side effects and toxicity.

Hence, the objectives of this research thesis are outlined as follows: I) investigate the importance of the *ethA-ethR* locus in mycobacteria virulence; and II) further understand the mechanisms behind ETH drug resistance, in a bid to identify novel mechanisms to improve the killing efficacy of ETH and the eventual goal for the re-consideration of ETH and other thiocarbamide-containing drugs as first-line antibiotics against tuberculosis.

1.6.1 Analyzing the Relevance of the *ethA/R* locus in Mycobacteria Virulence (Chapter 3)

Although the *ethA-ethR* locus has been characterized as the locus involved in ETH drug activation in mycobacteria, the actual physiological role of the *ethA-ethR* locus in mycobacteria has been largely overlooked by the scientific community. To date, while most studies have focused on dissecting the role of EthA and its transcriptional repressor EthR in ETH bio-activation, few attempts have been made to understand the function and physiological role of the *ethA-ethR* locus in Mycobacterium species. The function of EthA in the mycobacterial cell has never been experimentally addressed although it was previously proposed to be involved in cell detoxification through toxic ketones removal and/or in mycolic acid metabolism (132). Since the presence of an EthA-encoding gene ortholog could be found in all of the mycobacterial genomes (124), it is anticipated that EthA serves an important and conserved function in mycobacteria. Yet, it does not appear to be essential since ETH-resistant *M. tuberculosis* clinical isolates can be found with mutations in *ethA* that likely impair its physiological function as well (127). The presence of several genes encoding BVMO-like compounds together with an abundant number of other oxidizing enzymes, such as P450 cytochromes, has led to the idea that such high oxidative potential in mycobacteria may help the pathogen resist oxidative stress *in vivo*(127). In this context, it was proposed that EthA and other BVMOs may play a role in detoxifying the bacterial cell by removing toxic ketones (132). Moreover, the importance of this factor *in vivo* during macrophage or host infection has never been reported.

Hence, the first research objective investigated the relevance for the *ethA-ethR* locus in mycobacteria virulence. This was conducted by deleting the *ethA-ethR* locus in several Mtb backgrounds to create *ethA/R* KO mutants. The phenotypes of these mutants were then characterized in a series of mammalian cell infection assays, animal work and mycolic acid analyses to further discern the role of this locus for virulence in Mtb.

The results and discussion for this research objective are presented in Chapter 3.

1.6.2 Investigation of ETH Drug Activation and Resistance Mechanisms in Mycobacteria (Chapter 4)

While it is well established that the *ethA/R* locus in mycobacteria is involved in ETH bio-activation, recent studies have shown that this paradigm is more complex than initially thought and that other factors are involved in the regulation of this genetic locus (38, 139, 140). Further understanding the regulation of the *ethA/R* locus, especially during host-pathogen infections, could reveal valuable clues in the quest for novel approaches to enhance the efficacy of ETH usage in patients. As a preliminary step to investigate whether ETH bio-activation may be influenced upon host-pathogen interactions, the killing efficacies of ETH, ISO and TAC were compared during macrophage infection and *in vitro* culture, and revealed greater killing efficacy during macrophage infection. Based on these results, gene expression studies were then conducted for both *ethA* and *ethR* to detect for differential expression levels of these genes during macrophage expression that could account for the greater killing efficacy of ETH during macrophage infection in comparison to *in vitro* culture. Additionally, the possibility of ETH bio-activation within macrophages was studied by monitoring the fate of the drug by high resolution magic angle spinning (HRMAS)-NMR to address whether macrophages have the intrinsic ability to activate ETH in the absence of mycobacteria.

The EthA/EthR system has been described to be essential for the bio-activation of ETH in mycobacteria, with EthA as the only known ETH bio-activator. However, the molecular mechanisms of ETH bio-activation by EthA remain vague, and the presence of a fairly large proportion of ETH-resistant clinical isolates with no known genes linked to ETH resistance (126)suggests

the existence of additional bio-activation factors and/or drug resistance mechanisms. Hence, the second main objective of this research thesis aimed to further dissect the mechanisms involved in ETH bio-activation, and in particular to explore whether another pathway of ETH bio-activation independent of EthA/R may exist in Mtb. ETH susceptibility in the absence of the *ethA/R* locus was thus analysed, revealing varying degrees of ETH resistance amongst various Mtb strains. Generation of ETH resistant spontaneous mutants was then employed to identify factors involved in a possible EthA/R-independent pathway of ETH bio-activation.

The results and discussion for this research objective are presented in Chapter 4.

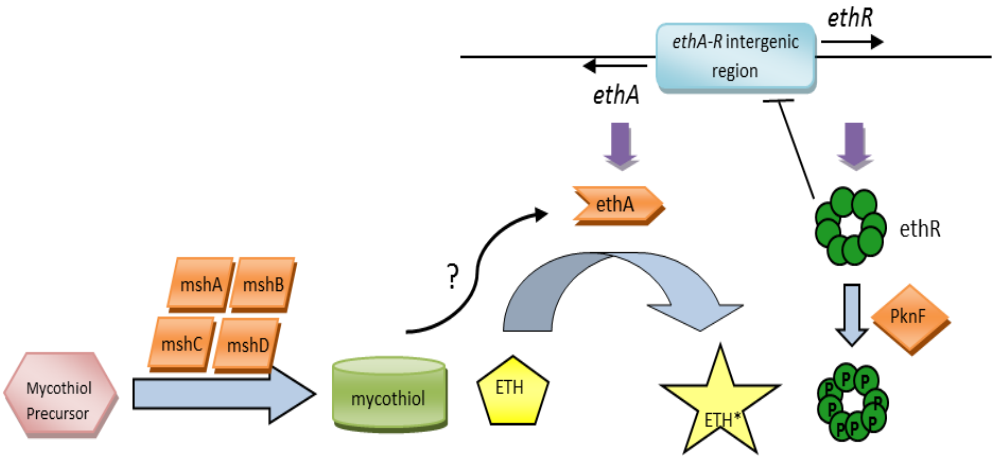

Figure 15: ETH bio-activation and the modulation of the *ethA-ethR* locus

ETH is activated by the monooxygenase EthA into its activated form, ETH*, for its antibiotic action. The expression of EthA is regulated by the transcriptional repressor EthR, and both *ethA* and *ethR* are located in the same operon with a shared intergenic promoter region. EthR dimers bind cooperatively as a homo-octamer to the specific operator in the *ethA-ethR* intergenic promoter region, repressing both *ethA* and *ethR* expression. A mycobacteria serine/threonine protein kinase (STPK) negatively regulates the physical binding of EthR to the DNA region via phosphorylation of the EthR homo-octamer, hence promoting *ethA-ethR* expression. Additionally, the mycothiol synthesis pathway and its end product, mycothiol, have been implicated in ETH bio-activation as well.

1.7 Clinical Significance of this Study

With dwindling treatment options for MDR and XDR-TB that are decades old, one of the pertinent key issues faced by the TB research community is the daunting challenge of synthesizing new anti-TB drugs. The last drug with a new mechanism of action approved for TB, rifampicin, was discovered in 1964, about four decades ago. Since then, few promising anti-TB drugs have been discovered, much less successfully entered the TB clinical pipeline (110). One of the major reasons for this limited success is our poor understanding of *M. tuberculosis* physiology and the disconnect between *in vitro* and *in vivo* behaviour of *M. tuberculosis* mycobacteria which has translated into the screening of numerous lead compounds with great *in vitro* killing efficacy but weak or no *in vivo* potency (145, 146). Both research and medical communities agree that it is of utmost urgency to identify novel anti-TB drugs that could reduce the timeframe for current anti-TB therapies and that are effective against MDR and XDR-TB. Being further hampered by the unfavourable economics of TB drug development (110), the identification and commercialization of new anti-TB drugs may however take another decade. In addition, more appropriate clinical trials to properly evaluate the efficacy of anti-TB drugs used in MDR and XDR-TB patient groups are necessary along with the improvement in TB diagnostics for a wider coverage of drug susceptibility testing (110).

While the development of new anti-TB drugs may take decades due to the various reasons listed above, improving the efficacy of existing drugs may represent an alternative strategy of choice that should not be disregarded. This

approach however necessitates further understanding in the mechanism of action of mycobacterial drugs and their bio-activation, especially drugs which have been suggested to have multiple targets and pathways, such as INH (114, 147) and ETH (126), thus increasing the exploitation potential for drug improvements. Despite ETH being one of the most effective drugs for the treatment of MDR-TB patients, due to the toxic side effects of ETH, ETH prescription is often associated with poor patient compliance which further aggravates drug-resistance in Mtb. Moreover, clinical dosage of ETH has to be limited as a consequence of its narrow therapeutic index, hence inhibiting the full killing potency of ETH upon Mtb. The recent discovery of small molecules capable of boosting ETH killing efficacy support the idea that it is possible to improve ETH treatment through dosage reduction, thus minimizing side effects and improving patient compliance (148, 149). A search for novel ETH resistance mechanisms, in particular alternative ETH bio-activation mechanisms, not only has the potential to increase the therapeutic index of ETH in a similar manner, thus improving ETH potency without increasing and perhaps even decreasing its toxic effects; but may also help improve the screening accuracy (PCR based) during drug susceptibility testing of MDR-TB strains with the introduction of additional gene candidates in the screening panel.

Chapter 2: Materials & Methods

All experiments involving live *Mycobacterium tuberculosis* were performed in a BSL3 laboratory following Standard Operating Procedures (SOPs) approved by the Institutional Bio-safety Committees (IBC) from Defence Science Organization (DSO) National Laboratories and National University of Singapore (NUS).

2.1 Microbiology

2.1.1 *E. coli* growth conditions

All *E.coli* strains were grown in Luria-Bertani (LB) broth and agar (Difco). When appropriate, hygromycin and kanamycin were added at 150 and 50 μg/ml into the medium, respectively. Chemically competent *E.coli* TOP10 strain (Invitrogen) was used for propagation of all plasmids in this study.

2.1.2 Mycobacterial Strains and Growth Conditions.

M. bovis BCG (Pasteur strain ATCC 35734), *M. tuberculosis* Erdman, H37Rv and CDC1551 and derivative strains were grown at 37°C in Middlebrook 7H9 liquid media (Difco) supplemented with ADS (0.5% bovine serum albumin-fraction V, 0.2% dextrose, 0.085% saline) unless otherwise stated; with OADC (0.5% bovine serum albumin-fraction V, 0.2% dextrose, 0.085% saline, 0.005% oleic acid and 0.0004% catalase) enrichment when necessary, or 7H11 agar, 0.05% Tween 80 (Tw) and 0.2% glycerol supplemented with OADC. Appropriate antibiotics [80μg/ml Hygromycin (Roche), 20μg/ml Kanamycin (Sigma)] were added when required.

2.2 Cell Biology

2.2.1 Cell culture

THP-1 (ATCC TIB-202), A549 (ATCC CCL-185) and Huh-7 (Health Science Research Resources Bank JCRB0403) cell lines were maintained and stored according to the ATCC guidelines. THP-1 cells were differentiated into adherent macrophages by seeding $5x10^4$ monocytes per well (in 24-well plates) with 0.04µg/ml Phorbol 12-myristate 13-acetate (PMA) (Sigma) 24-26 hours prior to infection.

To obtain murine bone marrow derived macrophages (BMMO), murine bone marrow cells were isolated from the femurs from adult BALB/c mice and differentiated into macrophages over 7 days in Dulbecco modified Eagle medium (DMEM) supplemented with 0.58g/litre L-glutamine, 1mM sodium pyruvate, 10% fetal bovine serum (FBS), 10mM HEPES, 100 units/ml penicillin-streptomycin (all reagents from Gibco), and 10ng/ml recombinant macrophage colony-stimulating factor (M-CSF) (R& D Systems). Culture media was refreshed on Day 2 and 5 post-seeding by centrifugation at 280g for 10 min at 4°C and resuspension of cell pellet in fresh complete BMMO media each time. On day 6 post-seeding, adherent BMMOs were washed once with PBS and harvested by incubating the cell layer in 1mM EDTA in PBS for 10min at 4°C, after which remaining adherent cells were gently scraped off with a plastic cell scraper (Techno Plastic Products). The cell culture dish was flushed with additional PBS, and the combined cell suspensions were then pelleted at 280g for 10min at 4°C, washed once with PBS and finally resuspended in complete BMMO media without penicillin/streptomycin to the

cell concentration required for seeding into 24- well plates ($5x10^4$ cells/well) 1 day prior to infection.

2.2.2 Ex vivo Mycobacteria Infection and Adherence Assays

Infection assays were performed by co-incubating mycobacteria and mammalian cells for 45 minutes at a multiplicity of infection (MOI) of 1 (THP-1 and BMMOs), 2 (Huh-7) and 3 (A549) in 24-well plates. At the indicated time points, the cell monolayers were washed thrice with PBS to remove extracellular bacteria and subsequently lysed with 0.1% Triton X-100 (Sigma) to release the intracellular bacteria. Appropriate dilutions of the cell lysates in 7H9 media were plated onto 7H11 for colony counting. Bacterial uptake percentages were calculated by normalizing Day 0 bacterial load to the respective inoculum, and survival percentages were calculated by expressing Day 2, 5 and 7 counts as a percentage of the initial Day 0 load. For adherence assays, 45 minutes co-incubation of mycobacteria and mammalian cells was performed at 4°C or in the presence of 10µg/ml cytochalasin D as described before (150). Monolayers were then thoroughly washed thrice with PBS to remove non-adherent bacteria, lysed with 0.1% Triton X-100, and appropriate dilutions of the cell lysates were plated onto 7H11 for colony counting.

2.3 Molecular Biology

2.3.1 Construction and Unmarking of KO mutants and complement strains

The *ethA/R* locus was deleted by double homologous recombination as described previously (151). Briefly, two primer pairs (listed in Table 3) were used to amplify the DNA regions flanking the *ethA/R* locus in *M. bovis* BCG and *M. tuberculosis* strains (Erdman, CDC1551 and H37Rv) via polymerase chain reaction (PCR). Bases in bold are extra nucleotides added for cloning convenience. The PCR-amplified regions (approximately 800bp long each) were sequenced and cloned directionally into vector pYUB854 such that the hygromycin-resistance cassette (*hyg*) lies in between the flanking regions. The *lacZ* ORF and promoter region from the pGoal17 plasmid (151) was then cloned into the unique *Pac*I site of the pYUB construct to obtain the final plasmid construct for electroporation. To prepare electrocompetent mycobacteria, mycobacteria cultures were grown to mid-log phase (0.4-0.6) in 7H9-ADS in the absence of glycerol, and re-introduced into fresh 7H9-ADS supplemented with 1.5% glycine (Sigma) 1 day prior to electroporation. On the day of electroporation, harvested mycobacteria cells were spun down and washed thrice with washing media (0.05% Tween80 and distilled water) before a final resuspension in 1ml wash media. For each electroporation, 200ml of electrocompetent mycobacteria were electroporated (2.5 kV, 800 Q, 25mF) with 2µg of recombinant plasmid and plated onto Hygromycin-containing 7H11 medium supplemented with 40µg/ml X-gal for incubation at 37°C. White hygromycin-resistant clones were selected after 16 days incubation and screened by PCR with a set of internal *ethA/R* primers, 5'-TCC

AGC GGT TTT CCG CGG TC-3'and 5'-TCC CGG TGC GCC ACA TGT TC-3'. Deletion of the *ethA/R* locus was further confirmed by Southern and Western blot analysis (see sections below).

To complement the *ethA/R* KO mutants, the 2.2kb *ethA/R* full-length locus was PCR amplified (Table 3), cloned into the multiple cloning site of the integrative vector pMV306 (42) and introduced into the genome of all *ethA/R* KO mutant constructs via electroporation as described above. The resulting transformants were plated onto Kanamycin-containing 7H11 agar and incubated at 37°C. After 16 days incubation, kanamycin-resistant colonies were PCR screened using the internal *ethA/R* primers as mentioned above.

Using the techniques described above, *ethA* KO and *mshA* KO mutants were constructed using vector pYUB854 as the backbone plasmid, whilst complement *ethR* and complement *mshA* mutants were constructed in selected Mtb strains using vector pMV306 as the backbone plasmid. Overexpressed *ethR* mutants were constructed using the multicopy replicative plasmid pMV262 (42). All modified plasmid constructs were synthesized and validated using oligonucleotides listed in Table 3.

Subsequent construction of the double *mshA/ethA/R* KO mutant was initiated by unmarking the *ethA/R* KO mutants which was necessary in order to remove the hygromycin cassette which was inserted in place of the *ethA/R* locus. To do so, the *ethA/R* KO mutants were transformed with plasmid pYUB870 which harbors a χδ-resolvase (tnpR)-encoding gene (152), thereby allowing the resolvase-mediated cleavage of the hygromycin cassette integrated at the *ethA/R* locus. Gentamicin-resistant clones were first selected

after incubation at 31°C for the resolvase activity and selected again on 7H11 containing 2% sucrose after incubation at 39°C. Loss of the hygromycin cassette and the retained deletion of the *ethA/R* locus were verified by PCR. Successfully unmarked *ethA/R* KO mutants were then used for deletion of *mshA* by classical double homologous recombination as described above, followed by complementation of *mshA* under the *hsp60* promoter (since the native promoter of *mshA* remains unknown) (Table 3).

2.3.2 Genomic DNA (gDNA) Extraction

Mycobacteria were grown to exponential phase and beyond (OD>0.6) and harvested for gDNA extraction. Cells were washed once with ultrapure water, resuspended in Buffer 1 (3% SDS, 1mM $CaCl_2$, 10mM Tris-HCl pH 8.0, 100mM NaCl and ultrapure water) and subjected to heat inactivation and cell lysis at 95°C for 20 minutes. The supernatant from the boiled cell suspension was extracted and adjusted to a final concentration of 2mM EGTA. An equal volume of phenol-chloroform-isoamyl alcohol (25:24:1) was added to extract the aqueous phase containing soluble gDNA. The separated aqueous phase was subjected to further adjustment to a final concentration of 0.3M sodium acetate and addition of 0.8 final volume of isopropanol for gDNA precipitation. The gDNA pellet was spun down at 14,000g for 15 min and washed once with 70% ethanol, dried and dissolved in TE buffer (10mM Tris-HCl pH 8.0, 0.2mM EDTA) overnight at room temperature before checking via Nanodrop2000c (Thermo-Scientific) and gel electrophoresis for visualization of gDNA.

2.3.3 Southern blot analysis

1-3 µg of gDNA was digested with *Sac*I (Promega), separated on a 1.5% agarose gel and treated as previously reported (153). DNA was transferred onto a Millipore Immobilon-Ny+ Transfer membrane and UV cross-linked. For detection of *ethA/R* and *ethA* KO mutants, a 415 bp DIG-labeled probe was amplified using a set of primers that binds approximately 1.5kb downstream of *ethR*, 5'-TGA GTT TAG TTG GGA CCT AGG CC -3'and 5'-CTA GAG TCA CAT CAG AAA CAT TTG A -3'. For detection of *mshA* and double *mshA/ethA/R* KO mutants, a 600 bp DIG-labeled probe was amplified using a set of primers that binds just upstream of *mshA*, 5'-CCC GTC CAC TCT GAA ATG CTC G -3'and 5'- ATC AAC CCT GAA CCG TCA TCG TGT -3'. Probe amplifications were done via PCR according to the manufacturer's instructions (DIG-labeling kit, Roche). Hybridization and signal detection were performed using a detection kit (Roche) according to the manufacturer's protocols. EasyHyb (Roche) was used as the prehybridization and hybridization solutions, and CSPD (Roche) was used as the detection substrate for chemical luminescence.

Plasmid	Sequence	RE used
pYUB-*ethA/R*KO		
FP1	5'-**TT** CTC GAG GTC CTG GCA TGA TGG GAC CG-3'	*XhoI*
RP1	5' **TT** AAG CTT GAC ATC CGG CTC ATC CGG C-3'	*HindIII*
FP2	5'-**TT** CTT AAG GTG CCG GAA GCC CGC GTG-3'	*AfIII*
RP2	5'-**TT** TCT AGA GGC CGC GAG CCG GAC CTG-3'	*XbaI*
pYUB-*ethA*KO		
FP1	5'- **TT**TTA ATT AAA CCC CCG ACC GAG TGC G-3'	*PacI*
RP1	5'- **TT**TCT AGA CAC GAT GAC AAC GTC GAG GT-3'	*XbaI*
FP2	5'- **TT**AAG CTT GAC GAG GGT CTG CGG TTC-3'	*HindIII*
RP2	5'- **TT**CTC GAG GTC AGT TTG CAG CAG CGG AT-3'	*XhoI*
pMV306-*ethA/R*		
FP	5'- **TT**TCT AGA GGC GCT AAA CCG TCG CTA AA-3'	*XbaI*
RP	5'- **TT**AAG CTT GAC CGA GCA CCC CCT ACC-3'	*HindIII*
pMV306-*ethA*		
FP	5'- **TT**TCT AGA GGC GCT AAA CCG TCG CTA AA-3'	*XbaI*
RP	5'- **TT** AAG CTT CC CCT AGG CAG CGA AGC-3'	*HindIII*
pMV306-*ethR*		
FP	5'- **TT** TCT AGA TAA TGT CGA GGC CGT CAA-3'	*XbaI*
RP	5'- **TT** AAG CTT GAC CGA GCA CCC CCT ACC-3'	*HindIII*
pMV262-*ethR*		
FP	5'- **TT** GGA TCC TAG TAA GCT GCC AGG GTG ACC-3'	*BamHI*
RP	5'- **TT** GTC GAC CGA GTG CGG CTT AGC GGT TCT-3'	*SalI*
pYUB-*mshA* KO		
FP1	5'- **TT**TTA ATT AAT GGT GGT GCA GTC GAC AGT G-3'	*PacI*
RP1	5'- **TT**TCT AGA GAT CAA CCC TGA ACC GTC ATC-3'	*XbaI*
FP2	5'- **TT**AAG CTT CTG GTA GCG GTG GGC AAG C-3'	*HindIII*
RP2	5'- **TT**CTC GAG TGT GAT CGC GAA TTT CTG AGT C-3'	*XhoI*
pMV306-*mshA*		
FP	5'- **TT**GGA TCC GCA AGG ATG GCA GGT GTG CG-3'	*BamHI*
RP	5'- **TT**GTC GAC GGT CGG CAA GGA GGA AGT CA-3'	*SalI*

Table 3: Oligonucleotides used during plasmid construction for gene deletion and complementation of mutants

FP: Forward primer; RP: Reverse primer. RE: Restriction Enzyme. RE sites in primer sequences are underlined.

2.3.4 Quantification of gene expression levels of selected Mtb genes

Real-time PCR (RT-PCR) was performed to analyse the mRNA levels of selected Mtb genes as previously reported(154). Briefly, Qiagen RNeasy Mini kit was employed according to the manufacturer's protocols to extract RNA from log-phase Mtb cultures or Mtb-infected THP-1 macrophages at indicated time points post-infection. 0.01-10 µg of DNase-I-treated RNA suspensions was reverse-transcribed to cDNA using an iScript cDNA synthesis kit (Biorad). Real time-PCR reactions were set up with iTaq SYBR Green Supermix with Rox (Biorad) utilizing designed primer sets as listed in Table 4. All listed primer sets were designed with either Primer Express 3.0 (Applied Biosystems) or Primer-Blast and pre-optimized for primer efficiencies ranging between 80-120%. Quantitation of the fluorescent-labeled PCR products were monitored over time employing the ABI PRISM 7000 SDS (Applied Biosystems) with a temperature cycling profile as follows: 2 min at 50˚C, 10 min at 95˚C and 59-61˚C (depending on primer sets) at 1 min for 40 cycles. At the end of each experiment, the final PCR mixes were ran on a 1.5% gel and the dissociation curve was analysed to confirm product specificity. The expression levels of each gene in all strains were then normalized to a housekeeping gene, either *sigA* or *16sRNA*, and compared to a specified reference strain for relative quantification. In all real time-PCR experiments, no template controls (NTC) and no reverse transcriptase controls (NRT) were included to check for the formation of any primer-dimers and exclude any genomic DNA contamination respectively.

H37Rv Locus	Gene name	Direction	Sequence
16S rRNA		FP	5'-GCA CCG GCC AAC TAC GTG-3'
		RP	5'-GAA CAA CGC GAC AAA CCA CC-3'
Rv2703	*sigA*	FP	5'-AGC TAG CCA AGC GGA TCG A-3'
		RP	5'-GCT AGC GAA ACC ACC AGG C-3'
Rv3854c	*ethA*	FP	5'-GTA CAC GCT AGG TTT CCG ATT
		RP	5'-GTA GTA GCC GCT GCA CAG AAA
Rv3855	*ethR*	FP	5'-CGA GGC CGA CGT TCT ACT TAT-
		RP	5'-GCG ACT TCG ACA CTG GTT GC-3'
Rv1393c		FP	5'-CCG GCT TCC ACA ACA CCT A-3'
		RP	5'-GTC TAG CAC CTT GAA GCC G-3'
Rv3049c		FP	5'-CCA CCG GCT TCC ACG TCA-3'
		RP	5'-CGA TCG CAT CGG CCA CGT-3'
Rv0892		FP	5'-CGT GTG TCG CGC CAG CTT-3'
		RP	5'-TGG CAA GCA CGA TGA CGT C-3'
Rv3083		FP	5'-CCA CCG GCT TCC ACG TCA-3'
		RP	5'-CGA TCG CAT CGG CCA CGT-3'
Rv0565c		FP	5'-ACG ACA TCG AAA CCC ACT TC-3'
		RP	5'-GAT AAT GTC CGC ATC GAG GT-3'
Rv0486	*mshA*	FP	5'-ACG AAT CGA CGT GGT CCA TCC-
		RP	5'-ACA ATG TCG GGT GCC TTC AGC-

Table 4: Sequences of Primer sets employed in RT-PCR assays

FP: Forward primer; RP: Reverse primer

2.3.5 Isolation of ETH-resistant spontaneous mutants

To generate spontaneous ETH^R clones from the Erdman *ethA/R* KO mutant, a protocol was adapted from both Luria and Delbruck (155) and Mathys et al. (156). Since the Erdman *ethA/R* KO mutants were lowly resistant (2-fold MIC increase in comparison to WT) to ETH, optimization was required to select appropriate ETH concentrations for the generation of spontaneous ETH^{Rhi} mutants in order to minimize background growth ie. clones that lowly resistant to ETH and where no spontaneous mutation has occurred. To do so, 10^8 and 10^7 bacteria directly obtained from a glycerol stock of Erdman *ethA/R* KO mutant strain were plated on 7H11-OADC full plates covering a range of ETH concentrations (40, 50, 60, 70, 80, 90µg/ml). CFU counts were enumerated from these plates to decide on appropriate ETH concentrations for the isolation of spontaneous ETH^R mutants. The results indicate that whether 10^7 or 10^8 bacteria was plated, high CFU counts (~200) were obtained at 40µg/ml, followed by a drastic drop in CFU counts (~20-80) with 50µg/ml ETH (Fig. 16). Following which, since CFU counts did not vary much over the range of 50-90µg/ml ETH and gave relatively low and countable CFU counts over these concentrations, 60, 70 and 80 µg/ml ETH were selected as appropriate ETH concentrations to maximize the number of truly spontaneous ETH^{Rhi} mutants.

To generate spontaneous ETH^{Rhi} mutants, an exponential phase 7H9-ADS liquid culture (OD600nm of 0.6-0.8) of the *ethA/R* KO mutant was used to inoculate 3 individual flasks of 7H9-ADS medium at an initial OD600 of 0.005-0.01. The cultures were incubated for 1-2 weeks and the OD600 noted. An estimated 10^8 and 10^7 bacteria were then plated onto 7H11 plates

containing selected ETH concentrations of 60-80µg/ml. ETH^{Rhi} colonies which could be sub-cultured were grown for gDNA extraction and also stored as glycerol stocks. The MIC and MBC of ETH were determined for these clones as described in Section 2.1.2, and extracted gDNA were sent for full genome sequencing at the Genome Institute of Singapore.

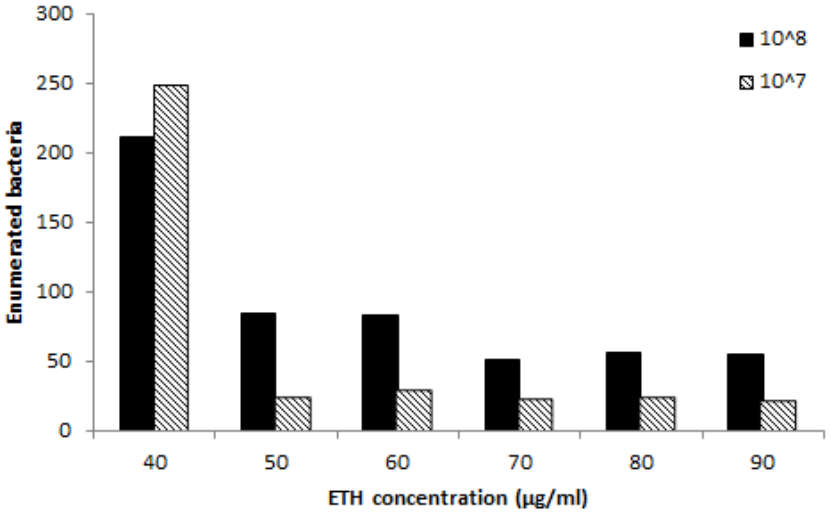

	ETH (µg/ml)					
Amount of Bacteria Plated	**40**	**50**	**60**	**70**	**80**	**90**
10^8	212	85	83	52	56	55
10^7	248	23	28	21	23	20

Figure 16: Amount of Bacteria Enumerated after plating Erdman *ethA/R* KO mutant at various ETH concentrations

10^7 or 10^8 bacteria from glycerol stock of *M. tuberculosis* Erdman *ethA/R* KO mutant were plated on 7H11-OADC full plates with various ETH concentrations (40, 50, 60, 70, 80, 90 µg/ml) and enumerated for CFU counts 16 days after incubation at 37°C.

2.4 Biochemistry

2.4.1 Western blot analysis

Mycobacteria grown to log-phase cultures were spun down and resuspended in ultrapure water, heat-inactivated at 95°C and passed through a 27g syringe needle 8-10 times to shear chromosomal DNA. Protein concentration was measured using Quick Start™ Bradford Protein Assay via a spectrophotometer. Protein sample buffer (8% sodium dodecyl sulfate [SDS], 20% β-mercaptoethanol, 20% glycerol, 0.04% bromophenol blue) was added to whole cell bacterial lysates. Lysates were subjected to SDS-PAGE with 12% polyacrylamide gels and electro-transferred onto polyvinylidene difluoride (PVDF) membranes via an Owl™ HEP Series Semidry Electroblotting system (Thermo Scientific) at 45mA for 2 hours. Blocking and incubation with antibodies were performed using 5% non-fat dry milk (Biorad) and 0.1% Tween 20 in Tris-buffered saline. Immunoblot was performed using primary rabbit polyclonal antibodies (diluted at 1:500) raised against an EthA epitope (GenicBio) and horseradish peroxidase (HRP)-conjugated goat anti-rabbit secondary antibodies (diluted at 1:2500) (Sigma). Detection was performed by enhanced chemiluminescence (ECL). Molecular sizes were determined using pre-stained molecular weight marker SDS-7B (Sigma).

2.4.2 Analysis of total, extractable and cell wall bound lipids.

Total lipid extraction from bacterial cells and preparation of fatty acid and mycolic acid methyl esters from extractable lipids and delipidated cells followed earlier procedures (157, 158). Briefly, selected mycobacteria strains were grown at 37°C in 7H9 media supplemented with ADS, 0.2% glycerol

and 0.05% Tyloxapol (Sigma) for 20 days, harvested, washed twice with ultrapure water (Gibco), resuspended in chloroform: methanol (2:1, v/v) and incubated at 4°C overnight to allow inactivation of the cells. The whole mixture was subsequently dried and subjected to a series of extractions with $CHCl_3$:CH_3OH (1:2) and two times with $CHCl_3$:CH_3OH (2:1). Each extraction was performed overnight at room temperature. The extracts obtained by centrifugation of the mixture at 1800 x g were collected, combined, dried and subjected to biphasic Folch wash as described previously (159). The upper phase was removed and discarded and the bottom phase was dried under a stream of N_2 and dissolved in $CHCl_3$:CH_3OH (2:1) in the ratio of 100µl of the solvent per 300 mg wet weight. Thin layer chromatography (TLC) of the lipid extracts was performed on silica gel plates (Merck) in different solvent systems [$CHCl_3$/CH_3OH/H_2O (20:4:0.5); $CHCl_3$/CH_3OH/NH_4OH/H_2O (65:25:0.5:4); n-hexane:ethylacetate (95:5)] to reveal total lipid species profiles. For further MAME analysis, MAMEs prepared from whole cells, extractable lipids and delipidated cells were ran in three different solvent systems [n-hexane:ethylacetate (95:5); petroleum ether: acetone (90:10); dichloromethane] using silver(Ag)-impregnated plates to reveal additional types of MAMEs. Lipids were visualized by spraying with cupric sulfate (10% in 8% phosphoric acid solution) or α-naphthol (0.5% α-naphthol in 5% sulfuric acid in ethanol) and heating.

2.4.3 Mass Spectrometry for Mycolic Acid Lipid Analysis

Mycobacterial cells grown in 7H9-ADS at mid-log phase were harvested in Teflon-fluorinated ethylene propylene tubes (Nalgene, Rochester, NY) and total lipids were extracted as described previously (160). Briefly, cell pellets

were resuspended in chloroform:methanol (2:1, v/v), incubated overnight at 4°C under constant shaking at 200 rpm and separated into organic and aqueous phases by adding deionized water. The white intermediate layer ("delipidated cells") was used for subsequent alkaline hydrolysis. To release esterified MAs from the cell wall, the defatted cells resulting from chloroform-methanol extraction were washed once with deionized water and dried. For alkaline hydrolysis, 1 ml of 1 M KOH/methanol was added for 2 h at 80°C at 600 rpm and resulting extracts were cooled to room temperature before acidification to pH 4.5 with HCl. Liberated MAs were extracted twice with 1 ml of diethyl ether. The ether phase were washed once with deionized water and dried. Samples were analyzed via a Q trap 4000 mass spectrometer as described previously (160).

2.5 Drug Assays

2.5.1 In vitro Drug Susceptibility Assays

Bacterial drug susceptibility assays were performed in 7H9 media supplemented with either ADS or OADC as reported previously (161). ETH (Sigma), ISO (NITD) and TAC (NITD) were dissolved in 90% DMSO, whilst INH (Sigma) was dissolved in ultrapure water for stock solutions. Using a broth microdilution method, 96-well flat bottom clear plates were prepared with twofold serially diluted concentrations of INH and ETH (0.02-5µM and 0.3-80µM respectively), one drug per row, and the last row filled with 7H9 media only to serve as drug-free control. BCG or Mt cultures were cultured up to log-phase and diluted in 7H9-ADS medium to obtain an optical density at 600nm (OD600) of 0.04. 100µl of this prepared inoculum were added to each test well containing an equal volume of drug containing 7H9 broth, bringing the final inoculum density to ~1 x 10^5 cfu/ml. The plates were then sealed in an air-tight box on water-soaked paper towels for 5-7 days at 37°C. On the 5^{th} day, OD600 values were recorded using a Biorad iMark Microplate absorbance reader, and minimum inhibition concentration curves were graphed using Graphpad PRISM to determine MIC values. The MIC50 in this study is defined as the lowest concentration of drug that is required to inhibit 50% growth of the specified strain in drug-free 7H9 media. Drug assays were performed thrice independently to confirm MIC values. After determining MIC50 values, 50µl of 1x MIC, 2x and 4x MIC from the assay plates were plated on 7H11 agar plates to determine minimum bactericidal concentration (MBC90) values when indicated. Plates were incubated at 37˚C for 2-3 weeks

before colony forming unit (CFU) enumeration. The MBC_{90} range (in μM) was defined as the range of drug concentrations within which the number of CFUs compared to the drug free control was reduced by 90% (1 log reduction).

2.5.2 Ex vivo Drug Susceptibility Assays

Infection assays were performed by co-incubating mycobacteria and THP-1 cells (see Section 1.2.1 for cell culture conditions) for 1 hour at MOI 1. At the end of 1 hour incubation, mycobacteria were removed and cell monolayers were washed thrice with PBS to remove any extracellular bacteria. The post-infected cells were then treated with various drug media of selected concentrations for 5 days, with media change to freshly prepared drug-containing media on Day 3 post-infection for cell maintenance. At Day 5, macrophages were harvested by washing each well twice with PBS and subsequent lysis with 0.1% Triton X-100 (Sigma) to release the intracellular bacteria. Appropriate dilutions of the cell lysates in 7H9 media were plated onto 7H11 for colony counting.

2.6 Animal Work

2.6.1 Mouse Infection

All animal experiments were carried out upon approval and under the guidelines of the Institutional Animal Care and Use Committee, National University of Singapore. Six- to eight-week-old female BALB/c mice were kept under specific-pathogen-free conditions in individual ventilated cages. For intranasal and intratracheal infections, sedated mice were either intranasally instilled with 5×10^6 CFUs of BCG or intratracheally administered with 500 cfu of CDC1551 in 20µl sterile phosphate-buffered saline (PBS) supplemented with 0.05% Tween 80 (PBST) (Sigma). Intravenous infection was performed retro-orbitally with 5×10^6 CFUs of BCG in 200µl sterile PBST. At the indicated times, 4 mice per group were euthanized, and individual lungs, spleens and livers were harvested and homogenized. Appropriate dilutions were plated onto 7H11 for colony counting.

2.7 Statistical Analysis

Unless otherwise stated, in the figures, bars represent means + standard deviations (SD) and averages were compared using a bidirectional unpaired Student ***t*** test with a 5% significance level (*, $\boldsymbol{P} \leq 0.05$).

Chapter 3: The role of the *ethA/R* locus in Mtb virulence

3.1 Construction, complementation and validation of ethA/R KO mutants in BCG, Erdman, H37Rv and CDC1551

The entire *ethA-ethR (ethA/R)* locus was deleted in several *Mycobacterium* wild type (WT) strains including *M. bovis* BCG (BCG), *M. tuberculosis* Erdman (Erdman), *M. tuberculosis* H37Rv (H37Rv) and *M. tuberculosis* CDC1551 (CDC1551) by double homologous recombination (Fig. 17A). Deletion of the *ethA/R* locus was verified by Southern blot (Fig. 17B) and Western blot analysis using an anti-EthA polyclonal immune serum (Fig. 17C). Complemented strains were also constructed by re-introducing the *ethA/R* locus back into the genome of the *ethA/R* KO mutants using the integrative plasmid pMV306 (162). Similar *in vitro* growth kinetic profiles in liquid culture medium were observed with both the parental, complemented and *ethA/R* KO mutant strains (Fig. 18) indicating that deletion of the *ethA/R* locus did not impair the general fitness of the mycobacteria during standard *in vitro* culture conditions.

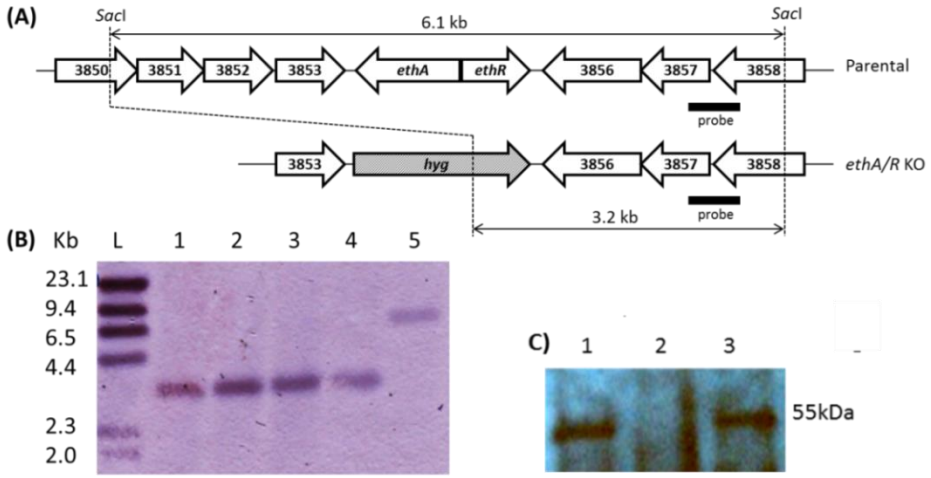

Figure 17: Construction of ethA/R KO mutants in BCG, MTB Erdman, H37Rv and CDC1551

A) Chromosomal organization of *ethA/R* was identical amongst all mutant strains. The arrows depict the lengths and directions of *ethA*, *ethR* and their neighbouring genes. Black bar corresponds to the probe used for Southern Blot analysis. B) Southern Blot analysis of chromosomal DNA. L, DNA Molecular Ladder; 1, BCG ethA/R KO; 2, MTB Erdman ethA/R KO; 3, MTB H37Rv ethA/R KO; 4, MTB CDC1551 ethA/R KO ; 5, BCG WT. C) Western Blot analysis of BCG whole cell lysate with anti-EthA polyclonal antibodies. 1, BCG WT; 2, BCG *ethA/R* KO; 3, BCG *ethA/R* KO complemented strain.

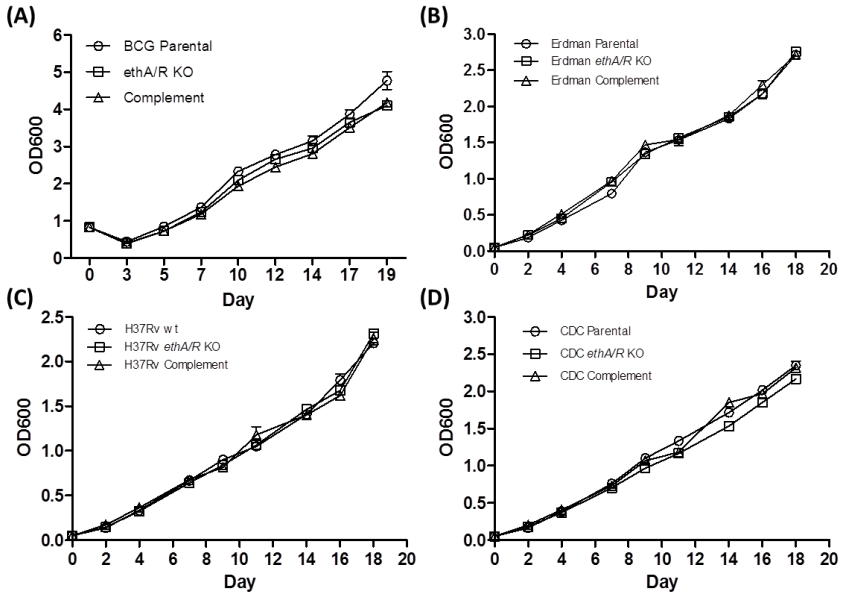

Figure 18: Growth kinetics of WT, KO and complemented strains in 7H11 medium

Growth Kinetics of A) *M. bovis* BCG, B) *M. tuberculosis* Erdman, C) H37Rv and D) CDC1551parental, *ethA/R* KO and Complement strains in 7H9 media over a period of 19-20 days. After precultures were adjusted to the same starting OD600, strains were grown in 7H9 at 37˚C over a period of 19 days. Every 2-3 days, the OD was taken to determine the growth of each strain.

3.2 M. bovis BCG ethA/R KO strain displays increased virulence in the mouse model.

To study the role of the *ethA/R* locus during infection, the infection profiles of the BCG *ethA/R* KO mutant and its parental and complemented counterparts were monitored in the mouse model. Upon nasal administration of comparable inoculums of each strain (data not shown), the bacterial load in the lungs, spleen and liver from infected animals was monitored over time. Comparable counts were obtained in the lungs at day 1 p.i. (Fig. 19A). In contrast, at day 10, 21, 35 and 56 p.i. the number of colonies recovered from the animals infected with the *ethA/R* KO strain was several orders of magnitude higher in all the organs examined when compared to the number of colonies obtained in mice infected with the parental and complemented strains (Fig. 19A-C). The difference in bacterial load between the parental and mutant strains was particularly striking in the liver where only the *ethA/R* KO mutant strain could establish infection and multiply transiently (Fig. 19C). Thus, the infection profiles obtained upon nasal infection indicate that absence of the *ethA/R* locus in BCG leads to a more virulent phenotype *in vivo*.

The enhanced virulent phenotype seen with the BCG *ethA/R* KO mutant upon nasal administration could be attributed to either enhanced colonization/persistence ability and/or increased ability of the bacteria to disseminate from the lungs to other systemic organs. To test both hypotheses, infection was performed via the intravenous route thereby bypassing the extrapulmonary dissemination step. Although less pronounced than for the nasal route of infection, generally, significantly higher bacterial loads were

again recovered from the BCG *ethA/R* KO-infected mice in comparison to mice infected with BCG WT and complemented strains (Fig. 19D-F).

Notably, intravenously-infected animals had similar mycobacterial loads in the lung, liver and spleen due to the absence of extrapulmonary dissemination (Fig. 19D, E, F). This led to the recovery of significantly higher bacterial loads from the liver of intravenously-inoculated mice with WT and complemented strains in contrast to intranasally-inoculated mice with the same strains. Besides this observation being attributed to the route of dissemination for infection, it has also previously been shown that differences in immune response following intravenous infection versus intranasal/intratracheal infections may add to differences in mycobacterial clearance from various extrapulmonary organs (163).

Together, these results thus indicate that the *ethA/R* KO BCG mutant strain displays intrinsic increased ability to persist in the murine organs compared to the WT strain. This suggests that while the *ethA/R* locus is not critical at the initial stage of infection (day 1 p.i.) for BCG, it may play a modulatory role in the mycobacterial colonization and persistence in the lungs, spleen and liver.

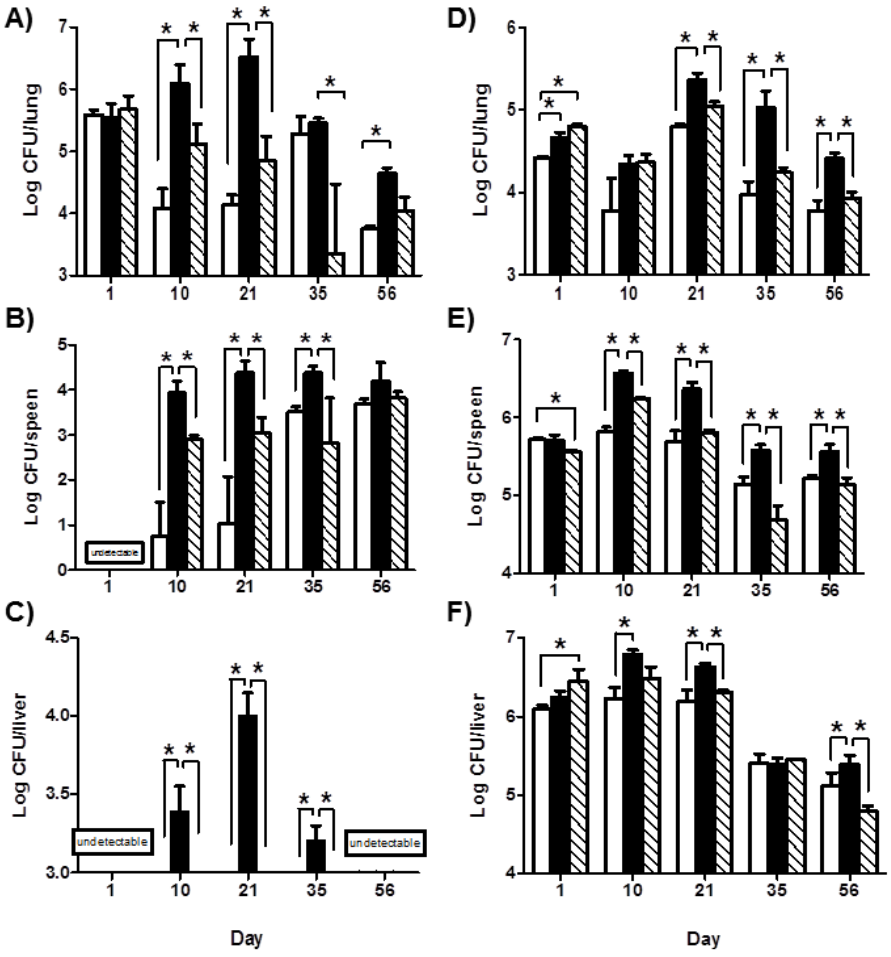

Figure 19: Infection profile of BCG ethA/R KO mutant in mice

Adult Balb/c mice were intranasally (A-C) or intravenously (D-F) infected with approx. $5x10^6$ CFU of *M. bovis* BCG WT (open bar), *ethA/R* KO (black bar) or complemented (stripped bar) strains. Bacterial loads were monitored in the lungs (A, D), spleen (B, E) and liver (C, F) from the infected mice. The results are expressed in Log10 CFU/ml as the average of 4 mice per group per time point ± SD. * $p < 0.05$.

3.3 M. bovis BCG ethA/R KO mutant displays a greater ability to adhere to mammalian cells.

To further investigate the increased ability of the BCG *ethA/R* KO mutant to colonize mouse organs**,** its infection profile in various mammalian cells was determined and compared to that obtained with the parental and complemented strains. Human macrophages (THP1), murine bone marrow-derived macrophages (BMMO), human hepatocytes (Huh7) and human pulmonary epithelial cells (A549) were infected at a multiplicity of infection (MOI) of 1, and at the indicated time points, the infected cells were lysed and appropriate dilutions were plated for colony counting. Comparable bacterial inoculums were added to the mammalian cells (data not shown). Significantly higher bacterial counts were obtained with the BCG *ethA/R* KO mutant strain across the various cell lines tested for all the time points analysed including Day 0, compared to the parental and complemented strains (Fig. 20). These data thus suggests that the BCG *ethA/R* KO mutant strain displays increased intrinsic ability to infect mammalian cells, regardless of cell type. Furthermore and importantly, this phenotype could be observed as early as at the first time point post-infection which corresponds to the initial 45 minutes of co-incubation between bacteria and mammalian cells (Fig. 20 and 21A). This observation could suggest that the BCG *ethA/R* KO displays greater adherence properties than its WT counterpart thereby allowing higher bacterial uptake within the host cells.

Additionally, Day 0 bacteria counts were expressed as a percentage of the given inoculum for each respective strain to further highlight the striking

differences in mycobacteria uptake by mammalian cells (Fig. 21A). Subsequent counts obtained from later time points were then expressed in reference to the initial Day 0 post-infection counts to check for differences in intracellular survival (Fig. 21B). The profiles obtained indicated that while there were no significant differences in the intracellular survival between the BCG *ethA/R* KO mutant, WT and complemented strains in human macrophages, the mutant displayed enhanced survival in murine macrophages throughout the course of infection (Fig. 21B). These data analyses imply that BCG *ethA/R* KO bacteria are more effectively taken up by the macrophages and may or may not display greater intracellular survival capability depending on the host species from which the macrophages were derived from.

To further test the hypothesis of increased adherence property of the BCG *ethA/R* KO mutant at the surface of macrophages, an adherence assay was performed whereby mycobacteria were co-incubated with THP1 cells at $4^{o}C$ or in the presence of cytochalasin D (CCD). Both conditions have previously been shown to prevent cellular uptake of bacteria (150, 164). Significantly higher bacterial counts were obtained with the BCG *ethA/R* KO mutant compared to the parental and complemented strains (Fig. 22). Moreover, the difference in bacteria counts obtained from parental and mutant-infected macrophages when cellular uptake was inhibited corresponds to the difference in counts between the respective strains under typical infection conditions, with differences close to half a log (Fig. 20A & 22). These data thus support that absence of the *ethA/R* locus in BCG confers a greater ability of the pathogen to adhere to mammalian cells.

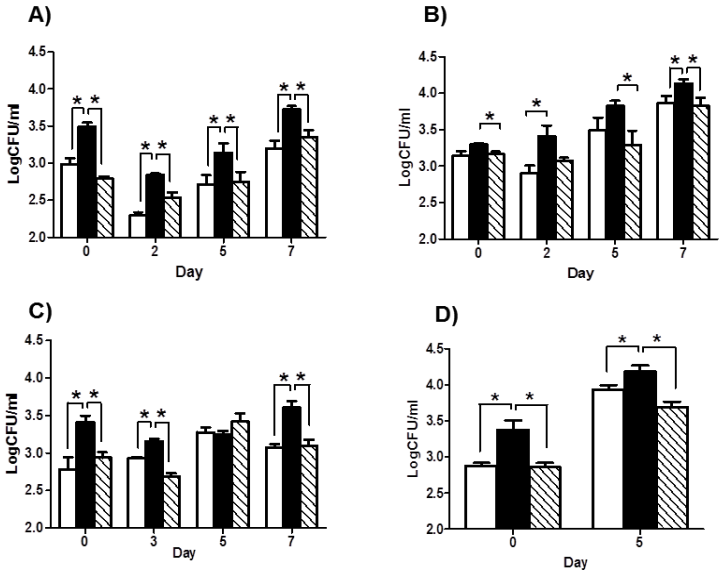

Figure 20: Infection profile of BCG ethA/R KO in mammalian cells

Human macrophages THP-1 (A), murine bone marrow-derived macrophages (BMMOs) (B), human hepatocyte cell line Huh-7 (C) and human pulmonary epithelial cell line A549 (D) were infected with WT (open bar), *ethA/R* KO (black bar) or complemented (stripped bar) strain at a MOI of 1 (THP-1 and BMMO), 2 (Huh-7) and 3 (A549). At the indicated time points, the cells were washed, lysed and appropriate dilutions were plated for colony counting. The results are expressed in Log10 CFU/ml and represents the average of quadruplicates ± SD. *, $p<0.05$.

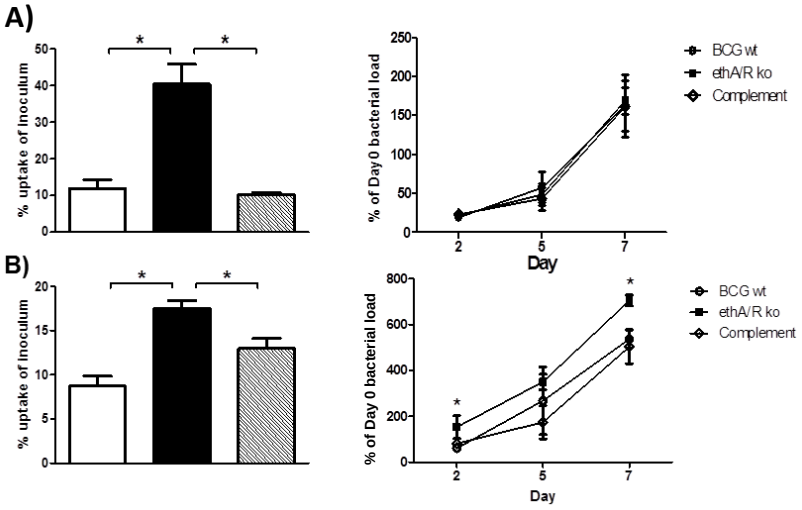

Figure 21: Uptake (Left Panel) and intracellular survival (Right Panel) profile of BCG ethA/R KO in macrophages

Uptake percentages upon macrophage infections with WT (open bar), *ethA/R* KO (black bar) or complemented (stripped bar) strains were calculated by expressing Day 0 bacterial loads as a percentage of the respective inoculum (Left Panel). Intracellular survival percentages were then calculated by expressing counts obtained at indicated time points as a percentage of Day 0 load. The results represent the average of quadruplicates ± SD. *, $p<0.05$ (Right Panel).These were performed in (A) human macrophages THP-1 and (B) murine bone marrow-derived macrophages (BMMOs).at a MOI of 1 as described in the legend of Figure 20.

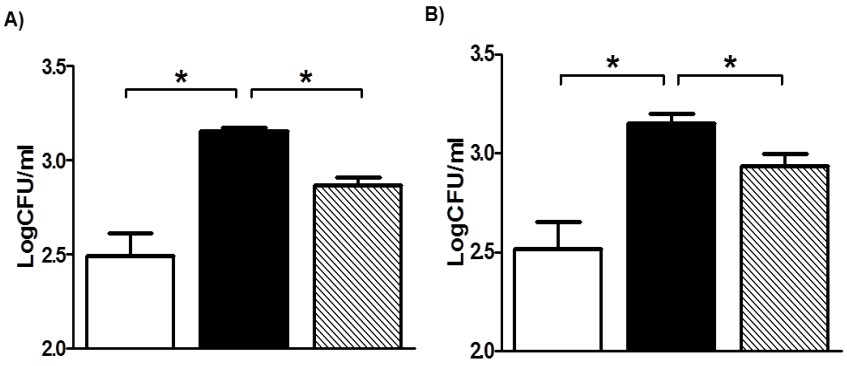

Figure 22: Adherence assay of BCG ethA/R KO to macrophages

THP-1 macrophages were infected with BCG WT (open bar), *ethA/R* KO (black bar) or complemented (stripped bar) strain at MOI of 1. After 45 minutes co-incubation at 4°C (A) or in the presence of cytochalasin D (B), the cells were washed and lysed. Appropriate dilutions of the lysates were plated for colony counting. The results are expressed in Log10 CFU/ml as the average of quadruplicates ± SD. *, $p < 0.05$.

3.4 The ethA/R locus affects the cell wall mycolic acids composition in M. bovis BCG.

The physiological role of membrane-associated EthA is unknown. However, given that BVMOs have been suggested to be involved in mycolic acid synthesis and/or degradation (132), it is plausible that the absence of EthA in the BCG *ethA/R* KO mutant may lead to some qualitative and/or quantitative differences in the cell wall lipid composition, in particular the mycolic acids (MA), that may account for the increased adherence properties of the BCG *ethA/R* KO mutant to mammalian cells.

The fatty acid methyl ester (FAME) and mycolic acid methyl ester (MAME) compositions were thus analyzed by thin layer chromatography (TLC) of the whole cell mycolates prepared from *ethA/R* KO, wild type and complemented strains. No visible differences in the FAME profiles of the whole cell lipid esters were observed (Fig.23A panel III). Similarly, no significant changes were observed in the total lipid species including trehalose dimycolates and monomycolates, phosphatidylethanolamine, phosphatidylinositol, cardiolipin, diacylated and monoacylated phosphatidylinositol di-mannosides, or higher phosphatidylinositol mannosides (Fig. 23A panels I-II). In contrast, slightly greater signal intensity was consistently seen with both alpha and keto MAME species in the *ethA/R* KO mutant (Fig. 23A panel III). To confirm and further analyze the slightly increased amounts of MAMEs seen with the KO mutant, TLC analysis was performed on whole cell mycolates, mycolates prepared from extractable lipids or cell wall bound mycolates in different solvent systems. Interestingly,

results consistently showed increased amounts of cell-wall bound MAMEs in the KO strain compared to the WT and complemented strains whereas no visible difference was observed in the amounts of MAMEs prepared from extractable lipids (Fig. 23B), suggesting that while the MAME differences were only localized to the cell wall, MAME profiles in extractable lipids were not affected.

To further analyse the qualitative difference in alpha and keto mycolic acids seen by TLC in the cell wall of the BCG *ethA/R* KO mutant, electrospray ionization-based multiple reaction monitoring (ESI-MRM) mass spectrometry was performed. This method allows qualitative and relative analysis of various species and sub-species of mycolic acids (160). The total amount of mycolic acids was increased by 83% in the *ethA/R* KO mutant compared to the parental strain, and re-introduction of the *ethA/R* locus in the complemented strain reduced the accumulation of mycolic acids back to levels comparable to that of the parental strain (Fig. 24A). In-depth analysis of the various mycolate sub-species from the BCG *ethA/R* KO mutant revealed significant increase in the overall amounts of C24:0 alpha-MA (170% increase compared to the parental strain), C26:0 keto-MA (56% increase) and C24:0 keto-MA (235% increase) mycolic acid sub-species (Fig. 24A). The quantitative differences of individual C24:0 and C26:0, alpha- and keto-mycolic acid sub-species between parental, KO and complemented strains have been heat-mapped to reflect localized differences between each mycolic acid subspecies (Fig. 24B). Together, these data demonstrate the existence of substantial alterations in the mycolic acid profile in the BCG *ethA/R* KO mutant compared to its parental and complemented counterparts, implying that EthA or EthR may be involved

in the metabolism of mycolic acids species and sub-species composition in the mycobacterial cell wall.

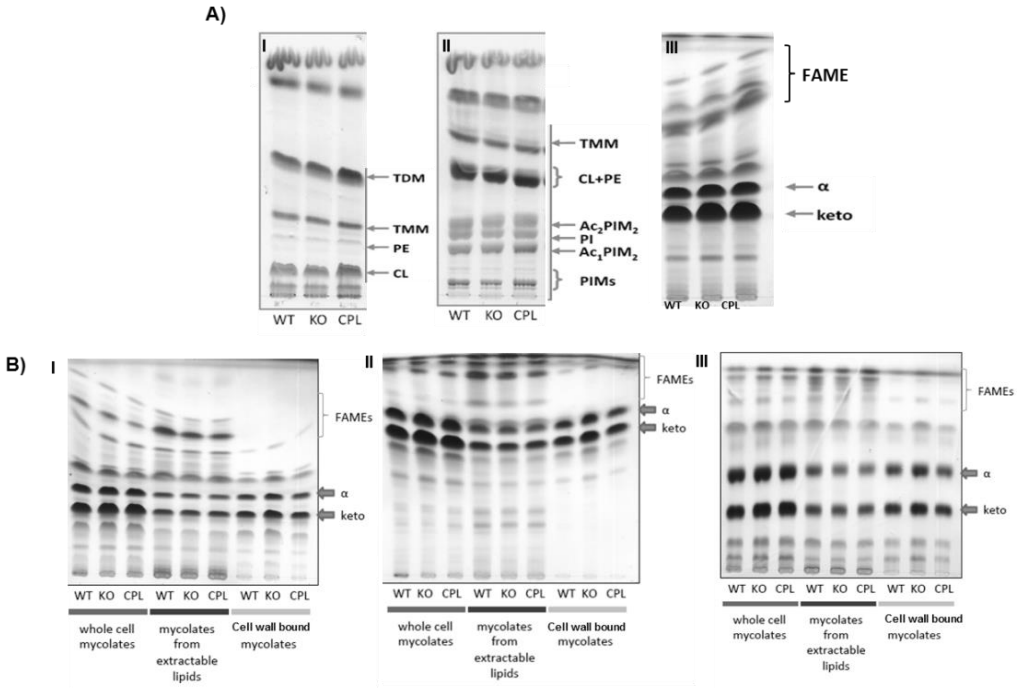

Figure 23: TLC analysis of the lipid composition in the BCG ethA/R KO mutant

A) Thin layer chromatography (TLC) of whole cell mycolates using different solvents: I CHCl3/CH3OH/H2O (20:4:0.5); II CHCl3/CH3OH/NH4OH/H2O (65:25:0.5:4); III n-hexane: ethylacetate (95:5). B) TLC analysis of FAME and MAME prepared from whole cells, extractable lipids or cell wall in different solvents: I n-hexane: ethylacetate (95:5); II petroleum ether: acetone (90:10); III dichloromethane on Ag-impregnated plates. WT, *ethA/R* KO and complemented BCG strains were grown at 37°C in 7H9 liquid medium for 20 days. The bacteria were harvested and processed for total, extractable and cell wall bound lipid extraction. Abbreviations: TDM, trehalose dimycolate; TMM, trehalose monomycolate; PEE, phosphatidylethanolamine; CL, cardiolipin; PI, phosphatidylinositol; Ac2PIM2, diacylated phosphatidylinositol di-mannoside; Ac1PIM1, mono-acylated phosphatidylinositol di-mannoside; PIMs, higher phosphatidylinositol mannosides. FAME: fatty acid methyl ester; α and keto: alpha- and keto-mycolic acid methyl esters respectively.
[TLCs were kindly performed by Dr Katarína Mikušová, Dr Jana Korduláková, Petronela Dianišková and Jan Madacki under collaboration.]

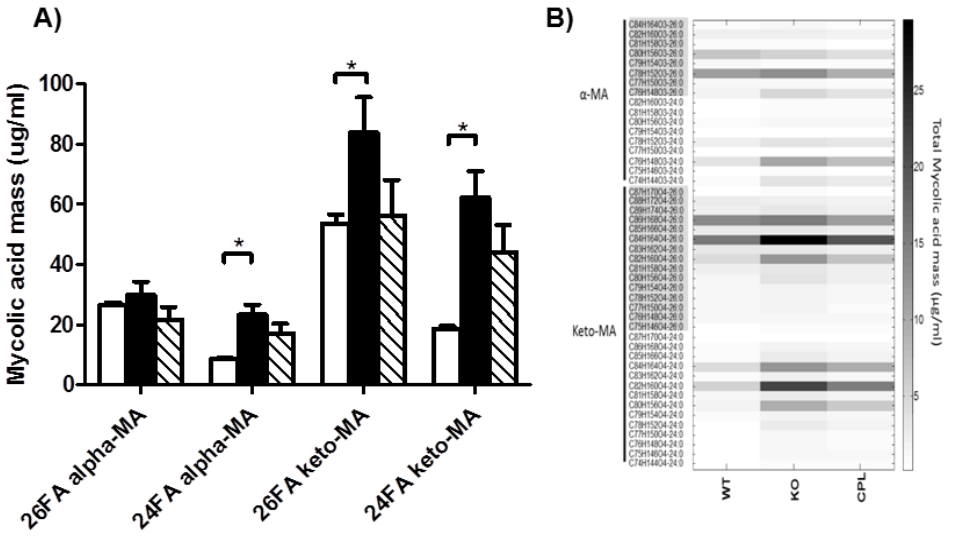

Figure 24: Mass spectrometry analysis of mycolic acids

Mycolic acids were extracted from mid-log phase liquid cultures (7H9). Samples were analyzed via a Q trap 4000 mass spectrometer. A) Individual sums of C26 alpha, C24 alpha, C26 alpha and C24 keto mycolic acid profiles in WT (open bar), *ethA/R* KO (black bar) and complemented (stripped bar) BCG strains. Results are expressed as the average of quintuplicates ± SD. * $p < 0.05$. B) Heat map representation of the mycolic acid profile in WT (n=5), ethA/R KO (n=5) and complemented (n=5) BCG strains.

Legend: 26FA alpha-MA: Carbon26-alpha-unit-containing mycolic acid, 24FA alpha-MA: Carbon24-alpha-unit-containing mycolic acid, 26FA MeO-MA: Carbon26-methoxy-unit-containing mycolic acid, 24FA alpha-MA: Carbon24-methoxy-unit-containing mycolic acid, 26FA keto-MA: Carbon26-keto-unit-containing mycolic acid, 24FA keto-MA: Carbon24-keto-unit-containing mycolic acid. The carbon number indicates chain length of the product ion.

[LC-MS was conducted together with Dr Shui Guanghou under collaboration.]

3.5 M. tuberculosis CDC1551ethA/R KO mutant displays increased adherence properties in vitro which correlated with mild enhanced virulence phenotype in vivo.

Although *M. bovis* BCG is commonly used as a surrogate organism to study *M. tuberculosis*, a high degree of phenotypic variability also exists amongst Mycobacteria strains including differences in terms of drug resistance, virulence and host immunity (165-168). Moreover, as mentioned earlier, BCG lacks the RD1 region which plays a crucial role in virulence in comparison to *M. tuberculosis* strains (44).

To investigate the role of the *ethA/R* locus in *M. tuberculosis* CDC1551, the infection profile of the CDC1551 *ethA/R* KO mutant and its parental and complemented counterparts in human macrophages (THP1) and human hepatocytes (Huh7) were monitored. The CDC1551 *ethA/R* KO mutant displayed infection profiles that were very similar to that observed with the BCG *ethA/R* KO mutant during *ex vivo* mammalian cell infection, where significantly higher bacterial counts were obtained for the *ethA/R* KO mutant across both cell lines and for all the time points analysed in comparison to its parental and complemented strains (Fig. 25).

These data thus support that the CDC1551 *ethA/R* KO mutant strain displays increased intrinsic ability to infect mammalian cells *ex vivo*. As seen for the BCG *ethA/R* KO mutant, importantly, this phenotype could be observed as early as at the first time point post-infection which corresponds to the initial 45 minutes of co-incubation between bacteria and mammalian cells

(Fig. 25). This observation suggests that the CDC1551 *ethA/R* KO mutant may also display greater adherence properties than its parental counterpart, which was indeed confirmed in an adherence assay. At 4°C, which inhibits cellular uptake as mentioned in the previous section, the CDC1551 *ethA/R* KO mutant was able to adhere better to THP1s, producing significantly higher counts by about 40% (Fig. 26).

To further understand the importance of the *ethA/R* locus in *M. tuberculosis* CDC1551and whether the *in vitro* findings could translate to an *in vivo* phenotype, the infection profile of the CDC1551 *ethA/R* KO mutant and its parental strain were monitored in the mouse model upon intra-tracheal administration of comparable inoculums of each strain (data not shown). The percentage of uptake determined by expressing the number of bacteria recovered at 3 hours post-administration as a percentage of the initial inoculum was found to be significantly higher for the CDC1551 *ethA/R* KO mutant in comparison to its parental strain (100% and 70% respectively) (Fig. 27A). This seems to directly correlate with the differential adherence properties between the KO and WT strains observed *ex vivo*. However, this difference was not seen with the BCG *ethA/R* KO mutant which displayed similar bacterial counts to the WT strain at day 1 post infection (p.i.) (Fig. 19A). This may be explained by the fact that a much higher infectious dose must be given to establish infection with BCG bacteria in the mouse model compared to *M. tuberculosis* ($5x10^6$ CFU for BCG vs 500 CFU for M. tuberculosis). It is thus likely that when giving $5x10^6$CFU of either BCG WT or *ethA/R* KO mutant bacteria, the initial adherence to the respiratory mucosa is comparable.

Next, the bacterial load present at different time points post-infection in the lungs, spleen and liver was expressed as a percentage of the initial bacterial uptake, in order to take into account the significant difference in bacterial uptake observed for both strains. It was found that the CDC1551 *ethA/R* KO mutant and its parental strain displayed comparable infection profiles in the lungs and spleen throughout the course of infection (Fig. 27B-C). A transient though non-significant increase in bacterial counts was seen in the spleen from the *ethA/R* KO-infected mice at Day 35 (Fig. 27C). No bacterial counts were obtained in the liver from both the parental and *ethA/R* KO strains throughout the course of infection, likely due to the small initial inoculum (500 CFU only) which was four logs less than that of the BCG inoculum. Thus, the CDC1551 *ethA/R* KO mutant infection profile obtained upon intra-tracheal infection suggests that absence of the *ethA/R* locus in *M. tuberculosis* CDC1551 allows greater bacterial adherence and uptake during the initial phase of infection, therefore implying a role in the establishment of infection. Presence or absence of the *ethA/R* locus at a later stage during the infection however seems to make no difference for *M. tuberculosis* whereas it was found very critical for *M. bovis* BCG. This observation indicates that *M. tuberculosis* relies on other virulence strategies to successfully infect its host, underscoring the differential virulence potential between *M. tuberculosis* and BCG, and indicating that observations made with BCG should not be extrapolated to *M. tuberculosis*.

Together, data obtained with both *M. bovis* BCG and *M. tuberculosis* CDC1551 *ethA/R* KO mutants indicate that absence of the *ethA/R* locus

confers greater adherence capabilities of mycobacteria to mammalian cells, which influences the ability of the pathogens to infect their host.

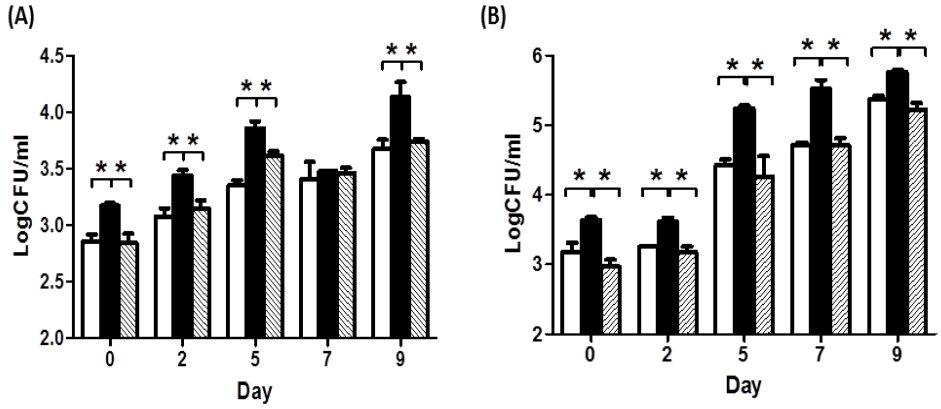

Figure 25: Infection profile of CDC *ethA/R* KO mutant in mammalian cells

Human macrophages THP-1 (A) and hepatocyte cell line Huh-7 (B) were infected with WT (open bar), *ethA/R* KO (black bar) or complemented (stripped bar) strain at a MOI of 1 (THP-1) and 2 (Huh-7). At the indicated time points, the cells were washed, lysed and appropriate dilutions were plated for colony counting. The results are expressed in Log10 CFU/ml and represents the average of quadruplicates ± SD. *, $p<0.05$.

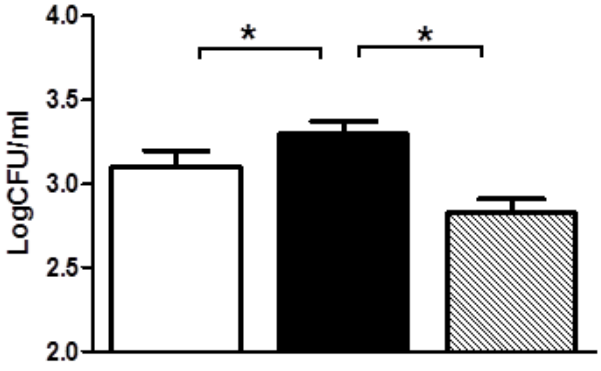

Figure 26: Adherence assay of CDC1551 *ethA/R* KO to macrophages

THP-1 macrophages were infected with CDC WT (open bar), *ethA/R* KO (black bar) or complemented (stripped bar) strain at MOI of 1. After 45 minutes co-incubation at 4°C, the cells were washed and lysed. Appropriate dilutions of the lysates were plated for colony counting. The results are expressed in Log10 CFU/ml as the average of quadruplicates ± SD. *, $p < 0.05$.

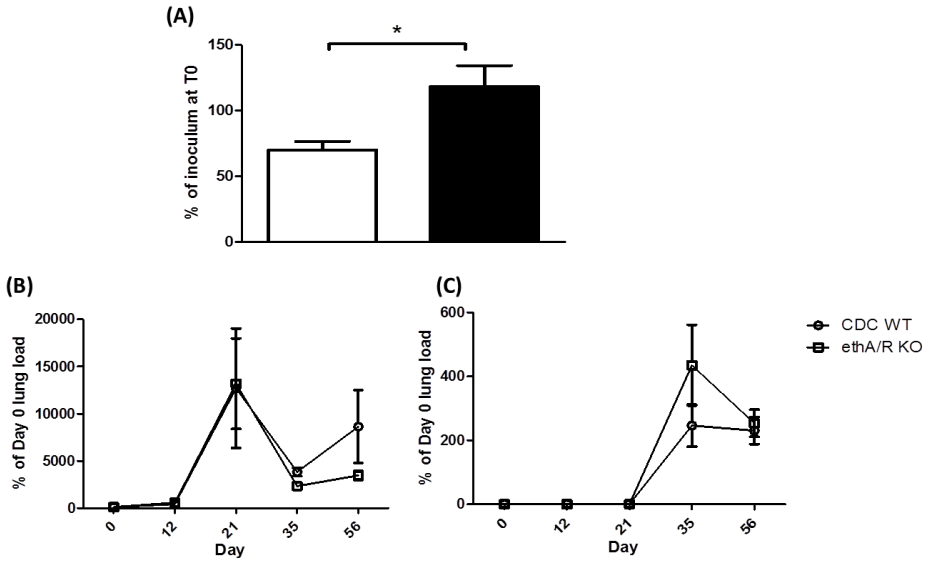

Figure 27: Infection profile of CDC1551 *ethA/R* KO mutant in mice

Adult Balb/c mice were intranasally infected with approx. 500 CFU of *M. tuberculosis* CDC wild type (open bar) or *ethA/R* KO (black bar). (A) Bacterial loads were obtained in the lungs from the infected mice at Day 1 post-infection and expressed as a percentage of the respective inoculums given per strain. Uptake percentages in the lungs (B) and spleens (C) were calculated by expressing Day 0 bacterial loads recovered from the lungs as a percentage of the respective inoculum. Intracellular survival percentages were calculated by expressing counts obtained at indicated time points as a percentage of Day 0 lung loads. The results represent the average of quadruplicates ± SD. *, p<0.05.Percentages reflected are the average of 4 mice per group per time point ± SD. * $p < 0.05$.

3.6 The M. tuberculosis Erdman ethA/R KO strain displays parental adherence properties during mammalian cell infection, which correlated with an unaltered mycolic acid cell wall composition.

For a more comprehensive understanding of the importance of the *ethA/R* locus in virulence, the infection profile of Erdman *ethA/R* KO mutant and its parental and complemented counterparts in human macrophages (THP-1) and murine bone marrow-derived macrophages (BMMO) was also monitored over time. Comparable bacterial inoculums were added to the mammalian cells (data not shown), and the Erdman *ethA/R* KO mutant strain showed no significant differences in bacterial counts across both macrophage cell lines in comparison to the parental and complemented strains over the course of infection (Fig. 28). These findings suggest that the *ethA/R* locus does not play a critical role in the adherence properties of *M. tuberculosis* Erdman.

As the BCG *ethA/R* KO mutant displayed increased virulence during host infection which correlated with an altered cell wall composition of mycolic acids, the lack of a differential adherence pattern for the Erdman *ethA/R* KO mutant suggests an unchanged cell wall composition. Consistently, TLCs of the mutant's whole cell mycolates revealed neither striking differences in various lipid species (Fig. 29A panels I-II) nor FAME and MAME profiles (Fig. 29B panel I). Further analysis of the localized extractable or cell wall-bound FAMEs and MAMEs from the Erdman *ethA/R* KO mutant and its parental and complemented counterparts also showed no conclusive differences between the three strains (Fig. 29B panels II-III).

In order to account for any possible relative differences in various mycolic acid species that may be undetectable via TLC, ESI-MRM was performed. Although there was a slight but significant decrease in C24:0 alpha-MA and also a slight but significant increase in C24:0 keto-MA in the mutant strain (Fig. 30), these differences could not be attributed to the absence of *ethA/R* locus since the complemented strain displayed a pattern similar to that of the KO mutant. We speculate that the minor differences seen with the KO and complemented strains compared to the parental strain could be due to the very sensitive nature of mass spectrometry quantification and minor sample loss during MA extraction, which involves several lengthy steps that could confound MA amounts. These observations thus suggest that unlike BCG andCDC1551, absence of the *ethA/R* locus in *M. tuberculosis* Erdman background does not lead to a significant change in the cell wall lipid composition.

Together, the combined findings indicate that the suggested role of the *ethA/R* locus in mycolic acid cell wall composition and its consequential effects on adherence to mammalian cells and persistence *in vivo* varies amongst different *Mycobacteria* species. Moreover, the data presented here further validate the correlation between mycobacteria virulence and mycolic acid cell wall composition.

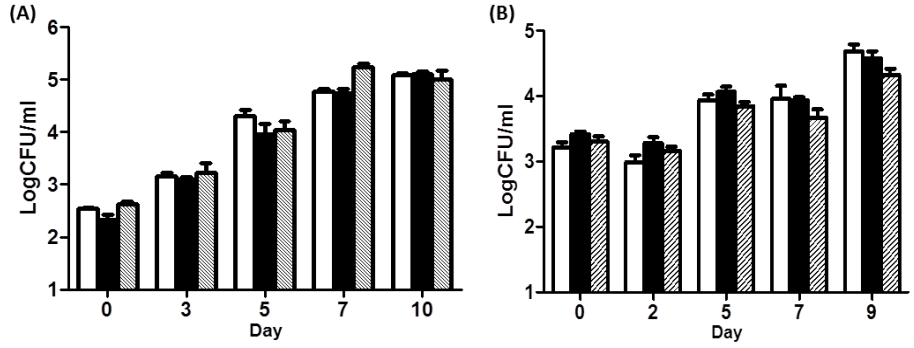

Figure 28: Infection profile of Erdman *ethA/R* KO mutant in mammalian cells

Human macrophages THP-1 (A) and murine bone marrow-derived macrophages (BMMOs) were infected with WT (open bar), *ethA/R* KO (black bar) or complemented (stripped bar) strain at a MOI of 1. At the indicated time points, the cells were washed, lysed and appropriate dilutions were plated for colony counting. The results are expressed in Log10 CFU/ml and represents the average of quadruplicates ± SD. *, $p<0.05$.

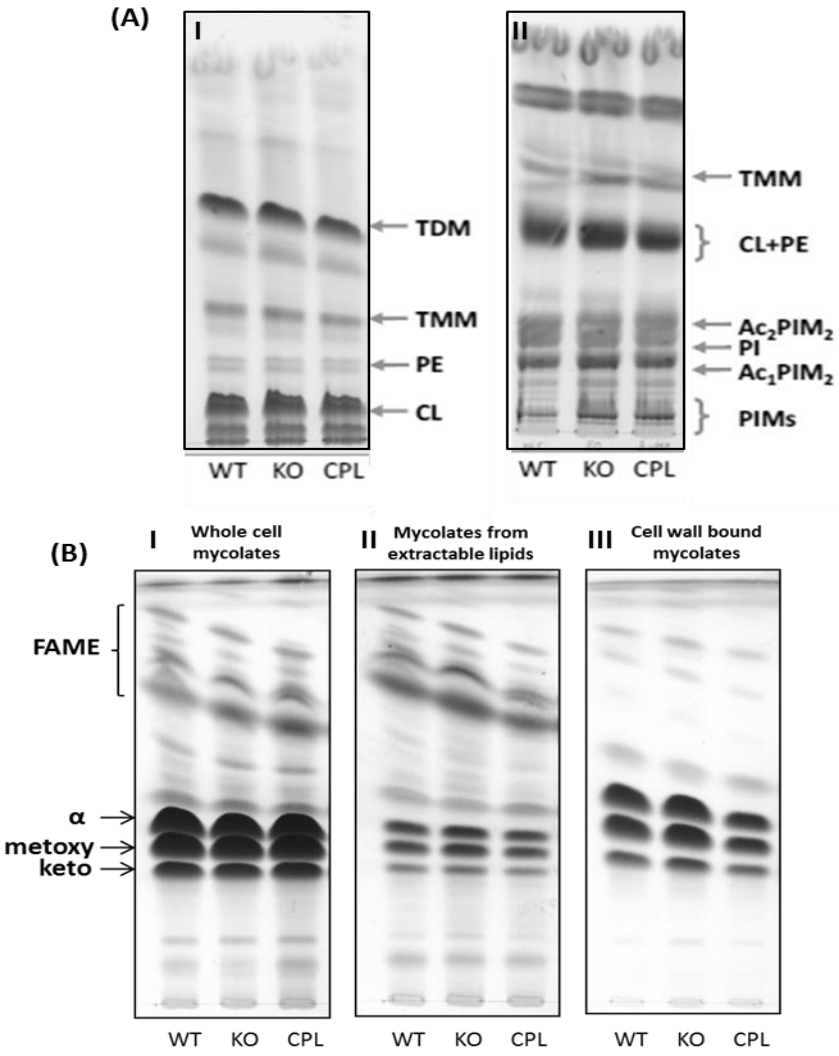

Figure 29: TLC analysis of the lipid composition in the Erdman *ethA/R* KO mutant

A) Thin layer chromatography (TLC) of whole cell mycolates using different solvents: I CHCl3/CH3OH/H2O (20:4:0.5); II CHCl3/CH3OH/NH4OH/H2O (65:25:0.5:4). B) TLC analysis of FAME and MAME prepared from whole cells, extractable lipids or cell wall n-hexane: ethylacetate (95:5) WT, *ethA/R* KO and complemented *M. tuberculosis* Erdman strains were grown at 37°C in 7H9 liquid medium for 20 days. The bacteria were harvested and processed for total, extractable and cell wall bound lipid extraction. Abbreviations: TDM, trehalose dimycolate; TMM, trehalose monomycolate; PEE, phosphatidylethanolamine; CL, cardiolipin; PI, phosphatidylinositol; Ac2PIM2, diacylated phosphatidylinositol di-mannoside; Ac1PIM1, mono-acylated phosphatidylinositol di-mannoside; PIMs, higher phosphatidylinositol mannosides. FAME: fatty acid methyl ester; α and keto: alpha- and keto-mycolic acid methyl esters respectively.

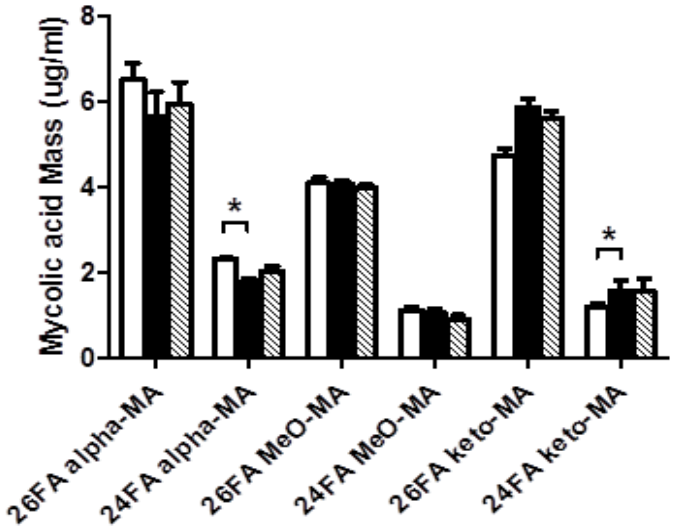

Figure 30: Mass Spectrometry Analysis of Mycolic Acids

Mycolic acids were extracted from mid-log phase liquid cultures (7H9). Samples were analyzed via a Q trap 4000 mass spectrometer. A) Individual sums of C26 alpha, C24 alpha, C26 alpha and C24 keto mycolic acid profiles in WT (open bar), *ethA/R* KO (black bar) and complemented (stripped bar) Erdman strains. Results are expressed as the average of quintuplicates ± SD. * $p < 0.05$. B) Heat map representation of the mycolic acid profile in WT (n=5), ethA/R KO (n=5) and complemented (n=5) Erdman strains.
Legend: 26FA alpha-MA: Carbon26-alpha-unit-containing mycolic acid, 24FA alpha-MA: Carbon24-alpha-unit-containing mycolic acid, 26FA MeO-MA: Carbon26-methoxy-unit-containing mycolic acid, 24FA alpha-MA: Carbon24-methoxy-unit-containing mycolic acid, 26FA keto-MA: Carbon26-keto-unit-containing mycolic acid, 24FA keto-MA: Carbon24-keto-unit-containing mycolic acid. The carbon number indicates chain length of the product ion.

3.7 Discussion

3.7.1 The role of the ethA/R locus in *M. bovis* BCG and *M. tuberculosis* CDC1551

As there is no experimental evidence that EthR directly modulates the expression of genes other than *ethA* and itself (136), we reasoned that any phenotypic differences observed between the parental and *ethA/R* KO strains would be very likely attributable to the lack of EthA monooxygenase activity, and unlikely to EthR-mediated repression of other unknown target genes, although we cannot completely rule out this remote possibility. Furthermore, although previous studies were able to create *ethR* KO mutants but yet were unsuccessful in their attempts to delete *ethA* for the study of ETH bio-activation (124, 127), to our knowledge, this is the first time the entire *ethA/R* locus has been deleted in mycobacteria for the characterization of the physiological role of this locus in the MTBC.

Deletion of the *ethA/R* locus in *M. bovis* BCG resulted in increased bacterial loads recovered from the mouse organs upon nasal infection, thus supporting a role for the *ethA/R* locus in modulating mycobacterial virulence. Consistently, increased *in vitro* adherence to mammalian cells were also observed with the BCG *ethA/R* KO mutant thus strongly supporting that the greater adherence ability of the *ethA/R* KO mycobacteria translated into greater persistence in the murine organs. In a relatively similar fashion, the lack of the *ethA/R* locus in *M. tuberculosis* CDC1551 resulted in greater *in vitro* adherence to mammalian cells and also an increase in the initial bacterial uptake in mice lungs upon *in vivo* infection; although this effect, unlike the

BCG *ethA/R* KO mutant, did not persist in the lungs or spleens throughout the course of infection. Nevertheless, it is apparent that the *ethA/R* locus in BCG and CDC1551 is able to affect the adherence properties of mycobacteria, and this affected adherence has an impact on mycobacteria virulence.

Interestingly, genetic studies have shown that 40-50% of the ETH-resistant clinical isolates harbour mutations in the *ethA* gene while the rest bear mutations in other genes such as *inhA* for example (126, 129). The possibility that the *ethA*-mutated ETH-resistant isolates display greater *in vitro* adherence properties and enhanced *in vivo* persistence ability would (at least partially) explain why the *ethA* locus is the most commonly mutated gene amongst existing ETH-resistant clinical isolates, as this would confer a selective advantage to these mutants.

TLC analysis revealed increased amounts of cell wall bound mycolates in the BCG *ethA/R* KO mutant compared to the parental and complemented strains. In-depth quantitative analysis of the cell wall bound mycolates via mass spectrometry further unveiled differences between the BCG parental and *ethA/R* KO strains in their composition of alpha- and keto-mycolic acids. Mycolic acids not only constitute the major mycobacterial hydrophobic barrier responsible for drug resistance and oxidative stress, but have also been shown to play an active role in host-pathogen interactions through host receptors binding (169) and immunomodulatory properties (162, 170). In addition, by controlling the fluidity and hence the outer permeability barrier of mycobacteria, mycolic acids directly control nutrients intake during mycobacterial growth in host tissues (85, 171). Surprisingly, even the most

subtle changes in the mycolic acid structure have been shown to have profound effects on the physiology and virulence of mycobacteria (171). We thus propose here that the overall increased amounts of keto-mycolates and alpha-mycolates in the BCG *ethA/R* KO may account for the observed increased adherence properties to mammalian cells. This working hypothesis is supported by a previous study where the absence of keto-mycolates was found to lead to profound alterations in the envelope permeability and to an attenuated phenotype in mice (85, 172). Conversely here, a significant increase in both alpha and keto-mycolates abundance correlated with a hypervirulent phenotype in mice. While the cell wall permeability of the *ethA/R* KO mutant strain has yet to be investigated, our data support that the altered mycolic acid profile has potentially modified the ability of the mycobacterial cell wall to interact with the mammalian cell surface.

Fraaije and colleagues previously proposed that the oxidative activity of EthA and other mycobacterial BVMOs may help the pathogen survive oxidative stress conditions encountered *in vivo*(132). The authors also speculated that EthA may participate to a detoxification activity through the removal of toxic ketones in mycobacteria. However, we found that EthA deletion neither impaired the *in vitro* general fitness of the mycobacteria, nor attenuated the infection capabilities of the mutant in macrophages, but instead enhanced its adherence properties and *in vivo* persistence. Alternatively, BVMOs in general have been shown to be involved in specific metabolic processes, through the conversion of relatively hydrophobic substances such as mycolic acids, although knowledge of mycolic acid metabolism still remains somewhat fragmentary (173). The altered mycolic acid profile in the

BCG *ethA/R* KO implies dysregulation of either the mycolic acid synthesis or degradation pathways, hence resulting in increased accumulation of long chain C24:0 and C26:0 alpha- and keto-mycolic acids. Although the exact mechanism of how the *ethA/R* locus modulates the composition of mycolic acid subspecies remains to be studied, the more pronounced keto-mycolic acid overproduction in the BCG *ethA/R* KO mutant compared to the change in alpha-mycolic acid levels leads us to speculate that EthA likely plays a metabolic role by oxidizing keto-mycolic acids to yield wax ester mycolic acids, which have been shown to be the result of a Baeyer-Villiger reaction on the keto group of keto-mycolic acids (174, 175) (Fig. 31).

Although the mycolic acid profile of the CDC1551 *ethA/R* KO mutant was not analysed in this study due to limited time and resources, it would have been insightful to do so in order for further evidence that the adherence properties correlate with changes in the mycolic acids composition in the cell wall. Data obtained with the Erdman *ethA/R* KO mutant support indeed such correlation. However, the increased adherence properties of the *ethA/R* KO CDC1551 mutant did not translate in a drastic increase in its ability to colonize the mouse lungs, spleen and liver, unlike the BCG *ethA/R* KO mutant. We propose that the different mouse infection profiles obtained with BCG and CDC1551 *ethA/R* KO mutant strains are due to the difference in virulence between BCG and *M. tuberculosis*. Indeed, it has been shown previously that the lack of the RD1 region in BCG makes this bacterium less able to invade its host successfully, and therefore increasing the adherence properties of BCG (through deletion of the *ethA/R* locus for example) leads to a significant increase in its colonization ability, whereas doing the same in *M. tuberculosis*

only mildly affects its virulence potential which relies on other mechanisms and strategies.

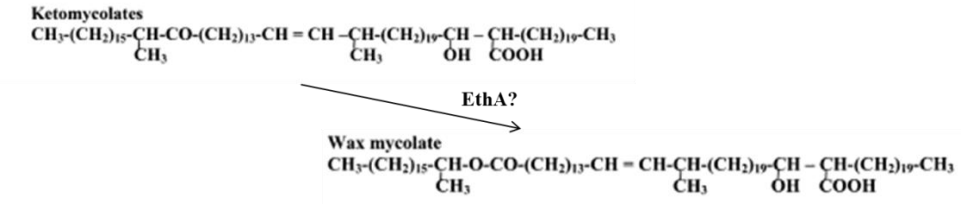

Figure 31: The Hypothetical Role of EthA

As a BVMO, EthA likely plays a metabolic role in mycobacteria by oxidizing keto-mycolates to wax ester mycolates, resulting in alterations in the mycolic acids cell wall of the bacterium.
Figure adapted with permission from Asselineau *et al.* (173)

3.7.2 The role of the ethA/R locus in *M. tuberculosis* Erdman

In an unexpected twist of findings, the *M. tuberculosis* Erdman *ethA/R* KO mutant did not display enhanced virulence *ex vivo,* nor did its cell wall composition differ from that of the parental phenotype, indicating that the *ethA/R* locus is not critical for virulence in *M. tuberculosis* Erdman. Notably, 5 other genes containing the BVMO signature motif besides EthA have previously been identified in the mycobacteria genome (132, 176). Considering that our findings in the previous section suggests a role in mycolic acids composition for EthA in BCG, it is plausible that in the Erdman *ethA/R* KO mutant, other BVMOs which possess similar catalytic functions as EthA are able to compensate for the deletion of the *ethA/R* locus, hence retaining a parental mycolic acid profile that does not affect the adherence property of Erdman. Moreover, this hypothesis is supported by the finding that expression levels of the genes encoding the 5 other BVMOs were significantly (up to 14 fold) lower in BCG compared to the levels measured in Erdman strain (Table 3). Thus, deletion of the *ethA/R* locus in BCG is likely to impact more drastically the overall BVMO activity in BCG than in Erdman.

3.8 Conclusions

In this section, we characterized the role of the *ethA/R* locus in virulence amongst 3 different strains of the MTBC – *M. bovis* BCG, *M. tuberculosis* Erdman and CDC1551 with the primary aim of studying the physiological role of EthA in various mycobacteria strains. The varying importance of the *ethA/R* locus in different Mtb strains has been demonstrated through the construction of EthA/R-deficient mutants in all 3 backgrounds. While this locus has been shown to play critical roles in adherence and subsequent virulence in both *M. bovis* BCG and *M. tuberculosis* CDC1551 host infections, it does not appear to impact the pathology of *M. tuberculosis* Erdman. Furthermore, the *ethA/R* locus appears to affect the cell wall mycolic acid composition in *M. bovis* BCG, but not that of *M. tuberculosis* Erdman. Lastly, the altered cell wall composition and enhanced virulence displayed by the *M. bovis* BCG *ethA/R* KO mutant corroborates with the unaltered cell wall composition and unaffected virulence of the *M. tuberculosis* Erdman *ethA/R* KO mutant, demonstrating that the mycobacterial cell wall mycolic acid composition correlates with the innate virulence of mycobacteria.

It is difficult to speculate why the *ethA/R* locus appears to be redundant in Erdman but yet affects virulence in BCG and CDC1551, especially comparing the mutant phenotypes observed between Erdman and CDC1551, which are both virulent *M. tuberculosis* strains that originate from the same lineage. Moreover, the entire *ethA/R* locus is well conserved between all mycobacteria strains used in this study; hence any deductions for the differing phenotypes observed between mutant strains would likely involve differences

in the entire genomes of Erdman, CDC1551 and BCG. However, since all 3 mutants did not appear to have impaired growth rates whether *in vitro* or *ex vivo*, we have established that this locus is not essential in mycobacteria, and it is not a critical factor for cell metabolism. Furthermore, though our study shows that the *ethA/R* locus affects virulence indirectly, it may also be feasible to investigate other roles for EthA that were not explored in this study, such as the detoxification of toxic ketones and esters that may aid in cell metabolism.

Many gene characterization studies in mycobacteria typically study the effects of gene removal/interruption in only 1 mycobacteria strain, commonly using the *M. tuberculosis* surrogates *M. bovis* BCG or *M. smegmatis* for safety reasons. Here, we have widened the scope of our study by characterizing the *ethA/R* locus in 3 different Mtb strains to reveal differential roles for the *ethA/R* locus amongst MTBC strains. In doing so, we demonstrate here the varying relevance of utilizing BCG for *M. tuberculosis* research, and highlight that care has to be taken in the extrapolation of these data to the clinical setting, particularly when these organisms are used to study Mtb virulence.

In conclusion, the work presented here suggests that the *ethA/R* locus is involved in the composition of cell wall mycolates in *M. bovis* BCG and *M. tuberculosis* CDC1551, specifically the relative amounts of alpha and keto mycolic acids, which impacts on the adherence properties of mycobacteria to mammalian cells *ex vivo* and their ability to colonize their host.

Chapter 4: Investigating ETH drug activation and resistance mechanisms in Mtb

4.1 Enhanced killing efficacy of ETH ex vivo versus in vitro against M. tuberculosis Erdman

To investigate whether ETH bio-activation may be influenced upon host-pathogen interactions, the killing efficacy of ethionamide (ETH), isoxyl (ISO) and thiacetazone (TAC) compounds against *M. tuberculosis* Erdman strain was determined under *in vitro* (during growth in liquid 7H9 medium) and *ex vivo* (during macrophage infection) conditions. A concentration range of each drug was tested and the minimal bactericidal concentration, which corresponds to 90% reduction (or 1 log) of the number of colony forming units (CFU) compared to the drug-free control (MBC90) was determined.

When tested during *in vitro* culture, MBC90 determined for ETH ranged between 2.5 and 5µM (Fig. 32A). In contrast, the MBC90 of ETH during macrophage infection was < 0.75µM, indicating that ETH was 3 to 6 times more potent in killing mycobacteria during macrophage infection in comparison to *in vitro* culture (Fig. 32B). Similar observations were made with ISO and TAC, for which the killing efficacy was approximately 14 and 57 times greater respectively during macrophage infection compared to *in vitro* culture (Fig. 32).

Furthermore, the MBC90 values of other non thiocarbamide-containing anti-TB drugs were also determined under both conditions. These included isoniazid, rifampicin, ethambutol, moxifloxacin, streptomycin, pyrazinamide and amikacin. In contrast to ETH, ISO and TAC, the MBC90 measured for all these drugs during *in vitro* culture was either similar or lower than the MBC90 measured during macrophage infection (Fig. 32C). These

observations therefore suggest that the greater killing efficacy observed during macrophage infection is specific to the thiocarbamide-containing anti-TB drugs.

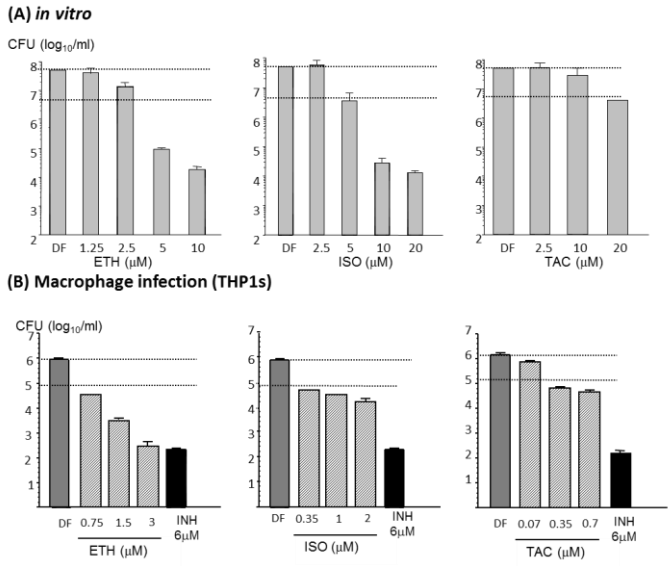

(C) MBC90 values

Drug	In vitro (mM)	THP-1 (mM)
ISONIAZID	0.12	0.5
RIFAMPICIN	0.01	0.08
ETHAMBUTOL	2.5	5
ETHIONAMIDE	**5**	**0.75**
ISOXYL	**5**	**0.35**
THIACETAZONE	**20**	**0.35**
MOXIFLOXACIN	0.2	0.2
STREPTOMYCIN	0.2	14
PYRAZINAMIDE	50	325
AMIKACIN	1	15

Figure 32: Killing efficacy of ETH, ISO and TAC compounds during in vitro (A) and macrophage (THP-1) infection (B) with *M. tuberculosis* Erdman strain

(A) *M. tuberculosis* Erdman bacteria were incubated in the presence of various concentrations of ETH, ISO or TAC, as indicated, and 5 days later, appropriate dilutions were plated for colony counting. (B) THP-1 macrophages were infected for one hour with M. tuberculosis at a multiplicity of infection of 1. The monolayers were then washed and culture medium containing ETH, ISO or TAC at the indicated concentrations was added. 5 days post-infection, the infected macrophages were lysed and appropriate dilutions were plated for mycobacteria colony counting. DF: drug-free. Each assay was performed twice or three times independently. (C) MBC90 values in µm of various first, second and third-line anti-TB drugs including ETH, ISO and TAC obtained from *in vitro* culture versus in THP1 macrophages.

4.2 EthA and ethR expression levels in M. tuberculosis Erdman are not significantly modulated during macrophage infection

Since the *ethA* and *ethR* genes encode for the ETH activator and repressor respectively, a possible explanation for the enhanced mycobacterial killing efficacy of the thiocarbamide-containing drugs during *ex vivo* conditions could be attributed to a differential expression of the *ethA* and/or *ethR* genes during macrophage infection compared to *in vitro* conditions. To test this hypothesis, the gene expression profiles of *ethA* and *ethR* in Erdman were analysed during macrophage infection and normalized to their expression levels during *in vitro* Mtb culture via quantitative real-time PCR. Considering a fold change threshold of 2 and above to be significant, the results indicated that neither *ethA* nor *ethR* genes were significantly modulated during macrophage infection (Fig. 33). While a slight down-regulation was observed for *ethR* at Day 1 and Day 4 post- infection (Fig. 33), this did not result in up-regulation of *ethA* as *ethA* expression levels remain unchanged in comparison to that of *ethA* mRNA levels during *in vitro* culture (Fig. 33). Although EthR has been shown to be the genetic repressor of the ETH activator EthA (124, 127), the minimal repression of *ethR* was likely insufficient to translate to a significant up-regulation of *ethA*. These results thus indicate that the greater killing efficacy of ETH during macrophage infection cannot be explained by a differential transcriptional activity of *ethA* and/or *ethR*.

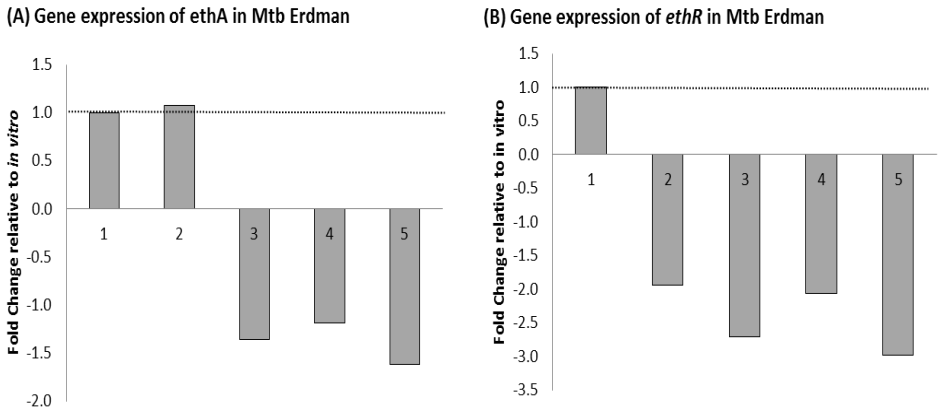

Figure 33: Quantitative analysis of *ethA* and *ethR* gene expression during macrophage infection

THP-1 cells were infected for 2 hours with Mtb Erdman at a multiplicity of infection of (MOI) of 10. The monolayers were then washed twice with PBS, and processed for RNA extraction. Real-time PCR was then conducted to compare regulation of (A) *ethA* and (B) *ethR* during macrophage infection were tabulated and compared to TB *in vitro* culture.

1 = Mtb Erdman *in vitro* culture, 2 = Mtb-infected macrophages at Day 0, 3 = Mtb-infected macrophages at Day 1, 4 = Mtb-infected macrophages at Day 3, 5 = Mtb-infected macrophages at Day 4

4.3 ETH metabolites are not detected in macrophages incubated with ETH

Human flavin-containing monooxygenases 1, 2 and 3 have been shown to catalyse the oxidation of ETH and TAC *in vitro*, forming the same products as EthA (177, 178). Thus, another plausible explanation for the enhanced killing efficacy of ETH during macrophage infection might be due to the innate ability of the macrophage itself to activate ETH before the compound reaches the mycobacterial cytoplasm. Due to the formation of very unstable and reactive intermediates during the activation steps of a pro-drug that may also further be modified during the extraction/purification procedures, a non-invasive, non-destructive method based on high resolution magic angle spinning (HRMAS-NMR) was previously developed to study ETH activation inside living mycobacteria (131). In order to address whether ETH is activated upon macrophage uptake, J774A.1 (murine) and THP-1 (human) macrophages were incubated in the presence of ETH and the fate of the drug and its metabolites (Fig. 11) was monitored by HRMAS-NMR analysis. However, no ETH intermediates were detected by this method, suggesting that ETH does not get activated within the macrophages (data not shown).

Together, the data presented from both the previous and current section suggest that the increased killing efficacy of ETH during macrophage infection cannot neither be explained by a differential transcriptional activity of the *ethA* and/or *ethR*, nor by a spontaneous activation of ETH within the macrophages. Further investigation would be necessary to understand and decipher the mechanisms involved but are not within the scope of this thesis.

4.4 A novel pathway of ETH bio-activation exists in M. tuberculosis Erdman and H37Rv strains

The minimum inhibitory concentration of drug required to inhibit 50% growth of mycobacteria in drug-free media (MIC) was determined for *ethA/R* KO mutant strains constructed in *M. bovis* BCG, *M. tuberculosis* Erdman, *M. tuberculosis* H37Rv and *M. tuberculosis* CDC1551 in order to determine the various levels of resistance to INH, ETH and other thiocarbamide containing drugs. INH was included as well as a negative control since bio-activation of INH is not EthA/R-dependent. Consistently, all *ethA/R* KO mutants displayed parental susceptibility to INH (Fig. 34). In contrast, and as expected, removal of the *ethA/R* locus in *M. bovis* BCG led to complete resistance to ETH (Fig. 34A). However, complete resistance to ETH was not seen with the MTB *ethA/R* KO mutants whereby a dose-dependent killing could still be observed as evidenced by the sigmoidal MIC curves obtained (Fig. 34B-D). The MIC_{50} values measured with the *ethA/R* KO MTB mutants were increased by 2-3X compared to their respective parental strains (Table 5). Furthermore, all the *ethA/R* KO mutant strains displayed increased resistance to TAC, with MIC_{50} values increasing by 2-8X (Table 5). As for ISO, with the exception of Erdman *ethA/R* KO mutant which was found slightly more resistant with a 2-fold increase in the MIC_{50} value compared to its parental counterpart, no significant changes in MIC_{50} were observed with the other mutant strains. Importantly, parental susceptibility to the three drugs was restored in each strain upon re-introduction of the *ethA/R* locus (Fig. 34, Table 5).

To confirm the MIC data reported above, the ETH concentration range within which 90% of the bacteria (also equivalent to 1 log) are killed (MBC_{90}), was determined for the *ethA/R* KO mutant, parental and complemented strains in all four backgrounds. Consistent with the MIC data, while BCG *ethA/R* KO displayed full resistance to ETH, dose-dependent killing was observed with all three MTB KO strains over the range of ETH concentrations assayed (Fig. 35). The MBC_{90} range of ETH on CDC1551 *ethA/R* KO mutant was increased by 8-16 fold compared to its parental and complemented counterparts (Table 6). In contrast, a mild 2-fold increase in ETH MBC_{90} was observed with *ethA/R* KO H37Rv and Erdman strains compared to their parental and complemented counterparts (Table 6). The *ethA/R* KO mutants in all backgrounds were constructed twice independently, and the MIC and MBC of ETH for this new set of mutants were determined. The results obtained were comparable to those obtained with the first series of KO mutants (data not shown).

Although the Mtb KO mutants demonstrated low resistance to ETH, the retained susceptibility to ETH and dose-dependent drug response despite the removal of the *ethA/R* locus in these mutants was a striking observation that warranted further investigation. To further understand the ETH-susceptiblephenotype observed with the Erdman and H37Rv *ethA/R* KO mutants in contrast to the ETH resistant phenotype obtained with the BCG *ethA/R* KO mutant, the DNA sequences of *inhA* and *ethA* (known genes identified in clinical isolates to be involved in ETH resistance phenotype) were obtained and compared between the Mtb strains (Erdman, CDC1551 and H37Rv) and BCG in order to rule out the possibility that a mutation in one of

these genes may be responsible for the phenotypic differences observed between the Mtb and BCG mutants. However, identical sequences were found for *ethA* and *inhA* genes for all 4 strains (data not shown), suggesting the possible association of other undiscovered genes with ETH resistance.

In conclusion, these data show that although the ETH MICs and MBCs values obtained for *ethA/R* KO MTB strains were higher than those measured with the corresponding parental and complemented strains, ETH susceptibility and dose-dependent drug response to ETH were retained. In particular, both Mtb Erdman and H37Rv strains remained very susceptible to ETH upon deletion of *ethA/R* locus with 3 and 2-fold increases in their MIC and MBC values respectively. The observations made with the Mtb strains were somewhat surprising given that the *ethA/R* locus was previously identified to be solely responsible for ETH bio-activation (149). Since the *ethA/R* locus is necessary for ETH bio-activation, removal of this locus was initially expected to lead to a distinct ETH-resistant phenotype (124). Deletion of the *ethA/R* locus was therefore expected to lead to full or very high resistance to ETH as observed with BCG *ethA/R* KO mutant. In contrast, the retained susceptibility to ETH despite removal of *ethA/R* in the three MTB strains suggests that the pro-drug ETH still gets activated into its bactericidal form in an EthA-independent manner, thus supporting the existence of an alternative bio-activation pathway for ETH in Mtb.

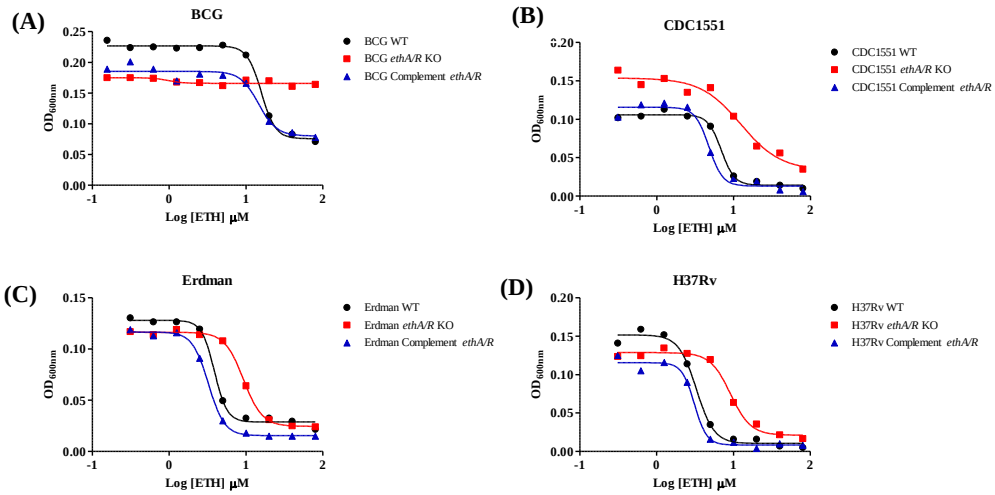

Figure 34: Minimum Inhibitory Concentrations of Ethionamide (ETH) and other drugs (in µm) during in vitro culture.

The MIC was defined as the minimum inhibitory concentration that is required to inhibit 50% growth of the specified strain in drug-free 7H9-ADS media. Drug assays were set up in 96-well plates using a broth microdilution method and their OD600 values read with a spectrophotometry microplate reader after 5 days after 5 days incubation at 37°C. OD600 values were tabulated into PRISM for fitting of MIC curves for (A) BCG, (B) CDC1551, (C) Erdman and (D) H37Rv and MIC50 values were read from PRISM.

Strain	INH	ETH	ISO	TAC
BCG	0.38	15.8	3.93	0.76
BCG *ethA/R* KO	0.35	NA	3.85	5.91
BCG complement *ethA/R*	0.39	14.4	4.04	0.27
CDC1551	0.22	6.90	12.4	9.20
CDC1551 *ethA/R* KO	0.22	12.4	11.5	19.2
CDC1551 complement *ethA/R*	0.20	4.77	14.0	6.42
Erdman	0.15	3.89	10.8	4.80
Erdman *ethA/R* KO	0.11	9.29	21.2	12.1
Erdman complement *ethA/R*	0.12	3.25	13.7	2.07
H37Rv	0.20	3.30	13.0	2.0
H37Rv *ethA/R* KO	0.20	9.16	10.6	12.3
H37Rv complement *ethA/R*	0.19	3.10	11.5	1.47

Table 5: Minimum Inhibitory Concentrations (MIC50) of Ethionamide (ETH) and other drugs (in µm) during in vitro 7H9-ADS culture.

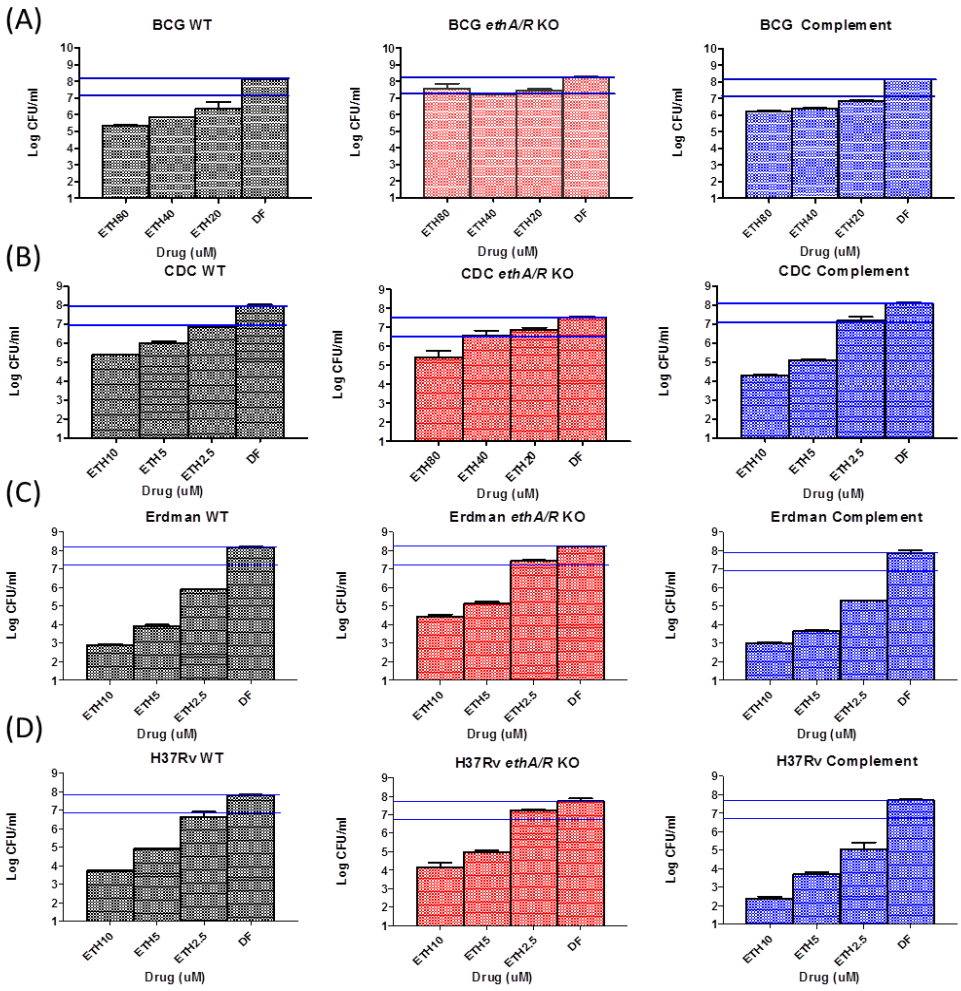

Figure 35: Minimum Bactericidal Concentration (MBC90) of Parental, *ethA/R* KO and complemented strain in the backgrounds of A) BCG, B) CDC1551, C) Erdman and D) H37Rv in the presence of ETH

After determining MIC, 50µl of selected drug concentrations from the assay plates were plated at appropriate dilutions on 7H11 agar plates to determine MBC. Plates were incubated at 37°C and scored for CFU after 14-16 days. MBC90 values in µm of various first, second and third-line anti-TB drugs including ETH, ISO and TAC obtained from *in vitro* culture versus in THP1 macrophages. *DF = Drug-free.*

	Parental Strain	*ethA/R* KO	Complement *ethA/R*
BCG	10-20	NA	10-20
CDC1551	2.5-5	40	2.5-5
Erdman	1.25-2.5	2.5-5	1.25-2.5
H37Rv	1.25-2.5	2.5-5	1.25-2.5

Table 6: Minimum Bactericidal Concentrations (MBC90) of Ethionamide (in µm) during in vitro culture.

Corresponding to Figure 34, the MBC90 range was defined as the range of ETH concentrations (in µM) within which 90% of the mycobacteria are killed compared to the drug-free control after 5 days incubation.

4.5 The alternative pathway of ETH bio-activation in M. tuberculosis Erdman and H37Rv is independent of the transcriptional repressor ethR.

To further investigate the possible existence of an alternative pathway of ETH bio-activation in MTB, we questioned whether the transcriptional repressor EthR which negatively modulates the *ethA/R* locus, would also modulate this alternative pathway. Indeed, EthR was predicted to bind to a number of promoter regions in addition to *ethA/R* promoter (http://genome.tbdb.org/tbdb_sysbio/Resources.html). Thus it is conceivable that EthR may repress the expression of another gene that is involved in ETH bio-activation. To address this hypothesis, the *ethR* open reading frame (ORF) was over-expressed in all three WT MTB strains under the control of the constitutive strong promoter *hsp60* and using the multicopy replicative plasmid pMV262. Real-time PCR analysis confirmed the over-expression of *ethR* (8-16 fold increase) in comparison to the parental strains (data not shown). The over-expression of *ethR* in these three strains was expected to lead to the strong repression of *ethA* expression as well as any other genes that may be negatively regulated by EthR. Should an alternative EthR-dependent pathway of ETH bio-activation exist in MTB, susceptibility to ETH would be affected when *ethR* is over-expressed.

However, the *ethR* over-expressing strains displayed MBC_{90} concentration ranges similar to those obtained with the *ethA/R* KO mutants (Table 7), retaining ETH susceptibility in a dose-dependent manner (Fig. 36). These results thus further support the existence of an alternative pathway of ETH

bio-activation in MTB and indicate that this pathway is likely to be EthR-independent.

To further confirm the existence of an EthR-independent pathway of ETH bio-activation in MTB, the *ethR* ORF was re-introduced back into the Erdman *ethA/R* KO mutant under the control of its original promoter using the integrative plasmid pMV306. We reasoned that expression of *ethR* in the *ethA/R* KO mutant would only impact on the susceptibility to ETH if the alternative pathway of ETH bio-activation is under the control of EthR. However, comparable dose-dependent killing profile and MBC_{90} ranges were obtained for both strains (Fig. 36, Table 7).

Finally, utilizing the previous strategy used for construction of the *ethA/R* KO mutants, the *ethA* ORF was deleted from all 4 mycobacteria strains, maintaining *ethR* ORF expressed at parental level. This approach allowed us to verify whether the absence of EthA alone would lead to similar observations made when the entire *ethA/R* locus has been deleted. The MIC (data not shown) and MBC values (Table 7) generated from these strains were similar to the values obtained with the *ethA/R* KO mutants, demonstrating that both EthA and EthR do not play a role in the alternative pathway of ETH bio-activation. Altogether, these findings strongly support the existence of an EthA/R-independent alternative pathway of ETH bio-activation in MTB strains.

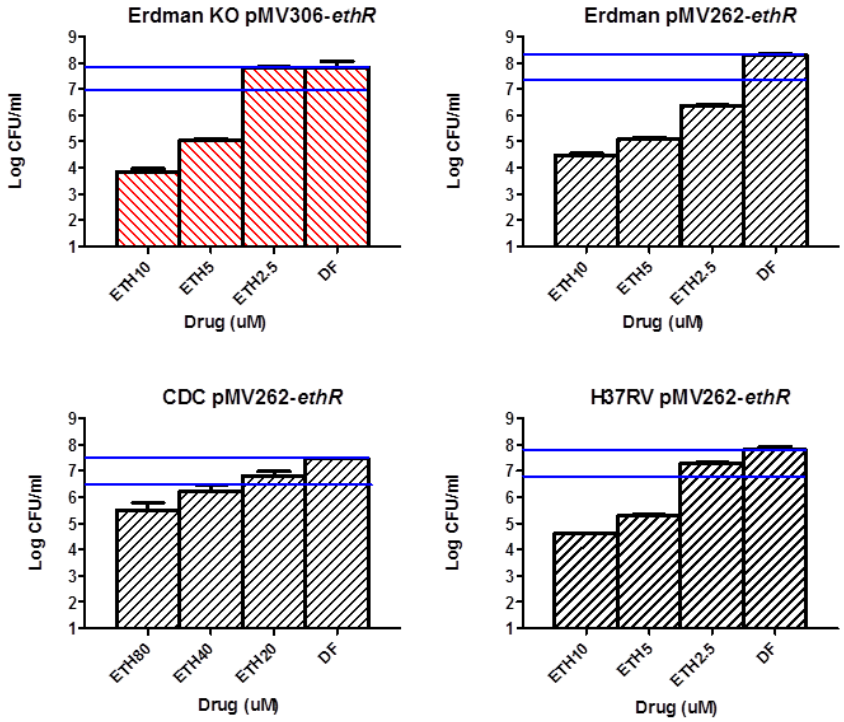

Figure 36: Minimum Bactericidal Concentration (MBC90) of ETH (in µm) in Erdman or CDC1551 ethA/R KO pMV306-ethR or Erdman or CDC1551 WT pMV262-ethR.

See experimental details in the legend of Fig. 34. DF, drug free. Solid lines represent 1 log change in CFU, ie. MBC90 values. DF = Drug-free.

	Parental strain	*ethA/R* KO	Complement *ethA/R*	pMV306-*ethR*	pMV262-*ethR*	*ethA* KO
CDC1551	2.5-5	20-40	ND	20-40	40	40
H37Rv	1.25-2.5	1.25-2.5	2.5-5	1.25-2.5	5	5
Erdman	1.25-2.5	2.5-5	ND	2.5-5	2.5	2.5

Table 7: Minimum Bactericidal Concentrations (MBC90) of Ethionamide (in µm) during in vitro culture.

See experimental details in the legend of Fig. 34.
pMV262-ethR: ethR was overexpressed in WT strains using replicative pMV262. pMV306-ethR: ethR was re-introduced into ethA/R KO mutants using integrative plasmid pMV306. The MBC90 was defined as the range of ETH concentration (in µM) within which 90% of the mycobacteria are killed compared to the drug-free control after 5 days incubation. ND: not determined.

4.6 Genomic Analyses of Spontaneous ETH mutants raised from Erdman ethA/R KO background

In order to identify the factors that are involved in the alternative pathway of ETH bio-activation in H37Rv and Erdman strains, spontaneous mutants that were highly resistant to ETH were generated from the Erdman *ethA/R* KO background. We reasoned that the absence of the *ethA/R* locus in the mutant should enable us to select for ETH^R clones for which a spontaneous mutation has occurred in a gene that is not involved in the classical EthA-dependent pathway of ETH bio-activation. Following the procedures described in section 3.3.5, passaged bacteria were plated onto agar plates containing a range of ETH concentrations (between 60-80μg/ml). Individual ETH^R colonies were picked and sub-cultured. Drug susceptibility assays were then determined for these ETH^R clones to confirm ETH resistance (data not shown).

Since InhA is the downstream target of activated ETH, a pre-screen was first conducted to exclude any spontaneous ETH^R mutants which harboured mutations in the *inhA* gene. Genomic DNA was extracted for PCR amplification and DNA sequencing of the *inhA* gene. Any spontaneous mutation that had occurred in this gene would have likely accounted for the observed ETH^R phenotype and was not of interest for this study. Out of the hundred clones analysed by PCR, only a handful of clones contained mutations in the *inhA* gene and were thus excluded. Notably, a large proportion of the spontaneous ETH^R mutants also could not be passaged *in vitro* and displayed weak growth in liquid media, hence these clones had to be excluded for full genome sequencing as well as it was technically impossible

to extract enough DNA from the cultures. The inability to passage these cultures suggests that the acquired mutations for these mutants were either unstable mutations or mutations in genes that are critical for growth.

Eventually, 2 clones with no mutation in *inhA* were selected and subjected to full genome sequencing (FGS). Although numerous mutations were identified through FGS, the list of mutations were restricted to insertion/deletions (INDELs) and non-synonymous SNPs (NS-SNPs), and further refined by eliminating NS-SNPs that resulted in conservative amino acid changes (ie. change to an amino acid with similar physiochemical properties) to eliminate as much noise and unspecific mutations as possible. These two clones were found to contain frameshift mutations in *mshA* caused by INDELs of a number of nucleotides. No other NS-SNPs were observed in these two clones when compared against the parental Erdman *ethA/R* KO strain, indicating that *mshA* is likely the gene accounting for ETH resistance. A second round of spontaneous ETH^R mutants was carried out independently applying the same exclusion criteria used for the first round and another 5 newly identified mutants were then subjected to full genome sequencing. This time, NS-SNPs in *mshA* were found in 4 out of 5 mutant clones, along with several other interesting genes candidates that could possibly account for ETH resistance as well (Table 9). A large proportion of the identified genes such as *galE3, cobD, plcB* and *pks5* were found to be involved in metabolism pathways. Another group of identified genes including *gltx, recD* and *topA* were involved in the transcriptional, translational and nucleotide assembly pathways; however these genes were eliminated due to their unlikely

involvement in ETH metabolism (as explained further in Section 4.2.10.2) (data not shown). Remaining identified genes such as Erdman_1484 and Erdman_0263 clones could not be categorized under any pathways and these genes remain unclassified.

While other gene candidates are worth further investigation as well, *mshA* was first selected for further characterization as *mshA* mutations had occurred at the highest frequency in six out of the seven clones. Previously, *mshA* mutations were shown to confer varying levels of co-resistance to INH and ETH in Mtb, after which MshA and its mycothiol associated pathway were suggested to play a role in ETH bio-activation (142). The same work has reported that *mshA* KO mutants in the Erdman, H37Rv and CDC1551 background are ETH^R. It was proposed that MshA is linked to ETH bio-activation due to its role in mycothiol biosynthesis. Interestingly, in both our current study and an independent group (38), only *mshA* mutations were obtained and not others in the mycothiol gene synthesis pathway including *mshB, mshC* or *mshD* during the generation of spontaneous ETH resistant mutants. However, the role of the glycosyltransferase MshA in ETH-mediated killing has yet to be described and understood fully and no further investigations had been made to analyze whether MshA action was associated with EthA-mediated ETH bio-activation. The identification of ETH^R *ethA/R* KO Erdman mutants with mutations in *mshA* here further affirms the role of MshA and mycothiol in ETH bio-activation and suggests that it may be in an *ethA/R*-independent fashion.

Gene Name	Gene	Known Function	Type of Mutations	Frequency of mutation
Erdman_0532	*mshA*	Mannosyl transferase	INDELs	2
			NS- SNPs	4
Erdman_3212	-	Malonyl CoA-acyl carrier protein transacylase	NS- SNPs	3
Erdman_0324	-	Transmembrane protein	NS- SNPs	2
Erdman_0263	-	Transmembrane protein	NS- SNPs	1
Erdman_0300	*fadE6*	Acyl-CoA dehydrogenase	NS- SNPs	1
Erdman_0588	*galE3*	UDP-glucose 4-epimerase	NS- SNPs	1
Erdman_0718	*fabD2*	Malonyl CoA-acyl carrier protein	NS- SNPs	1
Erdman_0819	-	Transcriptional regulator	NS- SNPs	1
Erdman_1118	*pabB*	Para-aminobenzoate synthase	NS- SNPs	1
Erdman_1484	-	Thioredoxin	NS- SNPs	1
Erdman_1488	*glgP*	Glycogen phosphorylase	NS- SNPs	1
Erdman_1647	*moxR1*	Transcriptional regulator	NS- SNPs	1
Erdman_1703	*pks5*	Polyketide synthase	NS- SNPs	1
Erdman_1821	*argB*	Acetylglutamate kinase	NS- SNPs	1
Erdman_2261	*pks12*	Polyketide synthase	NS- SNPs	1
Erdman_2377	*murE*	UDP-N-acetylmuramoylalanyl-D-glutamate-2,6-diaminopimelate ligase	NS- SNPs	1
Erdman_2459	*cobD*	Cobalamin biosynthesis protein	NS- SNPs	1
Erdman_2580	*plcB*	Membrane-associated phospholipase C	NS- SNPs	1
Erdman_2922	-	Prophage protein	NS- SNPs	1
Erdman_3922	-	Transcriptional regulator	NS- SNPs	1
Erdman_4115	*tyrA*	Prephenate dehydrogenase	NS- SNPs	1

Table 8: Mutations Identified from Spontaneous ETH-resistant mutants

Spontaneous ETH-resistant mutants were derived from a *M. tuberculosis* Erdman *ethA/R* KO mutant, screened for wild type *inhA* genes to exclude ETH^R mutants caused by *inhA* gene mutations, and 7 individual mutants were fully sequenced to identify novel genes involved in ETH bio-activation. Identified mutations were restricted to INDELs and NS- SNPs. The gene list was further refined by eliminating conservative NS-SNPs and excluding any hits in transcriptional, translational and nucleotide assembly pathways. Frequency of mutation indicates the number of mutants out of the 7 mutants sequenced that contains mutations in that particular gene. INDELS – Insertion/Deletion, NS-SNPs – non-synonymous single nucleotide polymorphisms. Gene name, gene and known function were referenced and extracted from Pubmed Genbank.
(http://www.ncbi.nlm.nih.gov/nuccore/379026087)

4.7 Analysis of mshA as a putative factor involved in the alternative pathway of ETH bio-activation in Mtb strains.

4.7.1 Construction, complementation and validation of *mshA* KO and *mshA/ethA/R* double KO mutants in Erdman, H37Rv and CDC1551

To verify the role of MshA in ETH bio-activation, the entire *mshA* locus was deleted from wild type *M. tuberculosis* Erdman, H37Rv and CDC1551, thus generating *mshA* single KO mutants. Furthermore, to investigate the role of MshA in the *ethA/R* KO mutants, *mshA* was also deleted in the *ethA/R* KO mutants. To do so, the *ethA/R* KO mutants were first unmarked to remove the hygromycin selection marker that had integrated at the *ethA/R* locus. Next, the unmarked *ethA/R* KO mutants underwent *mshA* deletion by classical double homologous recombination. This led to the generation of *mshA/ethA/R* (*m/e)* double KO mutants in all three backgrounds. All clones were verified by Southern blot (Fig. 36) and subsequently complemented with *hsp60-mshA* on the integrative plasmid pMV306, utilizing *hsp60* as its promoter since the native promoter of *mshA* remains uncharacterized (data not shown).

Growth kinetics profiles of the *M. tuberculosis* Erdman, H37Rv and CDC1551 *mshA* and *m/e* KO mutants in 7H9 and 7H9 supplemented with OADC were monitored over a period of 14 days. Expectedly, the *mshA* and *m/e* KO mutants were unable to grow in 7H9 supplemented with only ADS (bovine albumin-dextrose-sodium chloride) (Fig. 37D-F) as previously shown by Vilcheze *et al.* 2008 (38). Due to the presence of beef liver catalase in

OADC, growth of the mutants in 7H9 was restored with the addition of OADC in place of ADS as the growth supplement. Notably, in the presence of 7H9-OADC, Erdman parental, *mshA* and *m/e* KO mutants showed no differences in growth rate; however, H37Rv and CDC1551 *mshA* and *m/e* KO mutants displayed markedly attenuated growth rates in comparison to their respective parental strains particularly during the first 7 days of *in vitro* culture (Fig. 37A-C). Complementation of the KO mutants restored growth rates comparable to that of their parental strains (data not shown). Hence, we have verified that indeed, *M. tuberculosis* Erdman, H37Rv and CDC1551 *mshA* and *mshA/ethA/R* KO mutants require OADC to grow. Subsequently, all drug susceptibility assays involving *mshA* and *m/e* KO mutants were performed in 7H9-OADC.

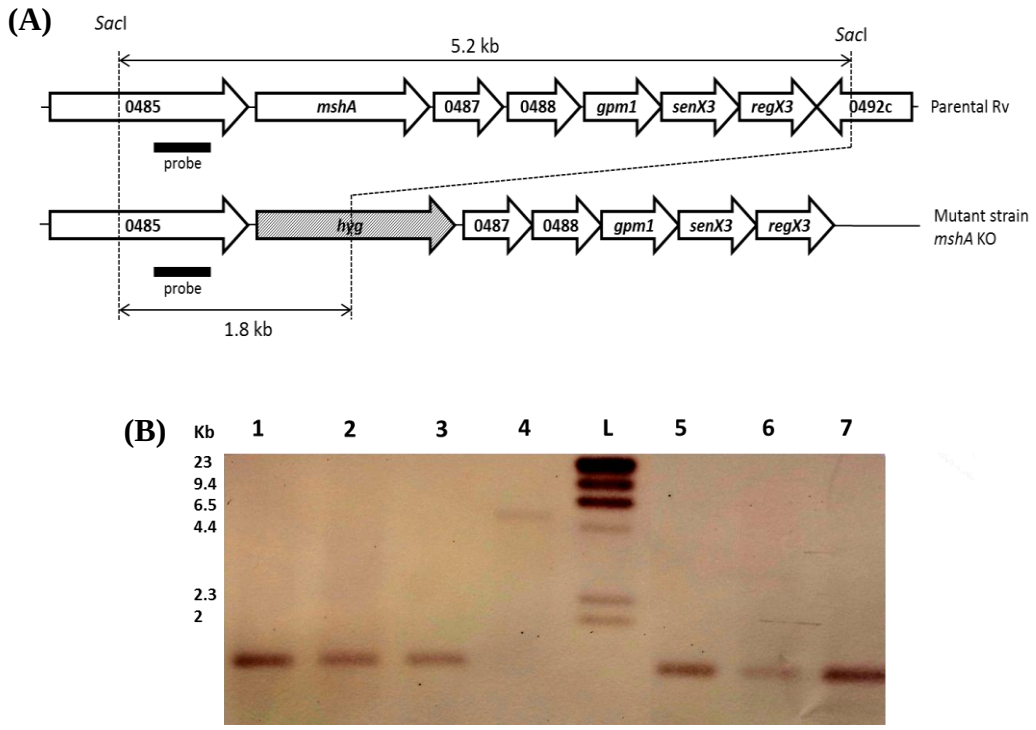

Figure 37: Construction of *mshA* KO and *mshA/ethA/R* double KO mutants in MTB Erdman, H37RV and CDC1551

A) Chromosomal organization of *mshA* was similar amongst all mutant strains. The arrows depict the lengths and directions of *mshA* and its neighbouring genes. Black bar corresponds to the probe used for Southern Blot analysis. B) Southern Blot analysis of chromosomal DNA. 1, MTB Erdman *mshA* KO; 2, MTB H37Rv *mshA* KO; 3, MTB CDC1551 *mshA* KO; 4, MTB CDC1551 WT ; L, DNA Molecular Ladder; 5, MTB Erdman *mshA/ethA/R* double KO; 6, MTB H37Rv *mshA/ethA/R* double KO; 3, MTB CDC1551 *mshA/ethA/R* double KO.

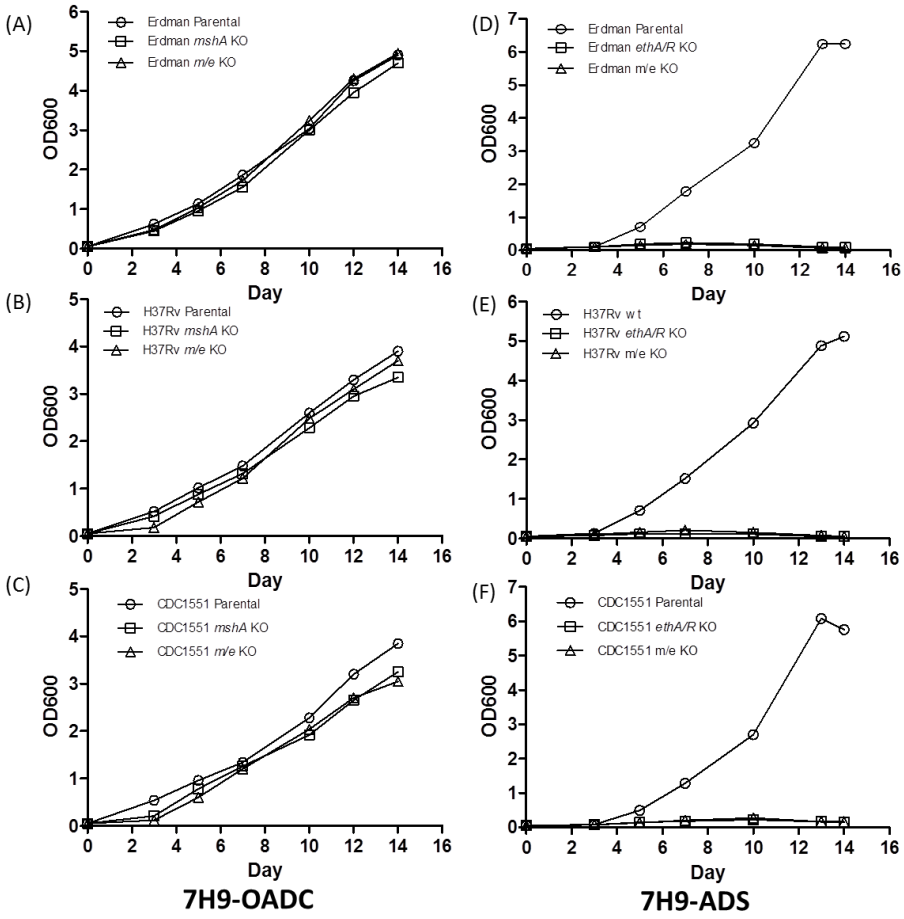

Figure 38: Growth Kinetics of *M. tuberculosis* Erdman, H37Rv and CDC1551 *mshA* KO and *mshA/ethA/R* double KO mutants in 7H9 OADC

Growth Kinetics of A) & D) *M. tuberculosis* Erdman, B &E) H37Rv, C &F) CDC1551 parental, *mshA* KO and *mshA/ethA/R (m/e)* double KO strains in 7H9 media supplemented with OADC (Left panel) or ADS (Right Panel) over a period of 14 days. After precultures were adjusted to the same starting OD600, strains were grown in 7H9 at 37˚C over a period of 14 days. Every 2-3 days, the OD was taken to determine the growth of each strain.

4.7.2 MshA is not involved in the alternative pathway of ETH bio-activation

To investigate the possible role of *mshA* in the alternative pathway for ETH bio-activation, drug susceptibility assays were conducted on the *mshA* single KO and *mshA ethA/R* (*m/e*) double KO mutants. The slower growth rates observed with the CDC1551 *mshA* and *m/e* KO mutants (Fig. 38) were taken into consideration by reading the plates at day 7 post-setup, instead of day 5 post-setup for the other strains with parental growth rates. Indeed, optimization studies showed that these mutants reached an OD_{600} at day 7 comparable to that of parental strain at day 5 in drug-free (DF) media, enabling unbiased comparison of MIC_{50} values (Table 11).

Remarkably, the combined absence of both *ethA/R* and *mshA* loci in all three MTB backgrounds abrogated ETH susceptibility, rendering the *m/e* double KO mutants completely resistant to ETH (Fig. 39 and Table 10). MIC_{50} values could not be obtained for these mutants since mycobacteria grew uninhibitedly even at the highest concentration of ETH (80µM) used (Table 10). These observations were supported by the lack of a dose-response curve (Fig. 39) and bacteria growth equivalent to that of untreated mycobacteria (data not shown) in all three *m/e* KO mutant strains. Re-introduction of *mshA* in the *m/e* KO mutants restored ETH susceptibility to levels similar to that observed with their respective *ethA/R* KO counterparts (Table 10). Thus, these data indicate that the combined removal of *mshA* and *ethA/R* loci in MTB leads to complete resistance to ETH, and further confirms the involvement of *mshA* in ETH killing efficacy.

Interestingly, deletion of *mshA* alone led to MIC_{50} values either comparable (Erdman background) or greater (H37Rv and CDC1551 backgrounds) than those obtained with their *ethA/R* KO counterparts (Fig. 39, Table 10). This observation thus suggests that *mshA* is at least, if not more; critical than the *ethA/R* locus for ETH killing efficacy. Complementation with *mshA* only partially restored the levels of ETH susceptibility, possibly due to the usage of *hsp60* promoter in place of its native promoter.

Additionally, and consistent with a previous report (179), the *mshA* KO mutants displayed mild increased resistance to INH with a 2-fold (Erdman) and 4-fold (H37Rv and CDC1551) increase of the MIC_{50} values compared to the parental strains (Table 10).

Together, these data confirm the contribution of *mshA* in ETH and (to a lower extent) INH killing efficacy in Mtb. In addition, the complete resistance to ETH upon deletion of *mshA* from *ethA/R* KO mutants suggests that the role of MshA in ETH killing efficacy is independent of EthA-mediated ETH bio-activation as previously proposed (42). These data thus further support that *mshA* is not involved in the alternative pathway of ETH bio-activation. Instead, since activated ETH and INH metabolites share the common drug target InhA, *mshA* may be involved in the latter steps of ETH drug action after its activation.

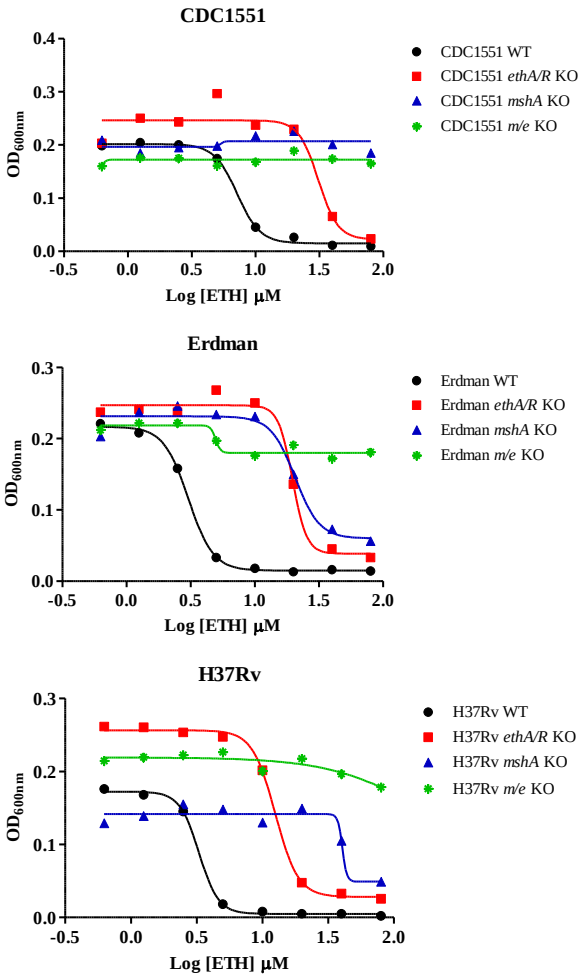

Figure 39: ETH MIC curves on *mshA* KO and *mshA ethA/R* double KO mutants.

Drug assays were set up in 96-well plates using a broth microdilution method and their OD600 values were read with a spectrophotometry microplate reader after 5-7 days. OD600 values were tabulated into PRISM for fitting of MIC curves, and MIC50 values were read from PRISM (Table 10).

Strain	INH	ETH
CDC1551	0.26	7.18
CDC1551 *ethA/R* KO	0.20	31.04
CDC1551 complement *ethA/R*	0.29	5.12
CDC1551 *mshA* KO	0.98	NA
CDC1551 complement *mshA*	0.43	11.82
CDC1551 *m/e* KO	0.57	NA
CDC1551 complement *m/e*	0.30	4.76
Erdman	0.18	3.04
Erdman *ethA/R* KO	0.18	19.69
Erdman complement *ethA/R*	0.17	2.67
Erdman *mshA* KO	0.49	20.63
Erdman complement *mshA*	0.28	5.42
Erdman *m/e* KO	0.37	NA
Erdman complement *m/e*	0.20	13.54
H37Rv	0.20	3.30
H37Rv *ethA/R* KO	0.28	12.55
H37Rv complement *ethA/R*	0.23	1.99
H37Rv *mshA* KO	0.85	40.67
H37Rv complement *mshA*	0.28	12.89
H37Rv *m/e* KO	0.80	NA
H37Rv complement *m/e*	0.27	11.12

Table 9: MIC50 values of INH and ETH on *mshA* KO and *mshA ethA/R* double KO mutants.

Drug assays were set up in 96-well plates using a broth microdilution method in 7H9-OADC and their OD600 values were read with a spectrophotometry microplate reader after 5 or 7 days. OD600 values were tabulated into PRISM for fitting of MIC curves, and MIC50 values were read from PRISM. NA = Not Available due to complete ETH resistance.

4.7.3 ETH drug susceptibility of Erdman *ethA/R* KO mutant varies in different nutritional supplements.

Due to the inability of *mshA* and *m/e* KO mutants to grow in 7H9 ADS, drug susceptibility assays involving these mutants were performed in 7H9-OADC. However, since the initial MIC values obtained in this work were generated in 7H9-ADS (Table 5), we re- established their MIC in 7H9-OADC to analyze for any differences in drug susceptibility in the presence of the 2 different supplements (Table 11). The MIC_{50} values obtained for INH were comparable regardless of the medium supplement (OADC or ADS) for the three MTB backgrounds (WT, *ethA/R* KO and complement) (Table 11). Similar MIC values for ETH were also observed with the three WT strains in both types of medium. However, the ETH MICs increased by 2-fold for all *ethA/R* KO mutants upon replacing ADS with OADC. Despite the greater resistance to ETH in the presence of OADC, dose-dependent drug susceptibility to ETH was nevertheless retained (data not shown). Therefore our data indicated that although some variation exists between the MIC values when using ADS or OADC as supplement, ETH susceptibility was still retained in the *ethA/R* KO MTB mutants.

	7H9-ADS		7H9-OADC	
	INH	ETH	INH	ETH
CDC1551	0.22	6.90	0.26	7.18
CDC1551 *ethA/R* KO	0.22	12.40	0.20	31.04
CDC1551 complement *ethA/R*	0.20	4.77	0.29	5.12
Erdman	0.15	3.89	0.18	3.04
Erdman *ethA/R* KO	0.11	9.29	0.18	19.69
Erdman complement *ethA/R*	0.12	3.25	0.17	2.67
H37Rv	0.20	3.30	0.20	3.30
H37Rv *ethA/R* KO	0.20	9.16	0.28	12.55
H37Rv complement *ethA/R*	0.19	3.1	0.23	1.99

Table 10: MIC_{50} values of INH and ETH in 7H9-ADS and 7H9-OADC.

Drug assays were set up in 96-well plates using a broth microdilution method and their OD600 values were read with a spectrophotometry microplate reader after 5-7 days. OD600 values were tabulated into PRISM for fitting of MIC curves, and MIC50 values were read from PRISM.

4.8 The EthA/R-independent alternative pathway of ETH bio-activation in M. tuberculosis Erdman and H37Rv strains does not involve other EthA-like BVMOs.

As mentioned earlier, EthA is a Bayer Villiger monooxygenase (BVMO) that metabolizes ETH into its active mycobactericidal compound. In addition to *ethA*, five other genes annotated in the H37Rv database (*rv1393c, rv3049c, rv0892, rv3083, rv0565c*) encode for proteins that display the BVMO signature motif (132, 176) and counterpart orthologs are also present in the genomes of the other Mycobacteria strains used in this study. Since BVMOs such as EthA are known to have broad substrate specificity, it is conceivable that the alternative ETH bio-activator present in these Mtb strains could also be a BVMO.

Taking into account that multiple *in vitro* passages occasionally lead to genetic mutations in the Mtb genome, the five BVMO-encoding genes in the Mtb and BCG strains used in this study were first fully sequenced to survey for any non-synonymous single nucleotide polymorphisms (SNPs) between the Mtb and BCG strains. Since BCG *ethA/R* KO was found to be completely resistant to ETH killing, we reasoned that should one of these putative BVMOs be involved in the alternative pathway of ETH bio-activation in MTB, differences at the DNA level may exist between the BCG and MTB strains. Using H37Rv as the reference genome, we therefore sequenced and compared all five other BVMO-encoding genes between the three MTB strains (CDC1551, Erdman, H37Rv) and BCG strain via BLAST (http://blast.ncbi.nlm.nih.gov/Blast.cgi). The BLAST results revealed 2 NS-

SNPs in *rv3083* (Ile81Ala and Val94Ile) between MTB strains and BCG. However, both NS-SNPs do not map within the 'Baeyer–Villigerase' (BVase) motif [FXGXXXHXXXW(P/D)] which is involved in the enzymatic activity of the protein (47). Therefore, these NS-SNPs are unlikely to account for a possible difference in the enzymatic activity of this putative BMVO between MTB and BCG strains.

In conclusion, the absence of significant differences at the DNA level of the five other BVMO-encoding genes between BCG and MTB strains argues against the hypothesis that one of these five BVMO-encoding genes may act as an alternative ETH bio-activator in MTB. In addition, the fact that none of these BVMO-encoding genes was identified upon FGS of the ETH^R spontaneous mutants further argues against their potential role in ETH bio-activation. Therefore, our data suggest that it is highly unlikely for the 5 other BVMO-encoding genes to be involved in the alternative pathway of ETH bio-activation identified in H37Rv and Erdman strains; however, the possibility of transcriptional or post-transcriptional modulation of these BVMOs cannot be ruled out.

4.9 Discussion

4.9.1 Comparison of ETH efficacy in vitro versus ex vivo

In the first part of this section, we observed an enhanced bactericidal effect of ETH and other thiocarbamide containing drugs during macrophage infection in contrast to *in vitro* conditions. Further investigations revealed that this effect could neither be accounted for by differential transcriptional activities of the *ethA/R* locus nor by spontaneous activation of ETH within the macrophages. Several other conjectures that could account for this interesting observation exist; however, these were not explored due to the technical limitations in our study.

Firstly, although the transcriptional activity of *ethA* and *ethR* was analyzed, post-transcriptional regulation or differential translational activity of these genes could have occurred which were not monitored in this study. Alternatively, thiocarbamide containing drugs may be able to accumulate better in macrophages, resulting in an actual intracellular drug concentration that is higher than that in the culture medium, thereby leading to an artefactual increase in drug killing efficacy. Lastly, it is proverbial that the physiology of Mtb varies widely in different microenvironments partly depending on the carbon and energy sources available. Naturally, the *in vitro* growth conditions versus the phagosomal environment vary greatly, which affects mycobacterial metabolism, thus possibly influencing ETH bio-activation. One manner in which ETH bio-activation could be affected could be an enhancement in the enzymatic activity of EthA in the presence of specific components that are only present in macrophages but not *in vitro.*

Yet, due to the difficulties in analysing pro-drug metabolism *in vivo*, to this date only 2 published reports exist on the study of ETH metabolism *in vivo* using this fairly new method of HRMAS-NMR by the same group (128, 131). Moreover, the challenges in studying these unstable and short-lived metabolites that are susceptible to oxidation coupled with the lack of understanding in ETH metabolism raises limitations in the use of this technique to study ETH bio-activation within the macrophage. Indeed, the macrophage environment varies vastly from the mycobacteria environment and thus it is difficult to conclude whether the lack of detection of ETH metabolites was due to a true inability of the macrophage to metabolize ETH, or the abundant amounts of reactive oxygen species (ROS) and reactive nitrogen intermediates (RNIs) present in macrophages that may have interfered with any intermediate metabolites the moment these were formed. Another theory that could be potentially challenging to investigate would be the metabolism of ETH being a synergistic reaction involving both the macrophage and the mycobacteria during macrophage infection.

Although the mechanisms behind these observed data are not fully deciphered yet, these findings can still be utilized to further our understanding of ETH bio-activation. As discussed in earlier sections, extremely high dosages of ETH (up to 10 times more than that of INH) are utilized for the treatment of MDR-TB in the clinical setting. Yet, the *in vitro* MIC value for ETH is 6-7 times lower than that of *ex vivo* MIC, in contrast to INH which displays the opposite trend (ie. *ex vivo* MIC is 4 times higher than *in vitro* MIC). This indicates that the co-incubation of Mtb-infected macrophages with

ETH is sufficient to achieve efficient and effective antibiotic effect, in contrast to previous deductions that the lower antibiotic activity of ETH as compared to INH was due to a generally lower efficiency of ETH bio-activation (180). Instead, these observations indirectly favour the counter theory, whereby the low bioavailability of ETH eventually results in poor drug distribution and thus, insufficient drug uptake by macrophages. While research efforts have been made in both aspects to either improve ETH efficacy by improving ETH bio-activation through the use of EthR inhibitors (149) or improving the drug formulation or delivery systems to reduce dosing frequency (which would reduce patient toxicity and improve patient compliance) (181), these findings give indication that perhaps the latter approach would be more feasible in the clinical setting with better clinical outcomes.

4.9.2 Molecular Mechanisms behind ETH Bio-activation

The second part of this section examines ETH drug susceptibility amongst *ethA/R* KO mutants in the BCG, Erdman, H37Rv and CDC1551 backgrounds in a bid to further analyze ETH bio-activation.Surprisingly, while BCG *ethA/R* KO mutant displayed complete resistance to ETH, ETH susceptibility and dose-dependent drug response to ETH were retained in the *ethA/R* KO MTB strains, with mild increase in their levels of resistance to ETH. Previous studies involving anti-mycobacterial pro-drugs INH and PZA have shown that absence of their respective bio-activators in MTB led to extremely high to complete levels of resistance (179, 182, 183). The reported MICs of INH for *katG*-deleted mutants and *katG* deficient MTB isolates (~80 mg/ml) (179) were 400 fold higher than the MIC measured with their WT and complemented counterparts (~0.02mg/ml), proving that deletion of *katG* is sufficient to confer high-level INH resistance (182). Similarly, PZA-resistant strains with *pncA*-encoded mutations that led to a loss in pyrazinamidase activity also displayed high levels of resistance to PZA, ranging from 100 to more than 800μg/ml versus 12.5 μg/ml in WT counterparts (183). Arguably, in the absence of their respective enzymatic bio-activator to convert these prodrugs into a catalytically active form, these stable and chemically inert drug forms are expected to remain inactive and non-bactericidal, thus accounting for the high to complete levels of drug resistance. Previous studies by Hanoulle *et al.* have shown that ETH is metabolized into an ETH-S-oxide derivate (ETH-SO) and ETH*, and subsequently into ETH-OH; out of which only ETH* was observed to accumulate exclusively within the bacterial cells

(128). On the other hand, ETH, ETH-SO and ETH-OH were found exclusively in the extracellular milieu, suggesting ETH* to be the prime active compound candidate for antibiotic action. Other than ETH*, all other ETH derivatives including prodrug ETH itself possess little or no anti-mycobactericidal activity (124, 130, 177, 184). Coupled with this knowledge, our data therefore challenge the paradigm of *ethA/R* locus as the sole player involved in ETH bio-activation in MTB (124, 127) and led us to propose the existence of an alternative pathway of ETH bio-activation independent of the *ethA/R* locus.

Although efforts were made in this study to compare the genome sequences of other BVMO-encoding genes amongst BCG and Mtb strains, no conclusive differences could be drawn between the strains. These findings led us to exclude the possibility of involvement of other BVMO-encoding genes in the alternative pathway of ETH bio-activation, although these genes cannot be ruled out completely either since their respective enzymatic activities in the various Mtb backgrounds has not been measured.

In fact, the genome of MTB encodes more than 30 putative monooxygenases which may have stemmed from evolution as a protective mechanism against various xenobiotic substances, leading Morlock *et al.* to contemplate the plausible existence of one or more enzymes with functional redundancy to EthA (124, 126, 127). The proliferation of these EthA homologs suggests that one or more of these enzymes may be capable of compensating for the loss of EthA for pro-drug function. However, the absence of NS-SNPs that map within the 'Baeyer–Villigerase' (BVase) motif [FXGXXXHXXXW(P/D)] and the absence of these BVMO-encoding genes

upon FGS of the ETH^R spontaneous mutants led us to exclude the likelihood of other BVMOs possessing analgous roles to EthA. Yet, these genes cannot be ruled out completely either since their respective enzymatic activities in the various Mtb backgrounds has not been measured. Transcriptional and post-transcriptional modulation of these BVMOs in similar *in vitro* conditions should be conducted to further validate this notion. Henceforth, we searched for novel factors that could account for additional mechanisms of ETH resistance by generating spontaneous ETH-resistant mutants from the lowly resistant Erdman *ethA/R* KO mutant and identified several potentially interesting gene candidates. Out of this list, MshA was selected as the pilot gene for further investigation in this thesis due to the existence of previous literature that suggested a role for this gene in ETH resistance (38).

ETH susceptibility assays of the *mshA* single KO and *mshA/ethA/R* double KO mutants revealed that the role of *mshA* in ETH killing efficacy was independent of *ethA/R*-mediated ETH bio-activation, and suggest that MshA and the mycothiol pathway play a role in ETH killing efficacy after ETH bio-activation. The different drug susceptibility profiles of ETH obtained from both sets of Mtb strains highlight the fact that different Mtb strains display very different phenotypes and raises a possible necessity to study various Mtb strains in future drug susceptibility assays instead of just one reference strain in order to further understand the complexity of drug resistance mechanisms in Mtb strains.

While clinical isolates resistant to ETH have been associated with mutations in its activator gene *ethA*, its molecular target *inhA* , and others, a

number of studies have reported that up to 20-50% of the ETH^R Mtb clinical isolates harbour no mutations in genes known to be involved in ETH resistance (126, 138, 149), adverting that the mechanisms involved in ETH bio-activation are more complicated than initially thought, thus supporting that additional investigation is necessary to fully decipher the molecular and genetic players. Also, despite the recent discovery of *mshA* as a novel player involved in ETH resistance, even then, few ETH^R clinical isolates were found to carry mutations in this gene; likely due to a loss of fitness in these mutants with the lack of mycothiol as a detoxification mechanism against toxic ROS (38). A very recent study found that only 1 out of 47 ETH^R clinical isolates (2%) harboured a mutation in *mshA.* Even more intriguing was the presence of 8 out of 47 isolates (17%) that had no mutations in any of the genes so far known to be involved in ETH activation (126, 129), suggesting that the mechanisms of ETH bio-activation in *M. tuberculosis* are more complex than initially thought and have yet to be deciphered. Furthermore, in a recent study on Mtb clinical isolates, investigators described ETH^R clinical isolates with wild type *ethA* gene but *inhA* promoter mutations which displayed varying levels of ETH resistance (138). The authors reported that 6 out of 15 isolates presented with unusually high levels of ETH resistance (100µg/ml) and proposed that this should not exclusively be attributed to the *inhA* promoter mutations, but rather, to an alternative mechanism of ETH resistance. Lastly, Baulard *et al.* have recently identified ETH boosters that appear to boost ETH bio-activation by turning on the transcription of a novel pathway for ETH bio-activation; but yet do not bind to EthR, giving rise to more evidence for the

existence of an alternative pathway of ETH bio-activation (Baulard, personal communication). Certainly, the combinations of all these findings taken together with the data presented here culminate in a highly plausible existence of an alternative pathway for ETH bio-activation.

In order to ascertain whether this hypothesized alternative activator has synonymous catalytic activity to EthA, one possible direction would be to use HRMAS-NMR as was previously done (131) to trace the fate of ETH and its derivative metabolites in the *ethA/R* KO Erdman and H37Rv mutants. Detection of similar metabolites as those found in the parental strain in the mutant would be a strong indication of the presence of an EthA-like activator in these mutants. Alternatively, an indirect way to confirm the presence of this hypothesized pathway would be to analyse the downstream effects of activated ETH by detecting by TLC for any possible inhibition of FAMEs and MAMEs in the *ethA/R* KO Erdman or H37Rv mutants, which has been shown previously to be inhibited only in the presence of ETH in its activated form (91).

Since MshA and its mycothiol-associated pathway were previously proposed to be involved in ETH bio-activation (142), we decided to ascertain its role in the alternative pathway of ETH bio-activation. Earlier studies observed an increase in the rate of NADPH-dependent mono-oxygenation of ETH by recombinant EthA that is directly proportional to the increase in mycothiol concentration, suggesting that mycothiol plays a role in the activation steps of ETH rather than in the formation of the ETH-NAD adduct (142). The findings presented in our study have demonstrated that removal of

mshA led to high levels of ETH resistance in all 3 Mtb strains. In fact, removal of *mshA* alone resulted in higher levels of ETH resistance than removal of the *ethA/R* locus in all the Mtb backgrounds including CDC1551 strain where a functional alternative pathway of ETH bio-activation is likely inexistent, therefore suggesting that *mshA* is not involved in ETH bio-activation. Furthermore, the low resistant phenotype to ETH in the Erdman and H37Rv *ethA/R* KO mutants shifted to full resistance to ETH upon deletion of *mshA*, suggesting that *mshA* may instead be involved in the downstream steps after ETH bio-activation. It is plausible that the final product of MshA, mycothiol, either stabilizes the formation of ETH intermediates or forms a complex with activated ETH as previously suggested by Vilcheze *et al.* (38),for which more in-depth studies will be necessary. Taking all these findings together, the totally ETH resistant phenotypes of the double *mshA/ethA/R* KO mutants and high ETH resistance phenotypes of the single *mshA* KO mutants in contrast to the low ETH resistance phenotypes of Erdman and H37Rv *ethA/R* KO mutants suggest that *mshA* plays a critical role in ETH killing efficacy. Additionally, these discoveries also further validate MshA and its mycothiol associated pathway as novel potential drug targets with the ultimate goal to enhance sensitivity to not only ETH but also to INH, by synthesizing compounds that lead to enhanced MshA expression levels. A similar approach has been reported with EthR inhibitors whereby small molecules able to inhibit EthR were shown to lead to increased EthA expression levels thereby improving the ETH bio-activation rate (149).

Taking all these data together, these conclusions raise the necessity to revisit the ETH bio-activation pathway in mycobacteria, which has been outlined in Figure 39. It appears that while MshA and its mycothiol-associated pathway are critical for ETH killing activity, their involvement would occur at a later stage, ie. after ETH bio-activation and after the formation of ETH metabolites. Previous studies found that EthA was able to metabolize thiacetazone into either a sulfenic acid intermediate under acidic/neutral conditions or a carbodiimide metabolite under basic conditions; and both metabolites readily react with glutathione (GSH) to either regenerate the parent drug for the former metabolite, or form a GSH-adduct for the latter (178). Since mycothiol is the mycobacterial analogue for GSH and EthA has also been shown to oxidize ETH into a sulfenic acid metabolite (130), ETH metabolites could react with mycothiol in a similar manner. Consequently, one could further speculate that such a reaction would either stabilize these reactive ETH metabolites or help in drug recycling, or perhaps even lower the intracellular concentration of MSH thus sensitizing mycobacteria to oxidative damage, or culminate in a combination of all three consequences. Furthermore, previous studies have demonstrated the lack of formation of the ETH-NAD adduct in the presence of recombinant EthA with NAD+, NADPH and mycothiol by monitoring the rate of inhibition of InhA (38), supporting that MSH is unlikely to be involved in the downstream formation of the ETH-NAD adduct. In light of our findings and the proposed role of mycothiol in ETH mycobactericidal activity, it is likely that the alternative pathway of ETH bio-activation identified in the Erdman and H37Rv strains still requires an

enzyme or protein conjugate of some sort to assist in the formation of ETH metabolites that has yet to be identified.

On that account, other novel genes have been identified through sequencing analysis of the spontaneous ETH^R mutants generated in this study, and it would be interesting to investigate their roles in ETH resistance upon further validation of these mutations via DNA sequencing in the respective mutants. It is possible that some of these hits could contribute to the alternative pathway of ETH bio-activation, in particular metabolism-related genes with similar catalytic activities as EthA; however we did not identify such genes in our list. We also ruled out genes involved in transcriptional, translational and nucleotide assembly pathways since it is highly likely that these mutations are most probably non-specific mutations that arose during the numerous rounds of passage; however, we cannot completely rule out the possible involvement of unknown transcriptional regulators such as Erdman_0819 and Erdman_3922 that may play a role in regulation of this pathway. Subsequent more interesting gene candidates worth studying apart from *mshA* would be Erdman_1484, a gene encoding for thioredoxin. Interestingly, in *Streptomyces coelicolour*, the amount of MSH has been shown to be under the control of a sigma factor σ^R, which is regulated by an antisigma factor RsrA via a thiol-disulphide redox switch involving thioredoxin (185);thus suggesting that such a thiol-disulphide redox switch may exist in mycobacteria as well, hence affecting mycothiol levels and subsequently causing ETH resistance. Moreover, since mycobacterial thioredoxins have been demonstrated to serve regulatory functions as

disulphide reductants that affect the metabolism of mycobacteria(186, 187), characterization of this gene may provide further insights into ETH bio-activation as well. Additionally, since small thiol molecules do not appear to be directly associated with the thioredoxin system in bacteria unlike that in mammalian cells (188), one could also speculate that thioredoxin may facilitate redox reactions specifically involved in the alternative pathway of ETH bio-activation, although biochemical studies would be necessary to explore this possibility. All things considered, this list of genes is undeniably worth further exploration for other novel factors influencing ETH killing efficacy.

Finally, we also discovered that the choice of nutrient supplement used when conducting ETH susceptibility assays can influence the outcome for the *ethA/R* KO mutants. The use of the nutritional supplement OADC causes Mtb *ethA/R* KO strains to develop slightly increased drug resistance towards ETH but not INH, whilst ADS allows mycobacteria to display a less resistant phenotype to ETH. The main differences in the 2 supplements are the additional beef catalase and oleic acid present in OADC that ADS lacks. In light of these findings, we reasoned that either of these additional components, more likely the catalase due to its involvement in detoxification processes, could also be contributing to ETH resistance. Should mycothiol and catalase affect ETH bio-activation in a similar manner due to their similarities in antioxidant functions (189), one would expect the addition of catalase to enhance ETH susceptibility in all Mtb strains (since removal of the *mshA* locus increased ETH resistance in all Mtb strains). On the contrary, the

addition of OADC increased ETH resistance in all 3 Mtb *ethA/R* KO mutants. The contrasting effect observed between MSH and OADC indicates that the mycothiol pathway and OADC affect ETH bio-activation via completely different modes of action. It seems likely that the beef catalase present in OADC may be implicated in the alternative pathway of ETH bio-activation, likely through the detoxification of ETH metabolites. Since catalases display high capacities in removing hydrogen peroxide which is a toxic by product of many metabolic reactions (190), this set of findings further supports the presence of an alternative pathway of ETH metabolism in Mtb which could explain the indirect effect of catalase in the alternative pathway of ETH bio-activation. Further studies would be necessary to verify this idea. Of note, most published studies on ETH resistance utilized OADC as their nutritional supplement of choice (124, 142).

Our work has demonstrated several novel findings. Firstly, it is worth to note that previous studies provided only indirect genetic evidence of the involvement of EthA/R in ETH bio-activation through either over-expression of *ethA* or *ethR*, or through *ethR* deletion in *M. bovis* BCG (124, 127). Here instead, we demonstrate for the first time that deletion of the entire *ethA/R* locus in MTB and BCG strains led to increased resistance to ETH, thus further confirming the crucial role of this locus in ETH bio-activation. Secondly, and less expectedly, the retained susceptibility to ETH in *ethA/R* KO MTB mutants led us to propose the existence of an alternative pathway of ETH bio-activation. Finally, while our data confirm the importance of MshA and the mycothiol pathway in ETH killing efficacy, they do not support its

involvement in EthA-mediated ETH bio-activation as previously proposed, and rather suggest that MshA and the mycothiol pathway act at a later step, after formation of the ETH cidal metabolite, ETH*. Hence, this work raises the necessity to revisit the ETH bio-activation pathway in pathogenic mycobacteria and calls for further investigation.

Chapter 5: Concluding Remarks

In closing, this thesis has explored the varying importance of the *ethA/R* locus for host virulence and drug susceptibility in several strains of Mtb. Characterization of the varied virulence profiles have demonstrated an indirect role for the *ethA/R* locus in virulence amongst specific Mtb strains; whilst the heterogeneous ETH resistance phenotypes obtained from the various Mtb *ethA/R* KO mutant strains have unexpectedly revealed an alternative mechanism for ETH bio-activation in certain Mtb strains. Although we have identified critical roles for the *ethA/R* locus in BCG and CDC1551 in terms of both host virulence and ETH drug susceptibility; conversely, the *ethA/R* locus appears to be less essential for both host virulence and ETH susceptibility in Erdman. While further in-depth studies will be necessary to verify this, we hypothesize either the presence of a compensatory factor for EthA that exists in Erdman and H37Rv but is absent in BCG and CDC1551, or the existence of additional detoxification mechanisms in BCG and CDC1551 that could simultaneously account for an increased resistance of CDC1551 and BCG against ROS and RNI. Considering the discovery of several other novel gene candidates that may potentially contribute to ETH drug resistance mechanisms from our pre-screens and the drug susceptibility profiles of these spontaneous ETH-resistant mutants being specific to ETH only, the former hypothesis is favoured; and further research in this area could reveal novel drug targets or aid in molecular diagnostics for the screening of MDR-TB in future.

Another recurrent issue raised in this thesis is the importance of selecting an appropriate and representative Mtb strain for experimental studies as reflected by the varying virulence and drug susceptibility phenotypes obtained amongst different Mtb strains. Though consisting of genetically related

members, the genome diversity amongst individual members varies considerably, and a minor amino acid or frameshift variant could have consequential effects. This decision should be dependent on factors such as the type of study being conducted, the available resources and the relative importance of future outcomes to the clinical setting. On hindsight, the study of virulence factors for Mtb should optimally utilize virulent *M. tuberculosis* strains and not avirulent BCG for more clinically relevant findings. Drug susceptibility and mechanism studies should not be limited to a single strain, but instead encompass a broad spectrum of Mtb strains in order to glean a better understanding of drug response in clinical settings that typically involve unidentified clinical Mtb isolates. Care should also be taken to not overgeneralize findings from mechanism studies based on just a single strain as these outcomes may not necessarily be extrapolated to other Mtb strains.

Lastly, we propose novel modifications in the mechanism for ETH bio-activation in mycobacteria upon consolidation of all findings in this thesis. Our findings in the first section suggest the existence of a compensatory factor for the *ethA/R* locus in Mtb strains that BCG lack. Assuming that this compensatory factor is innate and may also play a role in the alternative pathway of ETH bio-activation that may be further linked to MshA downstream, subsequent data from the second section of this thesis further supports this theory. Thus, based on existing literature and this thesis, ETH bio-activation should be reconsidered as a 2-step pathway (Fig. 40), with 1) the formation of unstable and reactive ETH metabolites; and 2) subsequent formation of the activated ETH, ETH*. Mycothiol appears to be implicated in the second step of this pathway downstream of ETH bio-activation, possibly

by stabilizing either intermediate ETH metabolites or ETH*. An alternative pathway of ETH bio-activation is proposed as well, with the possible involvement of catalase or its substrate, hydrogen peroxide, in the X pathway of ETH metabolism. These unexplored modifications warrant further research potential and specify novel investigative directions in further understanding ETH bio-activation.

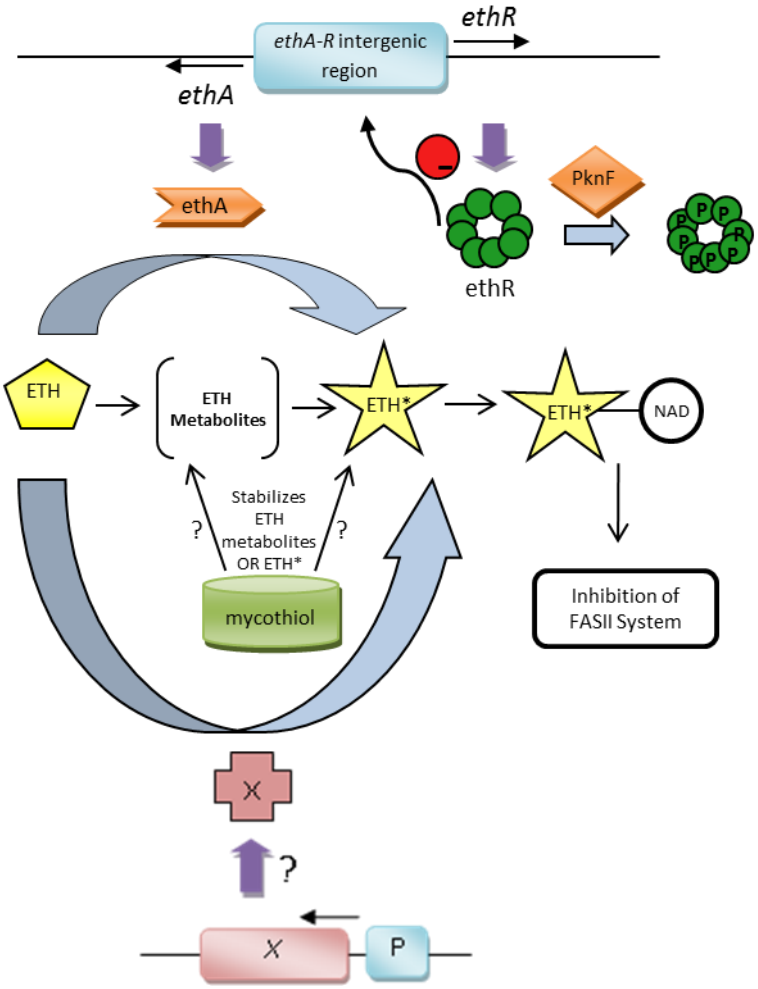

Figure 40: Existing and Proposed Alternative Pathway of ETH Bio-activation in *Mycobacterium tuberculosis*

ETH is activated by the monooxygenase EthA into its activated form, ETH*, for its antibiotic action. The expression of EthA is regulated by the transcriptional repressor EthR, and both ethA and ethR are located in the same operon with a shared intergenic promoter region. EthR dimers bind cooperatively as a homo-octamer to the specific operator in the ethA-ethR intergenic promoter region, repressing both ethA and ethR expression. A mycobacteria serine/threonine protein kinase (STPK) negatively regulates the physical binding of EthR to the DNA region via phosphorylation of the EthR homo-octamer, hence promoting ethA-ethR expression. Additionally, the mycothiol synthesis pathway and its end product, mycothiol, have been implicated in ETH bio-activation as well. Based on existing reports and this thesis, ETH activation should be considered as a 2-step pathway, with 1) the formation of unstable and reactive ETH metabolites; and 2) subsequent formation of the activated ETH, ETH*. Mycothiol appears to be implicated in the second step of this pathway, by stabilizing either ETH metabolites or ETH*. An alternative pathway of ETH bio-activation is proposed as well

References

1. **Zumla A, Mwaba P, Huggett J, Kapata N, Chanda D, Grange J.** 2009. Reflections on the white plague. Lancet Infect Dis **9:**197-202.
2. **Zumla A.** 2011. The white plague returns to London--with a vengeance. Lancet **377:**10-11.
3. **WHO.** 2011. Global tuberculosis control: WHO report 2011. World Health Organization, Press W, 20 Avenue Appia, 1211 Geneva 27, Switzerland.
4. **Dye C.** 2006. Global epidemiology of tuberculosis. Lancet **367:**938-940.
5. **Zumla A, George A, Sharma V, Herbert N, Baroness Masham of Ilton.** 2013. WHO's 2013 global report on tuberculosis: successes, threats, and opportunities. Lancet **382:**1765-1767.
6. **Farmer P, Bayona J, Becerra M, Furin J, Henry C, Hiatt H, Kim JY, Mitnick C, Nardell E, Shin S.** 1998. The dilemma of MDR-TB in the global era. Int J Tuberc Lung Dis **2:**869-876.
7. **WHO.** 2013. WHO Global Tuberculosis Report 2013. World Health Organization, 20 Avenue Appia, 1211 Geneva 27, Switzerland.
8. **Viskum K, Kok-Jensen A.** 1997. Multidrug-resistant tuberculosis in Denmark 1993-1995. Int J Tuberc Lung Dis **1:**299-301.
9. **Bass JB, Jr., Farer LS, Hopewell PC, O'Brien R, Jacobs RF, Ruben F, Snider DE, Jr., Thornton G.** 1994. Treatment of tuberculosis and tuberculosis infection in adults and children. American Thoracic Society and The Centers for Disease Control and Prevention. Am J Respir Crit Care Med **149:**1359-1374.
10. **Sahbazian B, Weis SE.** 2005. Treatment of active tuberculosis: challenges and prospects. Clin Chest Med **26:**273-282, vi.
11. **Falzon D, Jaramillo E, Schünemann HJ, Arentz M, Bauer M, Bayona J, Blanc L, Caminero JA, Daley CL, Duncombe C, Fitzpatrick C, Gebhard A, Getahun H, Henkens M, Holtz TH, Keravec J, Keshavjee S, Khan AJ, Kulier R, Leimane V, Lienhardt C, Lu C, Mariandyshev A, Migliori GB, Mirzayev F, Mitnick CD, Nunn P, Nwagboniwe G, Oxlade O, Palmero D, Pavlinac P, Quelapio MI, Raviglione MC, Rich ML, Royce S, Rüsch-Gerdes S, Salakaia A, Sarin R, Sculier D, Varaine F, Vitoria M, Walson JL, Wares F, Weyer K, White RA, Zignol M.** 2011. WHO guidelines for the programmatic management of drug-resistant tuberculosis: 2011 update. Eur Respir J **38:**516-528.

12. **Fattorini L, Piccaro G, Mustazzolu A, Giannoni F.** 2013. Targeting dormant bacilli to fight tuberculosis. Mediterr J Hematol Infect Dis **5:**e2013072.

13. **Ray S, Talukdar A, Kundu S, Khanra D, Sonthalia N.** 2013. Diagnosis and management of miliary tuberculosis: current state and future perspectives. Ther Clin Risk Manag **9:**9-26.

14. **Mandell GL, Douglas RG, Bennett JE, Dolin R, Brause BD, Fitzgerald DW, Hartman BJ, Johnson WD, Pamer EG, Rhee KY, Salvatore M, Sepkowitz KA.** 2010. Mandell, Douglas, and Bennett's principles and practice of infectious diseases, 7th ed. Churchill Livingstone/Elsevier, Philadelphia, PA.

15. **Hirayama Y, Yoshimura M, Ozeki Y, Sugawara I, Udagawa T, Mizuno S, Itano N, Kimata K, Tamaru A, Ogura H, Kobayashi K, Matsumoto S.** 2009. Mycobacteria exploit host hyaluronan for efficient extracellular replication. PLoS Pathog **5:**e1000643.

16. **Ernst JD.** 1998. Macrophage receptors for Mycobacterium tuberculosis. Infect Immun **66:**1277-1281.

17. **Aoki K, Matsumoto S, Hirayama Y, Wada T, Ozeki Y, Niki M, Domenech P, Umemori K, Yamamoto S, Mineda A, Matsumoto M, Kobayashi K.** 2004. Extracellular mycobacterial DNA-binding protein 1 participates in mycobacterium-lung epithelial cell interaction through hyaluronic acid. J Biol Chem **279:**39798-39806.

18. **Bermudez LE, Goodman J.** 1996. Mycobacterium tuberculosis invades and replicates within type II alveolar cells. Infect Immun **64:**1400-1406.

19. **Teitelbaum R, Schubert W, Gunther L, Kress Y, Macaluso F, Pollard JW, McMurray DN, Bloom BR.** 1999. The M cell as a portal of entry to the lung for the bacterial pathogen Mycobacterium tuberculosis. Immunity **10:**641-650.

20. **Saiga H, Nishimura J, Kuwata H, Okuyama M, Matsumoto S, Sato S, Matsumoto M, Akira S, Yoshikai Y, Honda K, Yamamoto M, Takeda K.** 2008. Lipocalin 2-dependent inhibition of mycobacterial growth in alveolar epithelium. J Immunol **181:**8521-8527.

21. **Griffiths G, Nyström B, Sable SB, Khuller GK.** 2010. Nanobead-based interventions for the treatment and prevention of tuberculosis. Nat Rev Microbiol **8:**827-834.

22. **Barry CE, Boshoff HI, Dartois V, Dick T, Ehrt S, Flynn J, Schnappinger D, Wilkinson RJ, Young D.** 2009. The spectrum of latent tuberculosis: rethinking the biology and intervention strategies. Nat Rev Microbiol **7:**845-855.

23. **Locht C, Rouanet C, Hougardy JM, Mascart F.** 2007. How a different look at latency can help to develop novel diagnostics and vaccines against tuberculosis. Expert Opin Biol Ther **7:**1665-1677.

24. **Gengenbacher M, Kaufmann SH.** 2012. Mycobacterium tuberculosis: success through dormancy. FEMS Microbiol Rev **36:**514-532.

25. **Dannenberg J, Arthur M.** 2006. Stages in the Pathogenesis of Human and Rabbit Tuberculosis, p 22-33, Pathogenesis of Human Pulmonary Tuberculosis. American Society of Microbiology.

26. **Cardona PJ, Ruiz-Manzano J.** 2004. On the nature of Mycobacterium tuberculosis-latent bacilli. Eur Respir J **24:**1044-1051.

27. **Russell DG.** 2007. Who puts the tubercle in tuberculosis? Nat Rev Microbiol **5:**39-47.

28. **Galagan JE.** 2014. Genomic insights into tuberculosis. Nat Rev Genet **15:**307-320.

29. **Fox GJ, Barry SE, Britton WJ, Marks GB.** 2013. Contact investigation for tuberculosis: a systematic review and meta-analysis. Eur Respir J **41:**140-156.

30. **Barry CE.** 2001. Interpreting cell wall 'virulence factors' of Mycobacterium tuberculosis. Trends Microbiol **9:**237-241.

31. **Dannenberg J, Arthur M., Rook GAW.** 1994. Pathogenesis of Pulmonary Tuberculosis: an Interplay of Tissue-Damaging and Macrophage-Activating Immune Responses—Dual Mechanisms That Control Bacillary Multiplication, p 459-483, Tuberculosis. American Society of Microbiology.

32. **Wellcome Images.** Retrieved from: http://wellcomeimages.org/indexplus/obf_images/5d/40/f87e040d6d72e470506f4d930f45.jpg

33. **Marais BJ, Brittle W, Painczyk K, Hesseling AC, Beyers N, Wasserman E, van Soolingen D, Warren RM.** 2008. Use of light-emitting diode fluorescence microscopy to detect acid-fast bacilli in sputum. Clin Infect Dis **47:**203-207.

34. **Cuevas LE, Al-Sonboli N, Lawson L, Yassin MA, Arbide I, Al-Aghbari N, Sherchand JB, Al-Absi A, Emenyonu EN, Merid Y, Okobi MI, Onuoha JO, Aschalew M, Aseffa A, Harper G, de Cuevas RM, Theobald SJ, Nathanson CM, Joly J, Faragher B, Squire SB, Ramsay A.** 2011. LED fluorescence microscopy for the diagnosis of pulmonary tuberculosis: a multi-country cross-sectional evaluation. PLoS Med **8:**e1001057.

35. **Steingart KR, Henry M, Ng V, Hopewell PC, Ramsay A, Cunningham J, Urbanczik R, Perkins M, Aziz MA, Pai M.** 2006. Fluorescence versus conventional sputum smear microscopy for tuberculosis: a systematic review. Lancet Infect Dis **6:**570-581.

36. **Bonnet M, Gagnidze L, Guerin PJ, Bonte L, Ramsay A, Githui W, Varaine F.** 2011. Evaluation of combined LED-fluorescence microscopy and bleach sedimentation for diagnosis of tuberculosis at peripheral health service level. PLoS One **6:**e20175.

37. **Wayne LG, Hayes LG.** 1996. An in vitro model for sequential study of shiftdown of Mycobacterium tuberculosis through two stages of nonreplicating persistence. Infect Immun **64:**2062-2069.

38. **Vilcheze C, Av-Gay Y, Attarian R, Liu Z, Hazbon MH, Colangeli R, Chen B, Liu W, Alland D, Sacchettini JC, Jacobs WR, Jr.** 2008. Mycothiol biosynthesis is essential for ethionamide susceptibility in Mycobacterium tuberculosis. Mol Microbiol **69:**1316-1329.

39. **Ryan GJ, Shapiro HM, Lenaerts AJ.** 2014. Improving acid-fast fluorescent staining for the detection of mycobacteria using a new nucleic acid staining approach. Tuberculosis (Edinb) **94:**511-518.

40. **Frothingham R, Hills HG, Wilson KH.** 1994. Extensive DNA sequence conservation throughout the Mycobacterium tuberculosis complex. J Clin Microbiol **32:**1639-1643.

41. **Colditz GA, Brewer TF, Berkey CS, Wilson ME, Burdick E, Fineberg HV, Mosteller F.** 1994. Efficacy of BCG vaccine in the prevention of tuberculosis. Meta-analysis of the published literature. JAMA **271:**698-702.

42. **Stover CK, de la Cruz VF, Fuerst TR, Burlein JE, Benson LA, Bennett LT, Bansal GP, Young JF, Lee MH, Hatfull GF.** 1991. New use of BCG for recombinant vaccines. Nature **351:**456-460.

43. **Forrellad MA, Klepp LI, Gioffré A, Sabio y García J, Morbidoni HR, de la Paz Santangelo M, Cataldi AA, Bigi F.** 2013. Virulence factors of the Mycobacterium tuberculosis complex. Virulence **4:**3-66.

44. **Mahairas GG, Sabo PJ, Hickey MJ, Singh DC, Stover CK.** 1996. Molecular analysis of genetic differences between Mycobacterium bovis BCG and virulent M. bovis. J Bacteriol **178:**1274-1282.

45. **Takayama K, Wang L, David HL.** 1972. Effect of isoniazid on the in vivo mycolic acid synthesis, cell growth, and viability of Mycobacterium tuberculosis. Antimicrob Agents Chemother **2:**29-35.

46. **Strain SM, Toubiana R, Ribi E, Parker R.** 1977. Separation of the mixture of trehalose 6,6'-dimycolates comprising the mycobacterial glycolipid fraction, "P3". Biochem Biophys Res Commun **77:**449-456.

47. **Coscolla M, Gagneux S.** 2010. Does M. tuberculosis genomic diversity explain disease diversity? Drug Discov Today Dis Mech **7:**e43-e59.

48. **Betts JC, Dodson P, Quan S, Lewis AP, Thomas PJ, Duncan K, McAdam RA.** 2000. Comparison of the proteome of Mycobacterium tuberculosis strain H37Rv with clinical isolate CDC 1551. Microbiology **146 Pt 12:**3205-3216.

49. **Domenech P, Reed MB.** 2009. Rapid and spontaneous loss of phthiocerol dimycocerosate (PDIM) from Mycobacterium tuberculosis grown in vitro: implications for virulence studies. Microbiology **155:**3532-3543.

50. **Wolf AJ, Linas B, Trevejo-Nuñez GJ, Kincaid E, Tamura T, Takatsu K, Ernst JD.** 2007. Mycobacterium tuberculosis infects dendritic cells with high frequency and impairs their function in vivo. J Immunol **179:**2509-2519.

51. **Armstrong JA, Hart PD.** 1971. Response of cultured macrophages to Mycobacterium tuberculosis, with observations on fusion of lysosomes with phagosomes. J Exp Med **134:**713-740.

52. **Armstrong JA, Hart PD.** 1975. Phagosome-lysosome interactions in cultured macrophages infected with virulent tubercle bacilli. Reversal of the usual nonfusion pattern and observations on bacterial survival. J Exp Med **142:**1-16.

53. **Clemens DL, Horwitz MA.** 1996. The Mycobacterium tuberculosis phagosome interacts with early endosomes and is accessible to exogenously administered transferrin. J Exp Med **184:**1349-1355.

54. **Crowle AJ, Dahl R, Ross E, May MH.** 1991. Evidence that vesicles containing living, virulent Mycobacterium tuberculosis or Mycobacterium avium in cultured human macrophages are not acidic. Infect Immun **59:**1823-1831.

55. **Sturgill-Koszycki S, Schlesinger PH, Chakraborty P, Haddix PL, Collins HL, Fok AK, Allen RD, Gluck SL, Heuser J, Russell DG.** 1994. Lack of acidification in Mycobacterium phagosomes produced by exclusion of the vesicular proton-ATPase. Science **263:**678-681.

56. **Malik ZA, Thompson CR, Hashimi S, Porter B, Iyer SS, Kusner DJ.** 2003. Cutting edge: Mycobacterium tuberculosis blocks Ca2+ signaling and phagosome maturation in human macrophages via specific inhibition of sphingosine kinase. J Immunol **170:**2811-2815.

57. **Jayachandran R, Sundaramurthy V, Combaluzier B, Mueller P, Korf H, Huygen K, Miyazaki T, Albrecht I, Massner J, Pieters J.** 2007. Survival of mycobacteria in macrophages is mediated by coronin 1-dependent activation of calcineurin. Cell **130:**37-50.

58. **Houben D, Demangel C, van Ingen J, Perez J, Baldeón L, Abdallah AM, Caleechurn L, Bottai D, van Zon M, de Punder K, van der Laan T, Kant A, Bossers-de Vries R, Willemsen P, Bitter W, van Soolingen D, Brosch R, van der Wel N, Peters PJ.** 2012. ESX-1-mediated translocation to the cytosol controls virulence of mycobacteria. Cell Microbiol **14:**1287-1298.

59. **Leake ES, Myrvik QN, Wright MJ.** 1984. Phagosomal membranes of Mycobacterium bovis BCG-immune alveolar macrophages are resistant to disruption by Mycobacterium tuberculosis H37Rv. Infect Immun **45:**443-446.

60. **McDonough KA, Kress Y, Bloom BR.** 1993. Pathogenesis of tuberculosis: interaction of Mycobacterium tuberculosis with macrophages. Infect Immun **61:**2763-2773.

61. **Myrvik QN, Leake ES, Wright MJ.** 1984. Disruption of phagosomal membranes of normal alveolar macrophages by the H37Rv strain of Mycobacterium tuberculosis. A correlate of virulence. Am Rev Respir Dis **129:**322-328.

62. **van der Wel N, Hava D, Houben D, Fluitsma D, van Zon M, Pierson J, Brenner M, Peters PJ.** 2007. M. tuberculosis and M.

leprae translocate from the phagolysosome to the cytosol in myeloid cells. Cell **129:**1287-1298.

63. **Manzanillo PS, Shiloh MU, Portnoy DA, Cox JS.** 2012. Mycobacterium tuberculosis activates the DNA-dependent cytosolic surveillance pathway within macrophages. Cell Host Microbe **11:**469-480.

64. **Wong KW, Jacobs WR.** 2011. Critical role for NLRP3 in necrotic death triggered by Mycobacterium tuberculosis. Cell Microbiol **13:**1371-1384.

65. **Simeone R, Bobard A, Lippmann J, Bitter W, Majlessi L, Brosch R, Enninga J.** 2012. Phagosomal rupture by Mycobacterium tuberculosis results in toxicity and host cell death. PLoS Pathog **8:**e1002507.

66. **Divangahi M, Mostowy S, Coulombe F, Kozak R, Guillot L, Veyrier F, Kobayashi KS, Flavell RA, Gros P, Behr MA.** 2008. NOD2-deficient mice have impaired resistance to Mycobacterium tuberculosis infection through defective innate and adaptive immunity. J Immunol **181:**7157-7165.

67. **Pandey AK, Yang Y, Jiang Z, Fortune SM, Coulombe F, Behr MA, Fitzgerald KA, Sassetti CM, Kelliher MA.** 2009. NOD2, RIP2 and IRF5 play a critical role in the type I interferon response to Mycobacterium tuberculosis. PLoS Pathog **5:**e1000500.

68. **Stanley SA, Johndrow JE, Manzanillo P, Cox JS.** 2007. The Type I IFN response to infection with Mycobacterium tuberculosis requires ESX-1-mediated secretion and contributes to pathogenesis. J Immunol **178:**3143-3152.

69. **Ehrt S, Schnappinger D.** 2009. Mycobacterial survival strategies in the phagosome: defence against host stresses. Cell Microbiol **11:**1170-1178.

70. **Zhao QJ, Xie JP.** 2011. Mycobacterium tuberculosis proteases and implications for new antibiotics against tuberculosis. Crit Rev Eukaryot Gene Expr **21:**347-361.

71. **Guenin-Macé L, Siméone R, Demangel C.** 2009. Lipids of pathogenic Mycobacteria: contributions to virulence and host immune suppression. Transbound Emerg Dis **56:**255-268.

72. **Hotter GS, Collins DM.** 2011. Mycobacterium bovis lipids: virulence and vaccines. Vet Microbiol **151:**91-98.

73. **Mehrotra J, Bishai WR.** 2001. Regulation of virulence genes in Mycobacterium tuberculosis. Int J Med Microbiol **291:**171-182.

74. **Sachdeva P, Misra R, Tyagi AK, Singh Y.** 2010. The sigma factors of Mycobacterium tuberculosis: regulation of the regulators. FEBS J **277:**605-626.

75. **Brodin P, Rosenkrands I, Andersen P, Cole ST, Brosch R.** 2004. ESAT-6 proteins: protective antigens and virulence factors? Trends Microbiol **12:**500-508.

76. **Simeone R, Bottai D, Brosch R.** 2009. ESX/type VII secretion systems and their role in host-pathogen interaction. Curr Opin Microbiol **12:**4-10.

77. **Takayama K, Wang C, Besra GS.** 2005. Pathway to synthesis and processing of mycolic acids in Mycobacterium tuberculosis. Clin Microbiol Rev **18:**81-101.

78. **Stanley SA, Cox JS.** 2013. Host-pathogen interactions during Mycobacterium tuberculosis infections. Curr Top Microbiol Immunol **374:**211-241.

79. **Hoffmann C, Leis A, Niederweis M, Plitzko JM, Engelhardt H.** 2008. Disclosure of the mycobacterial outer membrane: cryo-electron tomography and vitreous sections reveal the lipid bilayer structure. Proc Natl Acad Sci U S A **105:**3963-3967.

80. **Sani M, Houben EN, Geurtsen J, Pierson J, de Punder K, van Zon M, Wever B, Piersma SR, Jiménez CR, Daffé M, Appelmelk BJ, Bitter W, van der Wel N, Peters PJ.** 2010. Direct visualization by cryo-EM of the mycobacterial capsular layer: a labile structure containing ESX-1-secreted proteins. PLoS Pathog **6:**e1000794.

81. **ASSELINEAU J, LEDERER E.** 1950. Structure of the mycolic acids of Mycobacteria. Nature **166:**782-783.

82. **Qureshi N, Takayama K, Jordi HC, Schnoes HK.** 1978. Characterization of the purified components of a new homologous series of alpha-mycolic acids from Mycobacterium tuberculosis H37Ra. J Biol Chem **253:**5411-5417.

83. **Cole ST, Brosch R, Parkhill J, Garnier T, Churcher C, Harris D, Gordon SV, Eiglmeier K, Gas S, Barry CE, Tekaia F, Badcock K, Basham D, Brown D, Chillingworth T, Connor R, Davies R, Devlin K, Feltwell T, Gentles S, Hamlin N, Holroyd S, Hornsby T, Jagels K, Krogh A, McLean J, Moule S, Murphy L, Oliver K, Osborne J, Quail MA, Rajandream MA, Rogers J, Rutter S, Seeger K, Skelton J, Squares R, Squares S, Sulston JE, Taylor K, Whitehead S, Barrell BG.** 1998. Deciphering the biology of Mycobacterium tuberculosis from the complete genome sequence. Nature **393:**537-544.

84. **Bhatt A, Fujiwara N, Bhatt K, Gurcha SS, Kremer L, Chen B, Chan J, Porcelli SA, Kobayashi K, Besra GS, Jacobs WR.** 2007. Deletion of kasB in Mycobacterium tuberculosis causes loss of acid-fastness and subclinical latent tuberculosis in immunocompetent mice. Proc Natl Acad Sci U S A **104:**5157-5162.

85. **Dubnau E, Chan J, Raynaud C, Mohan VP, Lanéelle MA, Yu K, Quémard A, Smith I, Daffé M.** 2000. Oxygenated mycolic acids are necessary for virulence of Mycobacterium tuberculosis in mice. Mol Microbiol **36:**630-637.

86. **Gandhi NR, Nunn P, Dheda K, Schaaf HS, Zignol M, van Soolingen D, Jensen P, Bayona J.** 2010. Multidrug-resistant and extensively drug-resistant tuberculosis: a threat to global control of tuberculosis. Lancet **375:**1830-1843.

87. **Mukherjee JS, Rich ML, Socci AR, Joseph JK, Virú FA, Shin SS, Furin JJ, Becerra MC, Barry DJ, Kim JY, Bayona J, Farmer P, Smith Fawzi MC, Seung KJ.** 2004. Programmes and principles in treatment of multidrug-resistant tuberculosis. Lancet **363:**474-481.

88. **Zhang Y.** 2005. The magic bullets and tuberculosis drug targets. Annu Rev Pharmacol Toxicol **45:**529-564.

89. **Sharma S, Yoder MA.** 2011. New weapons in the war on tuberculosis. Am J Ther **18:**e101-112.

90. **Zumla A, Nahid P, Cole ST.** 2013. Advances in the development of new tuberculosis drugs and treatment regimens. Nat Rev Drug Discov **12:**388-404.

91. **Dover LG, Alahari A, Gratraud P, Gomes JM, Bhowruth V, Reynolds RC, Besra GS, Kremer L.** 2007. EthA, a common activator of thiocarbamide-containing drugs acting on different mycobacterial targets. Antimicrob Agents Chemother **51:**1055-1063.

92. **MACKANESS GB, SMITH N.** 1952. The action of isoniazid (isonicotinic acid hydrazide) on intracellular tubercle bacilli. Am Rev Tuberc **66:**125-133.

93. **Lambelin G.** 1970. Pharmacology and toxicology of Isoxyl. Antibiot Chemother **16:**84-95.

94. **Jaju M, Ahuja YR.** 1984. Combined and individual effects of isoniazid and thiacetazone on human lymphocyte chromosomes in vitro and in vivo. Hum Toxicol **3:**373-382.

95. **Chintu C, Luo C, Bhat G, Raviglione M, DuPont H, Zumla A.** 1993. Cutaneous hypersensitivity reactions due to thiacetazone in the treatment of tuberculosis in Zambian children infected with HIV-I. Arch Dis Child **68:**665-668.

96. **Stover CK, Warrener P, VanDevanter DR, Sherman DR, Arain TM, Langhorne MH, Anderson SW, Towell JA, Yuan Y, McMurray DN, Kreiswirth BN, Barry CE, Baker WR.** 2000. A small-molecule nitroimidazopyran drug candidate for the treatment of tuberculosis. Nature **405:**962-966.

97. **Woodcock JM, Andrews JM, Boswell FJ, Brenwald NP, Wise R.** 1997. In vitro activity of BAY 12-8039, a new fluoroquinolone. Antimicrob Agents Chemother **41:**101-106.

98. **Dawson R, Diacon A.** 2013. PA-824 , moxifloxacin and pyrazinamide combination therapy for tuberculosis. Expert Opin Investig Drugs **22:**927-932.

99. **Espinal MA, Laszlo A, Simonsen L, Boulahbal F, Kim SJ, Reniero A, Hoffner S, Rieder HL, Binkin N, Dye C, Williams R, Raviglione**

MC. 2001. Global trends in resistance to antituberculosis drugs. World Health Organization-International Union against Tuberculosis and Lung Disease Working Group on Anti-Tuberculosis Drug Resistance Surveillance. N Engl J Med **344:**1294-1303.

100. **Barnes PF, Bloch AB, Davidson PT, Snider DE, Jr.** 1991. Tuberculosis in patients with human immunodeficiency virus infection. N Engl J Med **324:**1644-1650.

101. **Snider DE, Jr., Roper WL.** 1992. The new tuberculosis. N Engl J Med **326:**703-705.

102. **Zignol M, Hosseini MS, Wright A, Weezenbeek CL, Nunn P, Watt CJ, Williams BG, Dye C.** 2006. Global incidence of multidrug-resistant tuberculosis. J Infect Dis **194:**479-485.

103. **Lawn SD, Wilkinson R.** 2006. Extensively drug resistant tuberculosis. BMJ **333:**559-560.

104. **Velayati AA, Masjedi MR, Farnia P, Tabarsi P, Ghanavi J, Ziazarifi AH, Hoffner SE.** 2009. Emergence of new forms of totally drug-resistant tuberculosis bacilli: super extensively drug-resistant tuberculosis or totally drug-resistant strains in iran. Chest **136:**420-425.

105. **Gandhi NR, Moll A, Sturm AW, Pawinski R, Govender T, Lalloo U, Zeller K, Andrews J, Friedland G.** 2006. Extensively drug-resistant tuberculosis as a cause of death in patients co-infected with tuberculosis and HIV in a rural area of South Africa. Lancet **368:**1575-1580.

106. **Shah NS, Wright A, Bai GH, Barrera L, Boulahbal F, Martín-Casabona N, Drobniewski F, Gilpin C, Havelková M, Lepe R, Lumb R, Metchock B, Portaels F, Rodrigues MF, Rüsch-Gerdes S, Van Deun A, Vincent V, Laserson K, Wells C, Cegielski JP.** 2007. Worldwide emergence of extensively drug-resistant tuberculosis. Emerg Infect Dis **13:**380-387.

107. **Wells CD, Cegielski JP, Nelson LJ, Laserson KF, Holtz TH, Finlay A, Castro KG, Weyer K.** 2007. HIV infection and multidrug-resistant tuberculosis: the perfect storm. J Infect Dis **196 Suppl 1:**S86-107.

108. **Cox H, Kebede Y, Allamuratova S, Ismailov G, Davletmuratova Z, Byrnes G, Stone C, Niemann S, Rusch-Gerdes S, Blok L, Doshetov D.** 2006. Tuberculosis recurrence and mortality after successful treatment: impact of drug resistance. PLoS Med **3:**e384.

109. **Sotgiu G, Ferrara G, Matteelli A, Richardson MD, Centis R, Ruesch-Gerdes S, Toungoussova O, Zellweger JP, Spanevello A, Cirillo D, Lange C, Migliori GB.** 2009. Epidemiology and clinical management of XDR-TB: a systematic review by TBNET. Eur Respir J **33:**871-881.

110. **Koul A, Arnoult E, Lounis N, Guillemont J, Andries K.** 2011. The challenge of new drug discovery for tuberculosis. Nature **469:**483-490.

111. **Bardou F, Raynaud C, Ramos C, Lanéelle MA, Lanéelle G.** 1998. Mechanism of isoniazid uptake in Mycobacterium tuberculosis. Microbiology **144 (Pt 9):**2539-2544.

112. **MITCHISON DA, SELKON JB.** 1956. The bactericidal activities of antituberculous drugs. Am Rev Tuberc **74:**109-116; discussion, 116-123.

113. **PANSY F, STANDER H, DONOVICK R.** 1952. In vitro studies on isonicotinic acid hydrazide. Am Rev Tuberc **65:**761-764.

114. **Vilchèze C, Jacobs WR.** 2007. The mechanism of isoniazid killing: clarity through the scope of genetics. Annu Rev Microbiol **61:**35-50.

115. **Vilchèze C, Morbidoni HR, Weisbrod TR, Iwamoto H, Kuo M, Sacchettini JC, Jacobs WR.** 2000. Inactivation of the inhA-encoded fatty acid synthase II (FASII) enoyl-acyl carrier protein reductase induces accumulation of the FASI end products and cell lysis of Mycobacterium smegmatis. J Bacteriol **182:**4059-4067.

116. **Vilchèze C, Weisbrod TR, Chen B, Kremer L, Hazbón MH, Wang F, Alland D, Sacchettini JC, Jacobs WR.** 2005. Altered NADH/NAD+ ratio mediates coresistance to isoniazid and ethionamide in mycobacteria. Antimicrob Agents Chemother **49:**708-720.

117. **Takayama K, Schnoes HK, Armstrong EL, Boyle RW.** 1975. Site of inhibitory action of isoniazid in the synthesis of mycolic acids in Mycobacterium tuberculosis. J Lipid Res **16:**308-317.

118. **Zhang Y, Heym B, Allen B, Young D, Cole S.** 1992. The catalase-peroxidase gene and isoniazid resistance of Mycobacterium tuberculosis. Nature **358:**591-593.

119. **Hazbon MH, Brimacombe M, Bobadilla del Valle M, Cavatore M, Guerrero MI, Varma-Basil M, Billman-Jacobe H, Lavender C, Fyfe J, Garcia-Garcia L, Leon CI, Bose M, Chaves F, Murray M, Eisenach KD, Sifuentes-Osornio J, Cave MD, Ponce de Leon A, Alland D.** 2006. Population genetics study of isoniazid resistance mutations and evolution of multidrug-resistant Mycobacterium tuberculosis. Antimicrob Agents Chemother **50:**2640-2649.

120. **Jenner PJ, Smith SE.** 1987. Plasma levels of ethionamide and prothionamide in a volunteer following intravenous and oral dosages. Lepr Rev **58:**31-37.

121. **Quemard A, Laneelle G, Lacave C.** 1992. Mycolic acid synthesis: a target for ethionamide in mycobacteria? Antimicrob Agents Chemother **36:**1316-1321.

122. **Banerjee A, Dubnau E, Quemard A, Balasubramanian V, Um KS, Wilson T, Collins D, de Lisle G, Jacobs WR, Jr.** 1994. inhA, a gene encoding a target for isoniazid and ethionamide in Mycobacterium tuberculosis. Science **263:**227-230.

123. **Rozwarski DA, Grant GA, Barton DH, Jacobs WR, Jr., Sacchettini JC.** 1998. Modification of the NADH of the isoniazid target (InhA) from Mycobacterium tuberculosis. Science **279:**98-102.

124. **Baulard AR, Betts JC, Engohang-Ndong J, Quan S, McAdam RA, Brennan PJ, Locht C, Besra GS.** 2000. Activation of the pro-drug ethionamide is regulated in mycobacteria. J Biol Chem **275:**28326-28331.

125. **Dessen A, Quemard A, Blanchard JS, Jacobs WR, Jr., Sacchettini JC.** 1995. Crystal structure and function of the isoniazid target of Mycobacterium tuberculosis. Science **267:**1638-1641.

126. **Morlock GP, Metchock B, Sikes D, Crawford JT, Cooksey RC.** 2003. ethA, inhA, and katG loci of ethionamide-resistant clinical Mycobacterium tuberculosis isolates. Antimicrob Agents Chemother **47:**3799-3805.

127. **DeBarber AE, Mdluli K, Bosman M, Bekker LG, Barry CE.** 2000. Ethionamide activation and sensitivity in multidrug-resistant Mycobacterium tuberculosis. Proc Natl Acad Sci U S A **97:**9677-9682.

128. **Hanoulle X, Wieruszeski JM, Rousselot-Pailley P, Landrieu I, Locht C, Lippens G, Baulard AR.** 2006. Selective intracellular accumulation of the major metabolite issued from the activation of the prodrug ethionamide in mycobacteria. J Antimicrob Chemother **58:**768-772.

129. **Boonaiam S, Chaiprasert A, Prammananan T, Leechawengwongs M.** 2010. Genotypic analysis of genes associated with isoniazid and ethionamide resistance in MDR-TB isolates from Thailand. Clin Microbiol Infect **16:**396-399.

130. **Vannelli TA, Dykman A, Ortiz de Montellano PR.** 2002. The antituberculosis drug ethionamide is activated by a flavoprotein monooxygenase. J Biol Chem **277:**12824-12829.

131. **Hanoulle X, Wieruszeski JM, Rousselot-Pailley P, Landrieu I, Baulard AR, Lippens G.** 2005. Monitoring of the ethionamide pro-drug activation in mycobacteria by (1)H high resolution magic angle spinning NMR. Biochem Biophys Res Commun **331:**452-458.

132. **Fraaije MW, Kamerbeek NM, Heidekamp AJ, Fortin R, Janssen DB.** 2004. The prodrug activator EtaA from Mycobacterium tuberculosis is a Baeyer-Villiger monooxygenase. J Biol Chem **279:**3354-3360.

133. **Betts JC, Lukey PT, Robb LC, McAdam RA, Duncan K.** 2002. Evaluation of a nutrient starvation model of Mycobacterium tuberculosis persistence by gene and protein expression profiling. Mol Microbiol **43:**717-731.

134. **Rodriguez GM, Voskuil MI, Gold B, Schoolnik GK, Smith I.** 2002. ideR, An essential gene in mycobacterium tuberculosis: role of IdeR in iron-dependent gene expression, iron metabolism, and oxidative stress response. Infect Immun **70:**3371-3381.

135. **Bhowruth V, Brown AK, Reynolds RC, Coxon GD, Mackay SP, Minnikin DE, Besra GS.** 2006. Symmetrical and unsymmetrical analogues of isoxyl; active agents against Mycobacterium tuberculosis. Bioorg Med Chem Lett **16:**4743-4747.

136. **Engohang-Ndong J, Baillat D, Aumercier M, Bellefontaine F, Besra GS, Locht C, Baulard AR.** 2004. EthR, a repressor of the TetR/CamR family implicated in ethionamide resistance in mycobacteria, octamerizes cooperatively on its operator. Mol Microbiol **51:**175-188.

137. **Frenois F, Baulard AR, Villeret V.** 2006. Insights into mechanisms of induction and ligands recognition in the transcriptional repressor EthR from Mycobacterium tuberculosis. Tuberculosis (Edinb) **86:**110-114.

138. **Huffman JL, Brennan RG.** 2002. Prokaryotic transcription regulators: more than just the helix-turn-helix motif. Curr Opin Struct Biol **12:**98-106.

139. **Frenois F, Engohang-Ndong J, Locht C, Baulard AR, Villeret V.** 2004. Structure of EthR in a ligand bound conformation reveals therapeutic perspectives against tuberculosis. Mol Cell **16:**301-307.

140. **Leiba J, Carrère-Kremer S, Blondiaux N, Dimala MM, Wohlkönig A, Baulard A, Kremer L, Molle V.** 2014. The Mycobacterium tuberculosis transcriptional repressor EthR is negatively regulated by Serine/Threonine phosphorylation. Biochem Biophys Res Commun **446:**1132-1138.

141. **Willand N, Dirie B, Carette X, Bifani P, Singhal A, Desroses M, Leroux F, Willery E, Mathys V, Deprez-Poulain R, Delcroix G, Frenois F, Aumercier M, Locht C, Villeret V, Deprez B, Baulard AR.** 2009. Synthetic EthR inhibitors boost antituberculous activity of ethionamide. Nat Med **15:**537-544.

142. **Vilchèze C, Av-Gay Y, Attarian R, Liu Z, Hazbón MH, Colangeli R, Chen B, Liu W, Alland D, Sacchettini JC, Jacobs WR.** 2008. Mycothiol biosynthesis is essential for ethionamide susceptibility in Mycobacterium tuberculosis. Mol Microbiol **69:**1316-1329.

143. **Vilchèze C, Av-Gay Y, Barnes SW, Larsen MH, Walker JR, Glynne RJ, Jacobs WR.** 2011. Coresistance to isoniazid and ethionamide maps to mycothiol biosynthetic genes in Mycobacterium bovis. Antimicrob Agents Chemother **55:**4422-4423.

144. **Rawat M, Kovacevic S, Billman-Jacobe H, Av-Gay Y.** 2003. Inactivation of mshB, a key gene in the mycothiol biosynthesis pathway in Mycobacterium smegmatis. Microbiology **149:**1341-1349.

145. **Pethe K, Sequeira PC, Agarwalla S, Rhee K, Kuhen K, Phong WY, Patel V, Beer D, Walker JR, Duraiswamy J, Jiricek J, Keller TH, Chatterjee A, Tan MP, Ujjini M, Rao SP, Camacho L, Bifani P, Mak PA, Ma I, Barnes SW, Chen Z, Plouffe D, Thayalan P, Ng SH, Au M, Lee BH, Tan BH, Ravindran S, Nanjundappa M, Lin X, Goh A, Lakshminarayana SB, Shoen C, Cynamon M, Kreiswirth**

B, Dartois V, Peters EC, Glynne R, Brenner S, Dick T. 2010. A chemical genetic screen in Mycobacterium tuberculosis identifies carbon-source-dependent growth inhibitors devoid of in vivo efficacy. Nat Commun **1:**57.

146. **Shandil RK, Jayaram R, Kaur P, Gaonkar S, Suresh BL, Mahesh BN, Jayashree R, Nandi V, Bharath S, Balasubramanian V.** 2007. Moxifloxacin, ofloxacin, sparfloxacin, and ciprofloxacin against Mycobacterium tuberculosis: evaluation of in vitro and pharmacodynamic indices that best predict in vivo efficacy. Antimicrob Agents Chemother **51:**576-582.

147. **Vilcheze C, Wang F, Arai M, Hazbon MH, Colangeli R, Kremer L, Weisbrod TR, Alland D, Sacchettini JC, Jacobs WR, Jr.** 2006. Transfer of a point mutation in Mycobacterium tuberculosis inhA resolves the target of isoniazid. Nat Med **12:**1027-1029.

148. **Flipo M, Desroses M, Lecat-Guillet N, Dirié B, Carette X, Leroux F, Piveteau C, Demirkaya F, Lens Z, Rucktooa P, Villeret V, Christophe T, Jeon HK, Locht C, Brodin P, Déprez B, Baulard AR, Willand N.** 2011. Ethionamide boosters: synthesis, biological activity, and structure-activity relationships of a series of 1,2,4-oxadiazole EthR inhibitors. J Med Chem **54:**2994-3010.

149. **Willand N, Dirié B, Carette X, Bifani P, Singhal A, Desroses M, Leroux F, Willery E, Mathys V, Déprez-Poulain R, Delcroix G, Frénois F, Aumercier M, Locht C, Villeret V, Déprez B, Baulard AR.** 2009. Synthetic EthR inhibitors boost antituberculous activity of ethionamide. Nat Med **15:**537-544.

150. **Balaji KN, Boom WH.** 1998. Processing of Mycobacterium tuberculosis bacilli by human monocytes for CD4+ alphabeta and gammadelta T cells: role of particulate antigen. Infect Immun **66:**98-106.

151. **Parish T, Stoker NG.** 2000. Use of a flexible cassette method to generate a double unmarked Mycobacterium tuberculosis tlyA plcABC mutant by gene replacement. Microbiology **146 (Pt 8):**1969-1975.

152. **Bardarov S, Bardarov Jr S, Jr., Pavelka Jr MS, Jr., Sambandamurthy V, Larsen M, Tufariello J, Chan J, Hatfull G, Jacobs Jr WR, Jr.** 2002. Specialized transduction: an efficient method for generating marked and unmarked targeted gene disruptions in Mycobacterium tuberculosis, M. bovis BCG and M. smegmatis. Microbiology **148:**3007-3017.

153. **Sambrook J, Russell DW.** 2001. Molecular cloning : a laboratory manual, 3rd ed. Cold Spring Harbor Laboratory Press, Cold Spring Harbor, N.Y.

154. **Cappelli G, Volpe E, Grassi M, Liseo B, Colizzi V, Mariani F.** 2006. Profiling of Mycobacterium tuberculosis gene expression during human macrophage infection: upregulation of the alternative sigma factor G, a group of transcriptional regulators, and proteins with unknown function. Res Microbiol **157:**445-455.

155. **Luria SE, Delbrück M.** 1943. Mutations of Bacteria from Virus Sensitivity to Virus Resistance. Genetics 28:491-511.

156. **Mathys V, Wintjens R, Lefevre P, Bertout J, Singhal A, Kiass M, Kurepina N, Wang XM, Mathema B, Baulard A, Kreiswirth BN, Bifani P.** 2009. Molecular genetics of para-aminosalicylic acid resistance in clinical isolates and spontaneous mutants of Mycobacterium tuberculosis. Antimicrob Agents Chemother **53:**2100-2109.

157. **Grzegorzewicz AE, Pham H, Gundi VA, Scherman MS, North EJ, Hess T, Jones V, Gruppo V, Born SE, Korduláková J, Chavadi SS, Morisseau C, Lenaerts AJ, Lee RE, McNeil MR, Jackson M.** 2012. Inhibition of mycolic acid transport across the Mycobacterium tuberculosis plasma membrane. Nat Chem Biol **8:**334-341.

158. **Stadthagen G, Korduláková J, Griffin R, Constant P, Bottová I, Barilone N, Gicquel B, Daffé M, Jackson M.** 2005. p-Hydroxybenzoic acid synthesis in Mycobacterium tuberculosis. J Biol Chem **280:**40699-40706.

159. **FOLCH J, LEES M, SLOANE STANLEY GH.** 1957. A simple method for the isolation and purification of total lipides from animal tissues. J Biol Chem **226:**497-509.

160. **Shui G, Bendt AK, Pethe K, Dick T, Wenk MR.** 2007. Sensitive profiling of chemically diverse bioactive lipids. J Lipid Res **48:**1976-1984.

161. **Kurabachew M, Lu SH, Krastel P, Schmitt EK, Suresh BL, Goh A, Knox JE, Ma NL, Jiricek J, Beer D, Cynamon M, Petersen F, Dartois V, Keller T, Dick T, Sambandamurthy VK.** 2008. Lipiarmycin targets RNA polymerase and has good activity against multidrug-resistant strains of Mycobacterium tuberculosis. J Antimicrob Chemother **62:**713-719.

162. **Vander Beken S, Al Dulayymi JR, Naessens T, Koza G, Maza-Iglesias M, Rowles R, Theunissen C, De Medts J, Lanckacker E, Baird MS, Grooten J.** 2010. Molecular structure of the Mycobacterium tuberculosis virulence factor, mycolic acid, determines the elicited inflammatory pattern. Eur J Immunol.

163. **de Steenwinkel JE, ten Kate MT, de Knegt GJ, Verbrugh HA, van Belkum A, Hernandez-Pando R, Bakker-Woudenberg IA.** 2011. Course of murine tuberculosis and response to first-line therapy depends on route of infection and inoculum size. Int J Tuberc Lung Dis **15:**1478-1484, i.

164. **Neo Y, Li R, Howe J, Hoo R, Pant A, Ho S, Alonso S.** 2010. Evidence for an intact polysaccharide capsule in Bordetella pertussis. Microbes Infect **12:**238-245.

165. **Shimono N, Morici L, Casali N, Cantrell S, Sidders B, Ehrt S, Riley LW.** 2003. Hypervirulent mutant of Mycobacterium tuberculosis resulting from disruption of the mce1 operon. Proc Natl Acad Sci U S A **100:**15918-15923.

166. **Cubillos-Ruiz A, Morales J, Zambrano MM.** 2008. Analysis of the genetic variation in Mycobacterium tuberculosis strains by multiple genome alignments. BMC Res Notes **1:**110.

167. **Manca C, Tsenova L, Bergtold A, Freeman S, Tovey M, Musser JM, Barry CE, Freedman VH, Kaplan G.** 2001. Virulence of a Mycobacterium tuberculosis clinical isolate in mice is determined by failure to induce Th1 type immunity and is associated with induction of IFN-alpha /beta. Proc Natl Acad Sci U S A **98:**5752-5757.

168. **Sreevatsan S, Pan X, Stockbauer KE, Connell ND, Kreiswirth BN, Whittam TS, Musser JM.** 1997. Restricted structural gene polymorphism in the Mycobacterium tuberculosis complex indicates evolutionarily recent global dissemination. Proc Natl Acad Sci U S A **94:**9869-9874.

169. **Nuzzo I, Galdiero M, Bentivoglio C, Galdiero R, Romano Carratelli C.** 2002. Apoptosis modulation by mycolic acid, tuberculostearic acid and trehalose 6,6'-dimycolate. J Infect **44:**229-235.

170. **Riley LW.** 2006. Of mice, men, and elephants: Mycobacterium tuberculosis cell envelope lipids and pathogenesis. J Clin Invest **116:**1475-1478.

171. **Liu J, Barry CE, Besra GS, Nikaido H.** 1996. Mycolic acid structure determines the fluidity of the mycobacterial cell wall. J Biol Chem **271:**29545-29551.

172. **Glickman MS, Cox JS, Jacobs WR.** 2000. A novel mycolic acid cyclopropane synthetase is required for cording, persistence, and virulence of Mycobacterium tuberculosis. Mol Cell **5:**717-727.

173. **Asselineau C, Asselineau J, Lanéelle G, Lanéelle MA.** 2002. The biosynthesis of mycolic acids by Mycobacteria: current and alternative hypotheses. Prog Lipid Res **41:**501-523.

174. **Toriyama S.** 1982. [Biosynthesis and regulation of cell wall mycolic acid in mycobacteria]. Kekkaku **57:**279-294.

175. **Etemadi AH, Lederer E.** 1965. [On the structure of the alpha-mycolic acids of the human test strain of Mycobacterium tuberculosis]. Bull Soc Chim Fr **9:**2640-2645.

176. **Bonsor D, Butz SF, Solomons J, Grant S, Fairlamb IJ, Fogg MJ, Grogan G.** 2006. Ligation independent cloning (LIC) as a rapid route to families of recombinant biocatalysts from sequenced prokaryotic genomes. Org Biomol Chem **4:**1252-1260.

177. **Francois AA, Nishida CR, de Montellano PR, Phillips IR, Shephard EA.** 2009. Human flavin-containing monooxygenase 2.1 catalyzes oxygenation of the antitubercular drugs thiacetazone and ethionamide. Drug Metab Dispos **37:**178-186.

178. **Qian L, Ortiz de Montellano PR.** 2006. Oxidative activation of thiacetazone by the Mycobacterium tuberculosis flavin

monooxygenase EtaA and human FMO1 and FMO3. Chem Res Toxicol **19:**443-449.

179. **Heym B, Zhang Y, Poulet S, Young D, Cole ST.** 1993. Characterization of the katG gene encoding a catalase-peroxidase required for the isoniazid susceptibility of Mycobacterium tuberculosis. J Bacteriol **175:**4255-4259.

180. **Belardinelli JM, Morbidoni HR.** 2013. Recycling and refurbishing old antitubercular drugs: the encouraging case of inhibitors of mycolic acid biosynthesis. Expert Rev Anti Infect Ther **11:**429-440.

181. **Kumar G, Sharma S, Shafiq N, Pandhi P, Khuller GK, Malhotra S.** 2011. Pharmacokinetics and tissue distribution studies of orally administered nanoparticles encapsulated ethionamide used as potential drug delivery system in management of multi-drug resistant tuberculosis. Drug Deliv **18:**65-73.

182. **Ng VH, Cox JS, Sousa AO, MacMicking JD, McKinney JD.** 2004. Role of KatG catalase-peroxidase in mycobacterial pathogenesis: countering the phagocyte oxidative burst. Mol Microbiol **52:**1291-1302.

183. **Morlock GP, Crawford JT, Butler WR, Brim SE, Sikes D, Mazurek GH, Woodley CL, Cooksey RC.** 2000. Phenotypic characterization of pncA mutants of Mycobacterium tuberculosis. Antimicrob Agents Chemother **44:**2291-2295.

184. **DeBarber AE, Mdluli K, Bosman M, Bekker LG, Barry CE, 3rd.** 2000. Ethionamide activation and sensitivity in multidrug-resistant Mycobacterium tuberculosis. Proc Natl Acad Sci U S A **97:**9677-9682.

185. **Park JH, Roe JH.** 2008. Mycothiol regulates and is regulated by a thiol-specific antisigma factor RsrA and sigma(R) in Streptomyces coelicolor. Mol Microbiol **68:**861-870.

186. **Machová I, Snašel J, Zimmermann M, Laubitz D, Plocinski P, Oehlmann W, Singh M, Dostál J, Sauer U, Pichová I.** 2014. Mycobacterium tuberculosis phosphoenolpyruvate carboxykinase is regulated by redox mechanisms and interaction with thioredoxin. J Biol Chem **289:**13066-13078.

187. **Van Laer K, Buts L, Foloppe N, Vertommen D, Van Belle K, Wahni K, Roos G, Nilsson L, Mateos LM, Rawat M, van Nuland NA, Messens J.** 2012. Mycoredoxin-1 is one of the missing links in the oxidative stress defence mechanism of Mycobacteria. Mol Microbiol **86:**787-804.

188. **Gustafsson TN, Sahlin M, Lu J, Sjöberg BM, Holmgren A.** 2012. Bacillus anthracis thioredoxin systems, characterization and role as electron donors for ribonucleotide reductase. J Biol Chem **287:**39686-39697.

189. **Lu J, Holmgren A.** 2014. The thioredoxin antioxidant system. Free Radic Biol Med **66:**75-87.

190. **Ritz D, Patel H, Doan B, Zheng M, Aslund F, Storz G, Beckwith J.** 2000. Thioredoxin 2 is involved in the oxidative stress response in Escherichia coli. J Biol Chem **275:**2505-2512.